Identification of a potential antimicrobial peptide derived from *Haliotis midae* haemocyanin

By Jarid North

Thesis submitted in fulfilment of the requirements for the degree of

Master of Science

Department of Molecular and Cell Biology

Faculty of Science

University of Cape Town

February 2019

Supervised by Assoc. Prof V. Coyne

DECLARATION

I hereby declare that this dissertation, submitted in fulfilment of the requirements for the degree of Master of Science in the Department of Molecular and Cell Biology at the University of Cape Town, is the result of my own investigations, apart from the referenced work of others.

Signed by candidate

_____

Jarid North

University of Cape Town

February 2019

Acknowledgements

I would like to acknowledge the support and guidance provided to me by my supervisor, Associate Professor Vernon. E. Coyne, during my postgraduate studies at the University of Cape Town: thank you for all the motivation to keep going throughout this project and for taking the time to understand my out-of-the box thinking. I learned a great deal throughout this process, so thank you for the opportunity to improve as a scientist and as a person.

I would like to thank the entire Molecular and Cell Biology Department, who always seemed willing to help whenever I asked, whether through advice or through the loan of reagents or materials. Special thanks also go to Dr Lara Donaldson and her lab for providing the BL21 *E. coli* strain used in this study, and to their member Nina Esterhuysen for being a close friend throughout my studies and making sure I made it to campus every day. Further gratitude must be extended to Tatiana Millard, who always seemed available for microbiological questions. I would also like to thank Dr Brandon Weber from the Centre for Imaging and Analysis for his help with the FPLC purification; if only we had been in contact earlier!

Particular mention must also go to the members of Lab 201, who were always around to provide input and assistance. Specifically, Jay-Dee Atkins for her wisdom and technical advice, Sarah Carroll for her constant encouragement and emotional support and Kyle Naylor for always letting me know when I did something wrong.

Finally, I would like to thank my family and friends, who, even though most had no idea what I was doing, provided constant support and encouragement. A special thank you must be passed along to my Tiger family – through Ultimate I found a place to balance my academic life and remain sane throughout my studies. Thank you for taking so much of my time away.

I would also like to formally acknowledge the financial assistance offered to me by the postgraduate funding office at the University of Cape Town, and the National Research Foundation for providing bursaries during my postgraduate studies.

Table of Contents

Identification of a potential antimicrobial peptide derived from Haliotis midae haemocyanin

By Jarid T. North

February 2019

Abstract

Haliotis midae aquaculture within South Africa remains afflicted by infectious diseases. Understanding of how the abalone's innate immune response functions is one of the greatest hindrances to assisting with the defence or detection of pathogenic attacks on farms. The multifunctional oxygen transporter haemocyanin was previously found to be upregulated in response to bacterial infection (Beltran 2015), indicating it may play a role in the defence response of *Haliotis midae*. The current knowledge regarding haemocyanin's role in the abalone innate immune response is incomplete. A number of studies have been published that investigated haemocyanin's potential as a broad spectrum antimicrobial peptide in many arthropod species. There has been only one study conducted in molluscs, which utilised synthetic peptides derived from a haemocyanin consensus sequence. In most organisms the haemocyanin protein is comprised of a string of eight roughly 50 kDa functional units (FU) annotated a-h. The current study determined the nucleotide sequence of the final four functional units on the C-terminal end of *H. midae* haemocyanin and examined the potential antimicrobial activity of the peptide product. The haliotisin coding sequence identified by Zhuang et al. (2015) was detected in FU-e of the *H. midae* haemocyanin and subcloned into an *Escherichia coli* expression vector for recombinant production of the peptide. This peptide showed some activity against *Staphylococcus aureus* and *E. coli*, suggesting it may function as an antimicrobial peptide. This study provides the first evidence that an antimicrobial peptide derived from the *H. midae* haemocyanin could be functioning as a component of the abalone innate immune response.

1.1 Introduction

Abalone are a commercially important marine species; the flesh from the large foot is consumed as a delicacy in east Asian regions, particularly in Japan and China, who import the most abalone globally (Mau & Jha 2018). The increase in the development of the abalone sector was also influenced by the development of a market for cocktail sized abalone. The market price for abalone fluctuates, depending on the quality and species produced, but is usually set around US$15–30/kg (Cook & Gordon 2010; Mau & Jha 2018). The largest suppliers of wild abalone are Australia, Japan, New Zealand, South Africa and the United States, while the largest producers of farmed abalone are China, Taiwan, South Africa, Australia and Chile (Mau & Jha 2018). South Africa is currently the fourth largest exporter of abalone globally and the largest exporter of cultured abalone outside of Asia (Kilian 2016; Troell et al. 2006). South African abalone inhabit primarily the west coast region, due to the colder waters (Vosloo et al. 2013).

During the 1970s, the South African abalone fishery sector was decommercialised because of its severe impact on the wild population. It was reopened in the early 2000s, but the annual catch allowance was severely reduced to 150 tonnes (Cook 2014). This limitation was put in place because of a decline in the population due to over-exploitation, illegal harvesting, disease and habitat degradation. Illegal harvesting over the last few decades remains a major contributor to the declining wild abalone population. Poaching levels escalated in the 1990s, and by 2002 more abalone was being confiscated than legally exported. This highly organised criminal industry led to wild *H. midae* being brought to the edge of commercial extinction (Steinberg 2005).

Farm-based production of abalone, however, increased dramatically over this time, with an almost-750% increase in farm production worldwide from 2002 to 2010 (Cook & Gordon 2010). Aquacultural practices have a high socioeconomic impact, providing employment, developing local farms and improving both domestic and international trade relations (Dixon et al. 2001). The shift away from commercial fishing towards an aquaculture-based practice not only produces a consistent, water-based food source but also relieves pressure on the wild population, allowing the wild abalone stocks to return to a healthy level. South African aquaculture-based abalone production is currently almost ten times greater than that of wild fisheries (Cook 2014; Department of Agriculture, Forestry and Fisheries 2016). The coastal waters of South Africa contain six different species of abalone, but *Haliotis midae* is the only species that is commercially exported, owing to its large size and relatively rapid growth rate (Sales & Peter J. Britz 2001).

1.1.1 *Haliotis midae* aquaculture

Haliotis midae is the primary species of abalone found along the South African shoreline. Commonly referred to as perlemoen, it is a species of large sea snail belonging to the superfamily Haliotidae (Wood & Buxton 1996). Within the aquaculture sector, the export of *H. midae* is South Africa's primary revenue source (Sales & Peter J Britz 2001; Raemaekers et al. 2011; M Troell et al. 2006; James 2018), and farming is South Africa's dominant source of abalone for export. The drive towards aquaculture-based practices is in part due to the rapid decline of wild abalone populations caused by overfishing and poaching, as well as favourable local conditions, such as access to relatively cheap labour and electricity, good base infrastructure and good water quality. As of 2016, a total of 18 abalone aquaculture farms were operational in South Africa (Department of Agriculture, Forestry and Fisheries 2016), making it the second highest contributor in the marine aquaculture sector, with 1 479.22 tonnes produced per annum. The export of which created an estimated revenue of R460 million (Department of Agriculture, Forestry and Fisheries 2016). Twelve of the aquaculture facilities that produce abalone are land-based with independent hatcheries and four operate as grow-out facilities only, where no hatching takes place and juveniles are grown to maturity. The final two facilities make use of sea cage culture, where cages with stock are maintained offshore within the ocean. The primary contributor to crop loss within the abalone aquaculture industry on a global scale remains infectious diseases (Lafferty et al. 2015).

1.1.2 Diseases affecting abalone aquaculture

Disease outbreaks in aquacultured abalone remain the most significant cause of economic loss globally (Sindermann 1984; Cook 2014). South African aquaculture farms lie primarily along the coastal regions and are thus heavily reliant on coastal water inputs to maintain their stocks, so that farmed abalone are susceptible to the same environmental fluctuations that threaten the wild population. A good example of this is the spread of harmful algal blooms (HAB) which have been found to cross over from wild populations into farming practices. A bloom in 1989 caused a mortality of 40 tons of wild abalone on the southwest coast of South Africa (Horstman et al. 1991), and a more recent event in 2017 near Walker Bay is having similar effects (Pitcher et al. 2019). More frequent extreme-weather conditions due to climate change have resulted in alterations in the temperature, salinity, oxygen and carbon dioxide levels of coastal waters (Morash & Alter 2016). Changes in the marine environment have led to predictions that the global wild mollusc population will dramatically decline between 2020 and 2050 (FAO 2016). Highly intensive farming practices further contribute to the unstable conditions and include farm-specific stressors such as elevated ammonia levels, high stocking densities, handling of abalone and nutrition

(Morash & Alter 2016; Hooper et al. 2011). Ammonia arises as the primary form of nitrogenous waste produced by the abalone as a toxic waste product of amino acid metabolism (Spotte 1970). In the natural oceanic environment the ammonia concentrations rarely reach toxic levels, but in semi-enclosed densely populated aquaculture facilities, ammonia can easily reach levels that affect physiological functions and induce stress (Spotte 1970; Morash & Alter 2016). The current culture methods for abalone also require various steps in which organisms need to be dislodged from their rearing substratum for the purposes of size grading, adjusting densities, tagging or transferring from indoor to outdoor culture facilities (Chacon et al. 2003; Hooper et al. 2011). To this effect, the abalone are moved either with or without anaesthetics and both have been shown to induce stress in the organisms. An increase in stressors has been linked to an increased susceptibility to infections (Hooper et al. 2007; Hooper et al. 2014; Malham et al. 2003), indicating that the stressful factors that affect farmed abalone also result in the decreased immune response of said organisms.

Pathogens that affect both wild and farmed abalone include bacteria, viruses, fungi and fungal-like pathogens, and protozoans (Bower et al. 1994; Paillard et al. 2004; Bondad-Reantaso et al. 2005; Macey et al. 2011), so combatting infections is not straightforward. The largest proportion of diseases within abalone is due to bacterial infection, with abalone mortality rates as high as 90% (Nicolas et al. 2002). For example, mass mortalities of the abalone species *Haliotis tuberculata L.* occurred on the French coast from 1997 into the early 2000s, the *Vibrio* species, identified as *V. carchariae*, spread from the south coast and along the west coast causing the death of between 60 and 80% of the abalone population. In 1999, this bacterium also affected a land-based farm in Normandy, where losses of up to 85% occurred. Other than sporadic instances of white pustules on the foot, there were no indications that the animals were afflicted prior to their death (Nicolas et al. 2002). Similarly, from the late 2000s, the bacteria *Vibrio parahaemolyticus* and *Vibrio alginolyticus* were the cause of mass mortalities in Taiwanese grow-out farms and settlement failure of spat larvae in nursery ponds (Bondad-Reantaso et al. 2005). Similar scenarios have played out in Japan, America, France, China and Australia (Lafferty et al. 2015; Lafferty & Kuris 1993; Mayfield et al. 2011; Sawabe et al. 2007; Nicolas et al. 2002). South Africa has faced similar issues: reports have been made of abalone infections by *Vibrio* and *Clostridium* bacteria, along with the occurrence of gut-associated parasites and the presence of paralytic, shellfish-poisoning toxins (Pitcher et al. 2001; Dixon et al. 1991; Mouton & Gummow 2011).

The variable living conditions of aquacultured abalone are optimal for the spread of pathogens. Stressful environmental conditions such as a change in temperature, pH or oxygen levels leads to reduced immunity

and allows for easier infection, while the proximity of neighbouring abalone due to high tank stocking densities allows the pathogen to spread quickly through an entire stock. These conditions are optimal for the spread of species such as *Pseudomonas*, *Aeromonas* and *Vibrio* (Sindermann 1984). Vibriosis caused by *Vibrio spp*. remains one of the most prevalent diseases in fish and other aquaculture-reared organisms and is responsible for mass mortality in aquaculture systems worldwide (Haldar & Chatterjee 2012).

Compounding these issues, pathogen transfer can occur between reared and wild populations of abalone (Arechavala-Lopez et al. 2013; Lafferty et al. 2015). As most land-based aquacultural systems are coastal, it is possible for one population to infect another, resulting in either major consequences for the wild population or major crop loss for farmed abalone. One prominent example of this would be the outbreak of abalone viral ganglioneuritis (AVG) in Australia. The disease spread from cultured abalone into the surrounding wild population resulting in mass mortalities (Corbeil et al. 2016). Pathogens do not travel exclusively through water, however – wild kelp, readily available on the nearby coastline, is used as the primary feed in many land-based aquaculture facilities, and pathogens in wild abalone populations are introduced onto farms via kelp collected close by (Mouton & Gummow 2011).

1.1.3 Health management on abalone farms

Currently, the primary focus for abalone farmers is on the prevention of pathogenic attack rather than therapy post infection. Prevention is primarily achieved by administering antibiotics to the feed (Handlinger et al. 2005). However, through misuse and overuse of antibiotics, there is an emerging threat of antibiotic-resistant bacteria that could infect the abalone and be transferred to humans upon consumption, causing consumers to be afflicted with a strain of bacteria that is resistant to all current treatment methods (Lee et al. 2003b; Schwarz et al. 2001). Another method for disease prevention is to reduce stocking densities or to invest more heavily in ensuring that water quality and diet are of a high enough standard to reduce opportunistic pathogen attacks. However, these solutions come with a high economic weight. Recently, the use of probiotics has gained popularity as an alternative to antibiotics (Balcázar et al. 2006; Kesarcodi-Watson et al. 2008). In one example, this worked by stimulating the immune response of the abalone through exposure to non-pathogenic bacterial species (Balcázar et al. 2006).

Despite the preventive methods described above, outbreaks of disease continue to plague the abalone aquaculture industry. Currently, the best methods for assessing whether a general abalone infection exists is through *in vitro* testing of the count and quantity of the different morphologies of haemocytes, as well

as through phagocytic capability and respiratory burst assays (Hooper et al. 2007). There are other methods for testing for specific infections, such as PCR, real time PCR, hybridization and histology but these are all costly and are only worth conducting if you have already determined that an infection exists within the abalone. However, much of our understanding of the functioning of the abalone immune response originates indirectly through research performed on other invertebrate species (Hooper et al. 2007; Song et al. 2003); the specifics of the abalone immune response needs investigation to confirm correlated functioning. A comprehensive exploration of the innate immune response of *H. midae* could provide insight into previously unknown molecular mechanisms of the abalone innate immune response.

1.2 Invertebrate immune response

The increased occurrence of infectious diseases in marine invertebrates emphasises the need to better understand how they cope with immunological challenges in both their natural habitats and in aquaculture (Terwilliger 2007). The term "invertebrate" is very broad and includes species making up around 95% of the animal kingdom split amongst 30 different phyla (May 1988). The term "invertebrates" includes molluscs, like abalone, but also many other marine invertebrates, and the largest group within the arthropods, the insects. The challenges faced by species within the invertebrate phylum vary greatly depending on their ecological niche. Immunological strategies employed by one group are thus different from those employed by the next group. Even within the same group, members sometimes use vastly different strategies of internal defence (Loker et al. 2004), and generalisations regarding "invertebrate immunity" should therefore be avoided until confirmed in the organism of interest. Our current understanding of abalone innate immunity is based on a very limited set of research conducted with abalone, a broader range of research undertaken with other gastropods and bivalves, a large body of research on other invertebrates, while the bulk of the research is inferred from vertebrate innate immune systems (Hooper et al. 2007).

Without a significant adaptive immune response, invertebrates are limited to their innate immune system. Lacking the "true" lymphocytes and functional antibodies found in vertebrates, the central dogma within evolutionary biology became that invertebrates rely entirely on their innate immunity (Rowley & Powell 2007). One possible explanation for how invertebrates survive without an adaptive immune system is that their innate defence systems are highly effective, while another is that there are more defences than are currently known (Loker et al. 2004). Lacking the complicated features that are required for an adaptive immune response, invertebrates are forced to employ other methods to generate diversity

and a complex response to attack (Hooper et al. 2007). The stages of the innate immune system begin with the first line of defence, which include physiochemical barriers such as the shell, skin and mucus layer. Following this, the cellular and humoral components are presented in a regulated manner to fight off infection (Girón-Pérez 2010).

The first stage of internal defence is the critical recognition stage. Invertebrates have an immune-neuroendocrine-recognising system that is capable of recognising self from non-self. This system is generally considered to be only slightly less complex than that found in its vertebrate counterpart (Ottaviani et al. 1998). The primary cell type used for recognition and cellular defence is the haemocytes, which can be divided roughly into two morphologies: hyalinocytes, which are smaller, with less cytoplasm and therefore fewer or no granules; and the granulocytes, larger cells with more cytoplasm accommodating a greater number of granules (Tiscar & Mosca 2004; Travers et al. 2008).

Molluscs and arthropods possess an open circulatory system, where the heart distributes haemolymph into the body cavity in such a manner that the organ systems are bathed in it, allowing immune response cells ample opportunity for chance encounters with foreign elements (Bayne 1990). Haemocytes are the main defence molecule in molluscs and are capable of chemotaxis, antigen recognition, attachment followed by agglutination, phagocytosis and elimination of invaders by respiratory burst (Hooper et al. 2007). The exact mechanisms for how these cells differentiate self from non-self and perform phagocytosis is not fully understood in the abalone system, but has been extensively characterised in other marine invertebrate species (Canesi et al. 2002; Canesi et al. 2006; Casas et al. 2011; Cardinaud et al. 2015).

Phagocytosis acts as the first line of internal innate immune defence (Bayne 1990) and has a clearly defined sequence: recognition; chemotaxis; attachment; ingestion; and destruction of the invading pathogen. Once the pathogen has been engulfed, the vacuole within the cytoplasm is referred to as the phagosome. This fuses with the lysosome, which contains degradative enzymes, to form the phagolysosome, which destroys, degrades and eliminates the foreign material via either an oxygen-dependant system (respiratory burst) or an oxygen-independent system (Bayne 1990; Hooper et al. 2007; Mogensen 2009). The cellular response during the innate immune response is complemented by the humoral response.

The haemolymph of abalone and other organisms with an open circulatory system is responsible for the transport of nutrients, oxygen, hormones and cells throughout the body (Fredrick & Ravichandran 2012).

Thus, beyond transporting haemocytes to the site of pathogenic attack, the haemolymph and its molecular constituents also play a role in innate defence. Humoral defence factors include lectins, agglutinins, lysosomal enzymes and, most importantly, antimicrobial peptides (Casas et al. 2011; Nappi & Ottaviani 2000; Marmaras & Lampropoulou 2009; Koutsogiannaki & Kaloyianni 2010). Agglutinins and agglutinin-like molecules such as lectins are responsible for the targeting of foreign material for degradation, while lysosomal enzymes are responsible for hydrolysing microorganisms (Tiscar & Mosca 2004).

The prophenoloxidase (proPO) system is an important component of the humoral immune response of invertebrates and is directly involved in non-self-recognition and defence (Pang et al. 2014). The molecule prophenoloxidase and its corresponding activating enzymes are stored in haemocyte granules and released upon haemocyte stimulation (Hooper et al. 2007). The subsequent proPO cascade modulates the activation of phenoloxidase. Activated phenoloxidases, whose counterpart is tyrosinase in mammals (Adachi et al. 2005), is responsible for catalysis of the initial stages of the biosynthetic pathway that eventually results in the formation of the microbiocidal pigment, melanin (Coates & Nairn 2014). Phenonoxidases catalyse two reactions: the hydroxylation of monophenols to o-diphenols and the oxidation of o-diphenols to o-quinones (Hooper et al. 2007). These reactions cause the production of reactive oxygen species (ROS) as by-products in the eventual formation of melanin (Coates & Nairn 2014; Söderhäll & Cerenius 1998). Melanisation is intimately associated with the appearance of factors that stimulate cellular defence by aiding the phagocytic and encapsulation processes (Cerenius et al. 2008).

Antimicrobial peptides, or AMPs, can act systemically or provide localised protection against environmental pathogens. They display hydrophobic and cationic properties and usually have a molecular mass that is less than 30 kDa.

1.2.1 Antimicrobial peptides

Although antimicrobial peptides have been described as ancient evolutionary weapons, AMPs have remained effective as defensive molecules despite their ancient lineage (Zasloff 2002). They possess a broad ability to kill microbes. To date, over 1 200 AMPs with a broad spectrum of activity have been classified from Eukaryotes, providing effective protection against both Gram-negative and -positive bacteria, yeast, fungi and, in some cases, even viruses and protozoa (Ellis et al. 2011). All AMPs are derived from a larger precursor protein and require post-translational modifications, such as proteolytic cleavage and, in some cases, glycosylation, to become biologically active (Zasloff 2002). Recently, there has been

evidence of proteins undergoing partial hydrolysis to generate antimicrobial peptides (Zhuang et al. 2015). The process of synthesising AMPs can take a few minutes or hours post-challenge (Fredrick & Ravichandran 2012).

Large AMPs, with sequences that are longer than 100 amino acids, either function as lytic proteins, nutrient-binding proteins, or specifically target microbial macromolecules; small AMPs, on the other hand, act by disrupting structures or functions within the cell wall of invading pathogens (Fredrick & Ravichandran 2012). AMPs have such high sequence diversity that the same nucleotide sequence is rarely recovered from two species, even if they are closely related, but there is significant conservation of the antimicrobial peptide amino acid sequences (Zasloff 2002). Some shared characteristics include small size, a cationic character and the presence of 30–50% hydrophobic residues (Ellis et al. 2011). Different AMPs are broadly categorised based on their secondary structure. In general, the molecule will adopt a shape that clusters the hydrophobic and cationic amino acids spatially in a discrete manner, allowing for an amphipathic design (Zasloff 2002). Linear peptides, such as the African clawed frog's magainin and the silk moth's cecropin, only adopt this organisation when they enter the membrane (Steiner et al. 1981; Zosloff 1988). A particular frog species belonging to the genus *Rana* modifies the design by adding a single loop formed via a disulphide bond at the carboxy end (Simmaco et al. 1998), whereas bacternecin and defensins possess a rigid anti-parallel β-sheet constrained by disulphide bonds as the framework (Romeo et al. 1988; Selsted et al. 1985). The diversity of AMPs probably reflects the species' adaptation to the unique microbial environments that characterise the niche it occupies. To effectively eradicate infections, most multicellular organisms will use a cocktail of AMPs comprised of multiple peptides belonging to several structural classes (Zasloff 2002).

Marine invertebrate research into the expression and action of AMPs has been focussed on bivalve molluscs and crustaceans (Ellis et al. 2011). From studies it has been found that different groups of AMPs display different antimicrobial activities and modes of action. They belong to one of three major groups: peptides with an α-helical shape; cyclic and open-ended cyclic peptides with pairs of cysteine residues; or peptides with an over-representation of some specified amino acids (Bulet et al. 2004; Dimarcq et al. 1998), and some peptides that don't fit any of these categories.

The membrane of bacterial cells is organised in such a way that the outer membrane is populated with negatively charged phospholipid headgroups (Zasloff 2002). This contrasts with animal cell membranes, which are mainly composed of the more neutrally charged phospholipids. As AMPs generally have a low

hydrophobicity, they will have a lower affinity for the self-cells and be more attracted to the invasive cells (Matsuzaki 2001).

With their amino acid composition, amphipathicity, cationic charge and small size, antimicrobial peptides are well suited to attach to and insert into bacterial membrane bilayers. In so doing, they form pores by one of three hypothesised methods: “barrel-stave”, whereby the peptide helices form a bundle in the

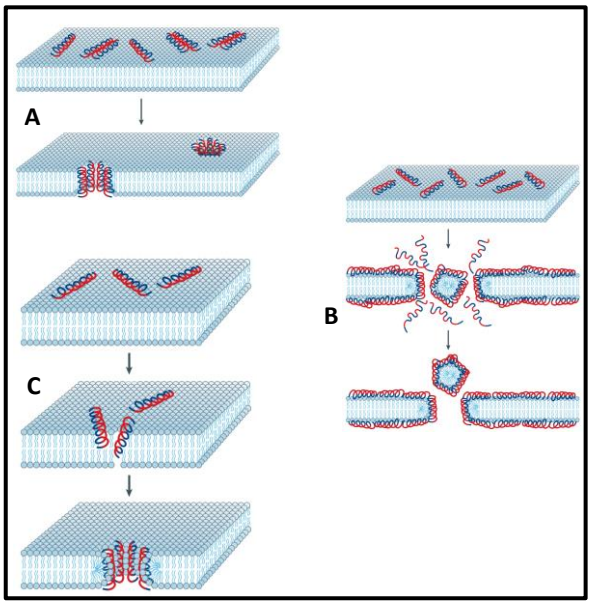

Figure 1.1: Antimicrobial peptides induce killing by creating pores in the bacterial membrane. Hydrophilic regions are shown in red and hydrophobic regions are blue. **A. The barrel-stave model**: Aggregated peptides insert into the membrane bilayer and orientate so that the hydrophobic portion of the peptide aligns with the lipid core region and the hydrophilic side forms the inside of the pore. **B. The carpet model**: The peptide orientates parallel to the surface of the lipid bilayer and forms an extensive layer or carpet. **C. The toroidal model:** The attached peptides aggregate and cause the lipid monolayers to bend continuously through the pore. Figure adapted from Brogden (2005).

membrane with a central channel; “carpet model”, whereby the peptides accumulate on the bilayer surface and force pieces of the membrane to be removed; and the “toroidal-pore model”, whereby peptide helices insert into the membrane and cause the lipid monolayers to bend continuously through the pore so that the water core is lined by both the inserted peptides and the lipid head groups (Brogden 2005). These are illustrated in Figure 1.1, adapted from the review by Brogden (2005).

Once a pore is created, the AMP kills the bacterial cell via one of the following proposed methods: fatal depolarisation of the normally energised bacterial membrane (Westerhoff et al. 1989); creation of physical holes that cause cellular contents to leak out (Yang et al. 2000); activation of deadly processes, such as induction of hydrolases, that degrade the cell wall (Bierbaum & Sahl 1985); or scrambling of the usual distribution of lipids between the leaflets of the bilayer, resulting in the disturbance of membrane functions (Matsuzaki 2001). Furthermore, there has been recent speculation that transmembrane pore formation may not be the only way in which antimicrobials function (Brogden 2005). The peptides may also damage critical targets after internalisation (Kragol et al. 2001) in that translocated peptides can alter formation of the cytoplasmic membrane septum, inhibit cell wall synthesis, inhibit nucleic acid synthesis, inhibit protein synthesis or inhibit the enzymatic activity of proteins (Brogden 2005).

1.3 Haemocyanin

The haemocyanin polypeptide sequence is the largest obtained to date for any respiratory protein (Harris et al. 2000; Lieb et al. 2000). Haemocyanin is one of the primary proteins in the haemolymph of the abalone's open circulatory system. The blue respiratory protein, present in the haemolymph of many molluscs and arthropods, possesses a copper type-3 centre that reversibly binds to oxygen molecules (Markl 2013; Van Holde et al. 2001). Recent studies suggest that this large, multimeric protein may have additional immune response attributes. Work done by the Marine Biotechnology laboratory in the Molecular and Cell Biology Department at the University of Cape Town found, through a proteomics-based study, that the haemocyanin present in the South African abalone *H. midae* was upregulated in response to bacterial infection (Beltran 2015). Before understanding how this protein may function during an immune response, it is necessary to discuss what makes the structure and evolution of this protein unique.

1.3.1 Structure

Typically, the structure of molluscan haemocyanin protein is a string of eight roughly 50 kDa functional units (FU) annotated a–h. This is reflected by its gene structure, which has eight structurally related coding regions, each separated by a variable linker region (intron) (Lieb et al. 2001). *Haliotis tuberculata* haemocyanin 1 has a high degree of similarity between respective functional units (around 45% similarity on the protein level). Corresponding functional units within *Octopus dofleini* share around 55% identity with the *H. tuberculata* haemocyanin at the protein level. This structural layout can be seen in Figure 1.2,

which shows the gene structures for the *Haliotis* and *Octopus* haemocyanin. The only relevant difference between the two is that the *Octopus* sequence lacks the C-terminal functional unit of its *Haliotis* counterpart (Lieb et al. 2001). For the most part, each of the functional units are encoded by a single unbroken exon, except for functional units a, f and g, which contain four, two and three exons respectively. These broken exons are separated by what is referred to as internal introns.

The internal and linker introns are strikingly different: the linker introns are very regular and have remained in the same position and phase since the evolution of the multiunit protein (Lieb et al. 2000; Altenhein et al. 2002), whereas the internal introns, by contrast, are far more scattered in their position and phase. The term "Phase" in this instance refers to which nucleotide in the codon the intron appears in. This organisation can be explained by a genetic mechanism that must have been used to generate the multiunit structure from a monomeric precursor (Lieb et al. 2001).

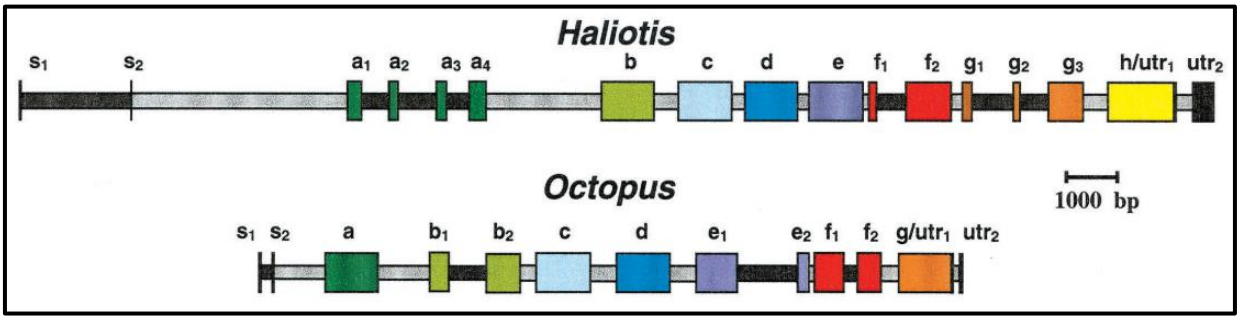

Figure 1.2: The gene structure of HtH1 (*Haliotis*) and OdH1 (*Octopus*). Each of the Functional Units (a-h) are indicated by a separate colour. Introns (grey for the linkers and black for internal) are shown to scale. utr indicates the 3' untranslated region. S1 and S2 correspond to the two exons encoding each signal sequence. Figure taken from Lieb et al. (2001).

1.3.2 Oxygen transport

Haemocyanins are extracellular oxygen-transporting metalloproteins, and each of the functional units are able to reversibly bind to a dioxygen molecule via their binuclear copper sites (Lieb & Markl 2004) (Figure 1.3). Each of these copper atoms is liganded to three histidine residues to form both the copper A and copper B sites (Lieb et al. 2001). The copper B site is the only region that shows similarity between molluscan and arthropod haemocyanin sequences, the limited similarity suggesting that these two phyla evolved independently (Lieb et al. 2001). The other site (A site) of abalone haemocyanin has a closer resemblance to that found in tyrosinases. It is likely that the tyrosinases and molluscan haemocyanin evolved from a common polypeptide chain that contained both the copper A and copper B sites (Lieb et al. 2001).

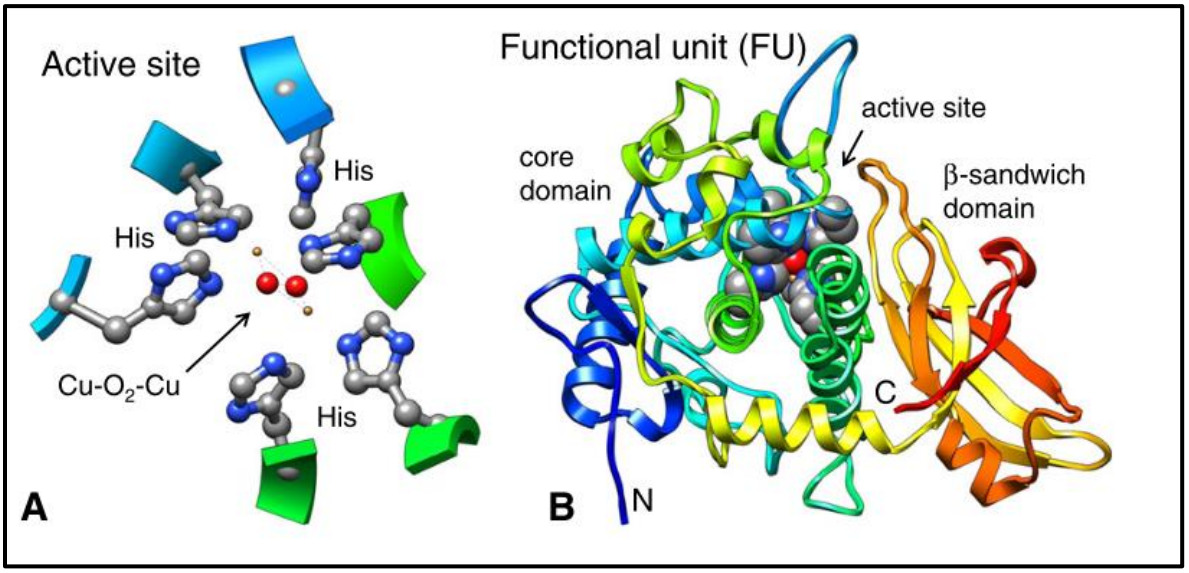

Figure 1.3: Structure of the molluscan haemocyanin subunit. **A** Active site with the two copper ions, six histidine residues and one bound dioxygen molecule (red). **B** A ribbon representation of a functional unit with the atoms of the single active site highlighted as spheres. Figure taken from Markl (2013)

Due to conversion of copper from the CU(I) state (deoxy form) to the oxygenated CU(II) state (Van Holde et al. 2001), a colour change from colourless to blue is evident in haemocyanin once an oxygen molecule is bound (Miller et al. 1998). A single haemocyanin polypeptide can carry as few as six oxygen molecules or as many as several hundred (Lieb et al. 2001).

1.3.3 Assembly of haemocyanin

In molluscs, each of the eight functional units has two well-defined domains. The α-helical domain, which includes the oxygen binding site, is connected by a hinge to a β-sandwich domain that is rich in β-sheets (Lieb et al. 2001) (Figure 1.4). Most organisms contain two separate isoforms of the haemocyanin protein, which can be differentiated either at the genetic level or by their formation of multidecameric proteins (Keller et al. 1999). For *Haliotis tuberculata*, these two isoforms are named *Haliotis tuberculata* haemocyanin 1 (HtH1) and *Haliotis tuberculata* haemocyanin 2 (HtH2). They share 66% similarity to one another and are thus distinguishable at the gene level (Altenhein et al. 2002).

One translated gene of the eight functional units makes up a single subunit of the final multimeric protein. Ten of these subunits arrange themselves together in order to form a decamer (Altenhein et al. 2002)

(Figure 1.4). The first isoform (HtH1) is found predominantly in this decameric form and the second isoform is found predominantly as a didecamer, formed via face-to-face assembly of two decamers.

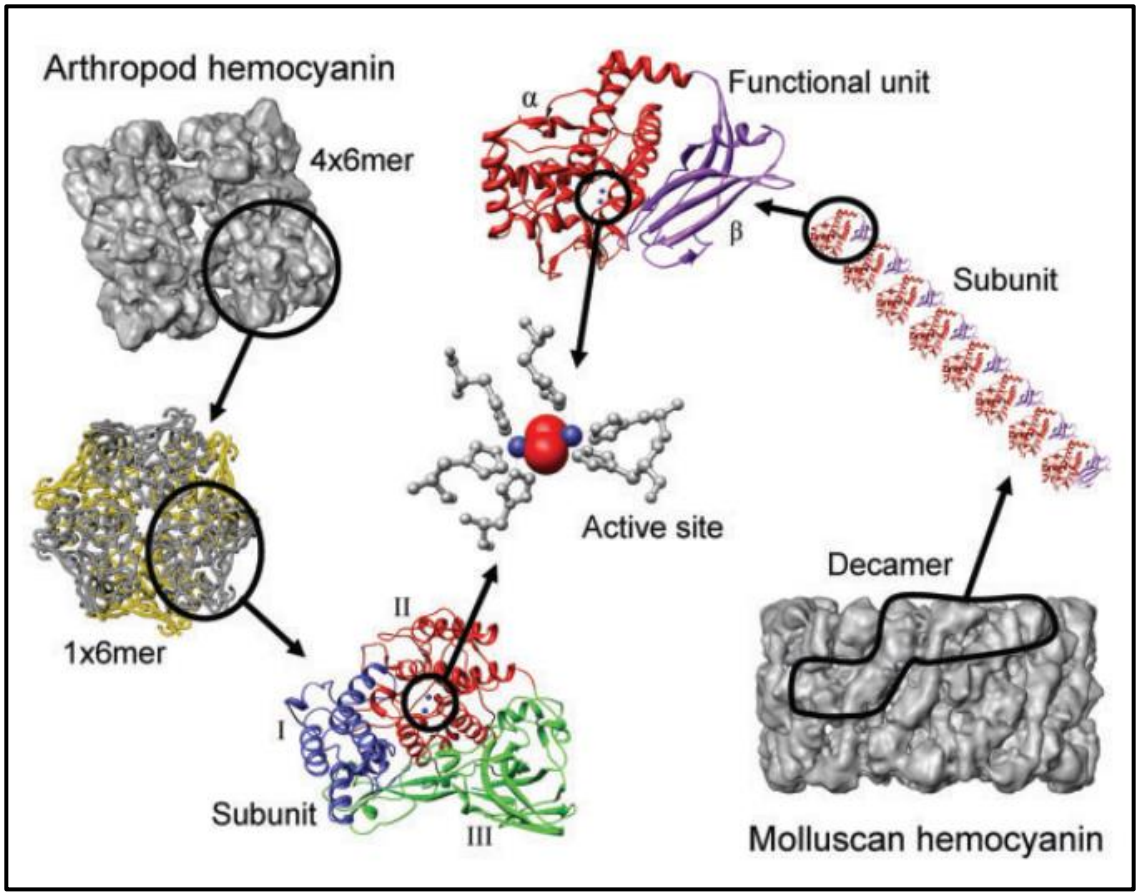

Figure 1.4: Structural representations of arthropod and molluscan haemocyanins. Figure taken from Decker (2007).

The assembled ring-like decamer consists of a wall of 60 globular functional units and a collar complex with the remaining 20 functional units. The first six functional units (FU-a–f) of a single subunit are generally considered to form the cylinder wall, while the rest form the collar (Markl 2013). The final functional unit (FU-h) contains a cupredoxin-like domain. This decameric molecule, which ends up being 4 MDa in size, has a diameter of 356 nm in its cylinder wall and 18 nm in height (Keller et al. 1999).

Haemocyanins are classified as glycoproteins, indicating that they are able to undergo glycosylation (Keller et al. 1999). The HtH1 protein contains 13 potential N-glycosylation sites, while HtH2 contains 11. It was further determined that the carbohydrate content of molluscan haemocyanins is unusually high (2–9% w/w) and that they also contain unusual monosaccharides (Kostadinova et al. 2013). While it is uncertain

whether all the glycosylation sites present are glycosylated at all times, these sites have been determined to play an important role in how haemocyanin functions within the innate immune response.

Recently, there has been a greater emphasis on haemocyanin function beyond its role in the transportation of oxygen, leading to several studies proposing that it may play a role in the innate immune system of invertebrates (Decker et al. 2007; Hristova et al. 2008; Dang et al. 2011; Beltran 2015; Zhuang et al. 2015). Due to the fact that invertebrates lack an adaptive immune response and therefore are necessitated to adapt the functioning of the proteins available to them, haemocyanin, with its unusually large size, provides a likely candidate for a component of the invertebrate innate immune response.

1.3.4 Role of haemocyanin in the immune response

In addition to its main function as an oxygen transporter, haemocyanins also appear to exhibit protective properties against bacterial, fungal and viral infections (Dolashka & Voelter 2013). Haemocyanins have recently been shown to act as phenoloxidases (POs) and are processed to become active antimicrobial peptides (AMPs). In arthropods, the phenoloxidases and haemocyanins appear to be closely related, while in Mollusca the haemocyanins are more closely related to tyrosinases of other phyla (Cerenius et al. 2008). Phylogenetic analysis of haemocyanin, phenoloxidase and other members of this gene family is consistent with both their phenoloxidase and oxygen-binding properties.

1.3.4.1 Haemocyanin as a phenoloxidase

Under certain conditions, haemocyanin has been shown to act as a phenoloxidase and therefore it is likely to participate in the immune response (Terwilliger 2007). It is possible that some haemocyanin proteins have their function transformed from oxygen transport to phenoloxidase activity only in response to major bacterial invasion. The melanisation pathway, under the control of phenoloxidase, has many precursor molecules, and therefore, has multiple stages that can be assayed for activity. Molecules like 5,6-dihydroxindole (DHI) and 5,6-dihydroxindole-2-carboxyllic acid (DHICA) function as precursors of eumelanin, which is a product of the melanisation pathway (Adachi et al. 2005). Polymers of the haemocyanin subunits isolated from *Marsupenaeus japonicus* haemolymph were capable of converting DHI into a black pigment, which indicates a phenoloxidase-like activity. The arthropod haemocyanin was also inhibited by inclusion of tyrosinase and phenoloxidase inhibitors in the assay. This indicates that the mechanisms employed by tyrosinases and phenoloxidases are similar to that utilised by haemocyanin and that both proteins are important in the conversion of DHI in the haemolymph, a necessary step in the

melanisation pathway (Adachi et al. 2005). Phenylthiourea inhibition of haemocyanin confirmed that copper plays a key role in the reaction.

Diphenoloxidase activity was also investigated in haemocyanin isolated from *Rapana venosa* haemolymph (Hristova et al. 2008). Under normal conditions, haemocyanin transported dioxygen molecules, whereas one of the oxygen molecules was used to facilitate chemical transformations during a severe bacterial infection. Using o-diphenol and L-Dopa as substrates, Hristova et al. (2008) demonstrated that haemocyanin had similar oxidation capabilities to that of phenoloxidases or tyrosinases, but that haemocyanin required proteolytic cleavage of either the N- or C-terminal end to disrupt the protein structure. This cleavage opens a large entrance to the active site, allowing access to phenolic substances. In molluscs, the C-terminal end of the peptide is removed, while in arthropods it is the N-terminal end (Hristova et al. 2008).

1.3.4.2 Haemocyanin as an antiviral

Haemocyanin has been shown to have antiviral capabilities. Using a two-dimensional gel electrophoresis (2-DGE) proteomic analysis, Dolashka et al. (2013) showed that, in response to viral arthropod infections, several haemocyte proteins, including haemocyanin, increased post-infection. As haemocyanin is a glycoprotein, it was hypothesised that the carbohydrate chains were interacting with surface-exposed amino acids or other carbohydrate residues on the virus through Van der Waals interactions. It was also discovered that molluscan haemocyanin functional units with specific glycosylation patterns possessed antiviral activity (Dolashka & Voelter 2013; Kostadinova et al. 2013).

Haemocyanin-derived peptides isolated from shrimp possessed properties of a non-specific antiviral nature that affected a range of cultured DNA and RNA fish viruses, while maintaining no cytotoxicity towards the host. The peptides were able to neutralise viruses and prevent viral replication (Zhang et al. 2004). Abalone haemocyanin was also shown to have a unique mechanism of antiviral protection against Herpes simplex virus 1 (HSV 1) infections (Zanjani et al. 2016). Through the use of *in vitro* assays, Zanjani (2016) was able to demonstrate that the purified haemocyanin from *H. rubra* had a dose-dependent, inhibitory effect against HSV-1 infection. The protein specifically inhibited attachment and entry by binding to the viral surface through the glycoproteins gD, gB and gC present on HSV-1, most likely by mimicking their receptors. Post entry, however, haemocyanin had no effect.

1.3.4.3 Haemocyanin as an antifungal

Haemocyanin has been observed to function as a precursor of antimicrobial and antifungal peptides (Coates & Nairn 2014). In response to fungal infections, the shrimp *Penaeus vannamei* and *Penaeus stylirostris* were found to have a higher concentration of the C-terminal end of haemocyanin (Destoumieux-Garzón et al. 2001), suggesting that this multifunctional polypeptide may play a role in protection against fungal infection. However, the mechanism of how this might be achieved has not yet been determined.

1.3.4.4 Haemocyanin as an antimicrobial peptide

Several haemocyanin-derived antimicrobial peptides have been discovered to date. The AMP Asticidin 1, a 16-amino-acid peptide isolated from the haemolymph of the crayfish *Pacifastacus leniusculus,* was found to have high bactericidal activity (Lee et al. 2003a). Lee (2003a) concluded that the peptide was derived from the C-terminal end of the crayfish haemocyanin and adopted a β-sheet conformation. The concentration of this peptide within the haemolymph increased greatly in response to microbial ligands. The release of astacidin 1 suggests the involvement of a lysosomal-derived, cysteine-rich protease that acts to cleave the AMP from crayfish haemocyanin. A further haemocyanin-derived AMP was isolated from haemolymph of the spider *Acanthoscurria rondoniae*. Termed rondonin, this peptide shared a high sequence homology to the C-terminus of several spider haemocyanin subunits (Riciluca et al. 2012). Additionally, two recombinant AMPs were designed to mimic the shrimp C-terminus of haemocyanin. Both of these peptides showed broad antifungal and antibacterial properties (Qiu et al. 2014).

1.3.5 Haliotisin

While the multifunctionality of haemocyanin as an AMP has been researched quite extensively in arthropods, few studies have been undertaken in molluscs, specifically abalone. One example of *Haliotis*-specific research was conducted by Zhuang et al. (2015), who identified a candidate antimicrobial peptide derived from the *H. tuberculata* haemocyanin sequence. This putative AMP region, which was termed haliotisin, is located in the linker region between the α-helical and β-sheet domains of the haemocyanin FU-e (Zhuang et al. 2015). Comparing this region to the Antimicrobial Peptide Database (Wang et al. 2009), the authors of the study determined that haliotisin could have antimicrobial properties. The haliotisin region was found to have high sequence similarity to the same region in haemocyanins from several *Haliotis* species. Zhuang et al. (2015) designed eight overlapping synthetic peptides that spanned the haliotisin region (Figure 1.5) and incubated each peptide with bacteria to determine whether haliotisin

exhibited antimicrobial activity. Growth of the Gram-positive bacterium *Bacillus subtilis* and the Gram-negative bacterium *Erwinia carotovora* was significantly inhibited depending on the synthetic peptide used in the assay.

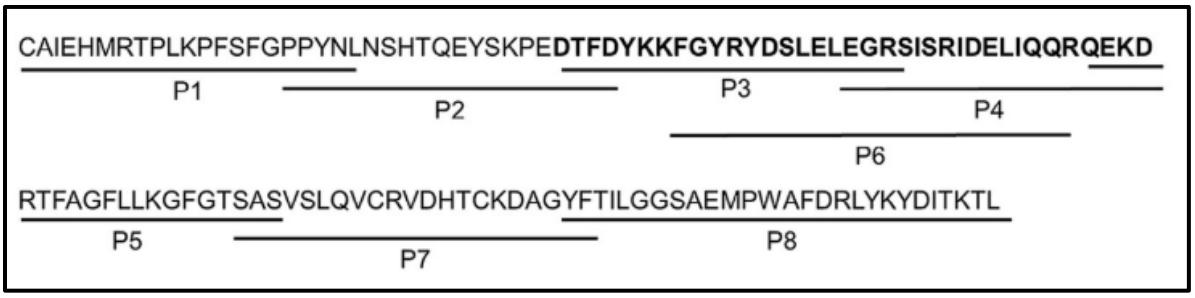

Figure 1.5: Full amino acid sequence of haliotisin from *H. tuberculata*, showing the location of each of the overlapping synthetic peptides tested by Zhuang et al. (2015). The bold region is the section found to be the most biologically active. Figure adapted from Zhuang et al. (2015).

Peptide 3 (P3) exhibited the strongest anti-proliferation activity when incubated with *B. subtilis*. The minimum inhibitory concentration (MIC) for this interaction was calculated to be between 0.3 and 1 µM. Peptide 6 (P6) also showed activity against *B. subtilis* but was only half as effective as P3, which was attributed to P6's lack of the N-terminal amino acids present in P3 (Figure 1.5) and indicated that the N-terminal portion of P3 may interact with an epitope that is present on the membrane of *B. subtilis*. Peptides 1, 2, 4, 5 and 6 (P1, P2, P4, P5 and P6) all exhibited antimicrobial activity towards *E. carotovora*. P6 was the only synthetic peptide able to inhibit the growth of both Gram-positive and -negative bacteria. It was suspected that this was due to the inclusion of both P3 and P4 as shown in Figure 1.5 (Zhuang et al. 2015).

Transmission electron microscopy (TEM) of *E. carotovora* incubated with P4 and *B. subtilis* incubated with P3 showed morphological abnormalities, including fragmentation of the pilli, a reduced number of flagella and the appearance of blisters on the surface of the bacterium. *E. carotovora* incubated with the P4 synthetic peptide also showed damage and irregularities in the cell wall when compared to cells incubated without the peptide (Zhuang et al. 2015).

The bold section in Figure 1.5 highlights one continuous peptide identified by Zhuang et al. (2015). This continuous peptide, which includes P3-P4-P5, seemed to exhibit the strongest antimicrobial activity. As a peptide, it has 29% hydrophobicity and is 6.75 kDa in size, indicating its potential as an AMP as it is small in size and consists of a high percentage of hydrophobic residues. While P3 and P4 both traverse the internal wall of the haemocyanin cylinder, a portion of the haliotisin peptide is located at the external

portion of the protein, allowing proteases access to potential cleavage sites that immediately follow P3-P4-P5, and thus provide a possible method of peptide release from the greater haemocyanin protein. Serine proteases such as trypsin, chymotrypsin and proteinase K were identified as potential effectors (Zhuang et al. 2015). This study was the first to show that molluscan haemocyanin may act as a source of anti-infection peptides.

1.4 Objectives of this study

Haliotis midae cultivation is a valuable sector of the South African aquaculture industry, as attested to by South Africa's status as the largest producer of commercial abalone outside of Asia (Troell et al. 2006). However, the industry suffers from significant financial losses as a result of regular outbreaks of pathogens and disease. Detection, prediction and management of such outbreaks requires a better understanding of how the abalone innate immune response operates. A large body of work has already been dedicated to characterising and decoding the innate immune response of other marine organisms and growing evidence suggests a high level of species-specific regulatory mechanisms, even within the same order (Hooper et al. 2007; Ghosh et al. 2011). The bulk of knowledge surrounding the abalone immune response has been generated from genomic (Wang et al. 2013; Travers et al. 2010), transcriptomic (De Zoysa et al. 2011a; De Zoysa et al. 2011b) and a few proteomic studies (Slattery et al. 2012; Beltran 2015).

Recently, through a proteomics-based study, it was found that haemocyanin, the oxygen transporter present in the haemolymph of *H. midae*, was upregulated in response to bacterial infection (Beltran 2015), suggesting that it could play a role in the abalone's innate immune response. The haemocyanin protein, integral to the transportation of oxygen throughout the abalone, has been reported to play a part in both the cellular and humoral response of the invertebrate innate immune response. Some mechanisms described in section 1.3.4 are: functioning as a phenoloxidase in the melanisation pathway (Adachi et al. 2005; Hristova et al. 2008; Coates & Nairn 2014); acting as an antiviral agent after glycosylation (Zhang et al. 2004; Zanjani et al. 2016); acting as an antifungal agent (Coates & Nairn 2014; Destoumieux-Garzón et al. 2001); and, most importantly for this study, acting as an antimicrobial peptide (Lee et al. 2003a; Riciluca et al. 2012; Qiu et al. 2014). These studies, largely investigating non-*Haliotis* invertebrates, imply that haemocyanin is a worthy candidate for further study regarding its possible role in the *H. midae* immune system. Further confirmation that haemocyanin can function as an AMP was reported by Zhuang et al. (2015) who identified the haliotisin peptide in *H. tuberculata* and demonstrated its antimicrobial activity against both Gram-positive and -negative bacteria.

This study aims to investigate a possible antimicrobial peptide derived from *H. midae* haemocyanin, and to this end, has three primary objectives. The first is to determine the sequence of *H. midae* haemocyanin in order to examine the structure of the protein and compare its similarity to other haemocyanin sequences and antimicrobial peptide sequences in order to locate a region that is similar to known antimicrobial peptides (the most likely candidate being the haliotisin peptide found by Zhuang et al. (2015)) for further investigation. The second objective of the study is to express the *H. midae* antimicrobial peptide using an *Escherichia coli* expression system to obtain sufficient quantities of the protein that would allow investigation of its potential antimicrobial activity. Thus, the final objective is to test the expressed *H. midae* haemocyanin peptide for antimicrobial activity. These objectives would provide information regarding the possible role of haemocyanin in the *H. midae* immune response.

2. Methods

2.1.1 Abalone storage conditions

H. midae used in this study were stored at the Department of Agriculture, Forestry and Fisheries Research Aquarium in Sea Point, Cape Town, South Africa. Abalone were kept in meshed baskets suspended in polyethylene tanks. Baskets were kept at a stocking density of roughly 30 abalone per basket. The tanks were maintained in the dark with circulating filtered seawater taken from the nearby ocean, and constant aeration. Abalone were fed a diet of *Ecklonia maxima* fronds twice weekly for the duration of the project, and the tanks were thoroughly cleaned at least once a week.

2.1.2 Haemolymph extraction and haemocyte counting

Haemolymph was extracted from abalone with a shell length of 10 cm or greater. Using a sterile 21-gauge needle and 1 ml syringe, haemolymph was extracted from the pedal sinus of an individual abalone. A 10 µl aliquot was added to nine parts anticoagulant Alsever's solution for haemocyte counting (0.1 M glucose ($C_6H_{12}O_6$), 0.3 M trisodium citrate ($C_6H_5Na_3O_7.2H_2O$), 0.5 M EDTA, 2.2% (w/v) sodium chloride (NaCl), 4.4% (w/v) formaldehyde (HCHO), pH7.5). Cell titre was determine using a haemocytometer and the relevant number of haemocyte cells were pelleted via centrifugation as needed for RNA or DNA extraction (described in 2.1.3 and 2.1.4).

2.1.3 RNA extraction and cDNA synthesis

RNA was extracted from between 3 and 4 million haemocyte cells using the RNeasy Mini Kit (QIAGEN) as per the manufacturer's instructions, with the following minor modifications: cells were pelleted by centrifugation at 300 x g for 5 minutes and the supernatant removed and discarded; to ensure thorough cell lysis, the haemocyte suspension was vortexed for 30 minutes at 4°C, and subsequent centrifugation steps were conducted at 10 500 x g; an additional wash step with the provided buffer was added and an additional centrifugation step was included to elute residual ethanol; finally, the RNA was eluted from the column using 35 µl of RNase-free distilled water. The concentration of RNA was determined using a NanoDrop ND-100 spectrophotometer (NanoDrop Technologies, Inc.), and a 500 ng sample was run on a MOPS/formaldehyde agarose gel to check the integrity of the RNA. The QuantiNova™ Reverse Transcription Kit (QIAGEN) was used for cDNA synthesis from 500 ng of haemocyte RNA according to the manufacturer's instructions, and haemocyte cDNA was either stored on ice and used immediately for PCR amplification or stored frozen at -80°C for not longer than a week.

2.1.4 Genomic DNA (gDNA) extraction

DNA extraction was performed using a DNeasy® Blood and Tissue kit (QIAGEN) as per the manufacturer's protocol. Between 5 and 6 million haemocyte cells were pelleted by centrifugation at 300 x g for 5 minutes and then resuspended in 200 µl of phosphate-buffered saline (PBS) supplemented with 20 µl of the provided proteinase K. From here, no alterations were made to the protocol and all solutions used were obtained with the kit. The concentration of DNA was determined using a NanoDrop ND-100 spectrophotometer (NanoDrop Technologies, Inc). Genomic DNA was stored at -80°C until needed for PCR amplifications.

2.2 PCR amplification and nucleotide sequence analysis

Polymerase chain reaction (PCR) was used to amplify fragments of the haemocyanin gene from either haemocyte gDNA or cDNA, prepared as described in sections 2.1.3 and 2.1.4. The purpose of the PCR was to obtain fragments that could either be used as sequencing templates or for subcloning into the pProEX expression vector as described in section 2.3.

2.2.1 Primer design

Due to the unusually large size of the haemocyanin gene, a technique known as primer walking was employed to design the sequencing primers required for this study. The polymerase used was GoTaq® DNA polymerase (Promega) and, due to its efficacy, the amplicon size was limited to a max of 1 kbp. Figure 2.1 illustrates the primer-walking strategy, while the primers used in the study are shown in Table 2.1.

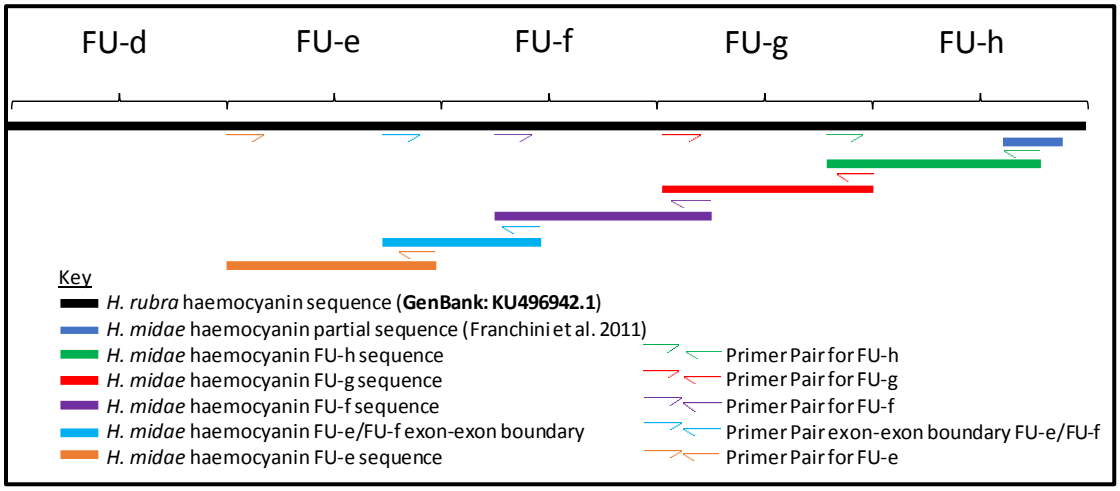

Figure 2.1: Diagram illustrating the primer walking strategy used for amplification and sequencing the functional units e, f, g and h of the *H. midae* haemocyanin. Solid bars represent sequence data, arrows represent regions of primer binding and the template sequence to which the primers were designed.

To start, annotated sequencing data was obtained from a study conducted at Stellenbosch University on *Haliotis midae* (Franchini et al. 2011). This contained a partial sequence for haemocyanin which served as the initial point for primer design. Using this sequence, a BLASTn search was performed to determine which fully sequenced *Haliotis* haemocyanin showed the highest similarity to that obtained for *H. midae*. *Haliotis rubra,* the Australian blacklip abalone, was found to have the highest sequence similarity to the partial segment of *H. midae* haemocyanin. Primers were designed using CLC (Main Workbench) v7.7 (QIAGEN). For the initial PCR product, the reverse primer was designed against the *H. midae* sequence, and its complimentary forward primer was designed against the *H. rubra* haemocyanin sequence. These primers produced the first PCR product (green) in Figure 2.1. Once this had been amplified and sequenced (section 2.2.2), the sequencing data was used for designing the next primer pair. The reverse primer was designed using the *H. midae* sequence data, and the corresponding forward primer was designed using the *H. rubra* haemocyanin sequence. These primers produced the second PCR product (red) (Figure 2.1). This method was repeated a further three times to obtain and sequence the third (purple), fourth (blue) and fifth (orange) PCR products shown in Figure 2.1. All possible primer pairs were analysed using Primer BLAST (Altschul et al. 1990) and PerlPrimer (v1.1.21; Marshall 2004) to ensure that no secondary structures would be generated and that there was no cross- and self-complementarity. In this manner, primer pairs were designed to sequence the final four functional units (FU- e-h) of the *H. midae* haemocyanin.

Table 2.1: PCR primers used to determine the nucleotide sequence of the carboxyl end of the *H. midae* haemocyanin gene.

Name of primer	Sequence
H. midae FU-h Fwd	TTGACTTCCTCTCCCTGC
H. midae FU-h Rev	CATTTCCTTCTCACCTCCCA
H. midae FU-g Fwd	CCCCCTTTACTGTTGTCATTCT
H. midae FU-g Rev	ACTACTGCCTTTACCCATCT
H. midae FU-f Fwd	TCTTTGCTGGTTTCCTGTTGT
H. midae FU-f Rev	GGCTGTGAAGTCGAGAGT
H. midae FU-e/FU-f intron Fwd	CCAGCAAAGACTCTAGCA
H. midae FU-e/FU-f intron Rev	TCTCCACGATATGCACCT
H. midae FU-e Fwd	TTGAGTCCTAGGGAGAGGGT
H. midae FU-e Rev	AGGTGCATATCGTGGAGAGT

2.2.2 PCR amplification and DNA sequencing

The template selected for each PCR amplification was dependent on whether the amplicon was expected to contain an intron or not. Although genomic DNA was preferentially used as the template whenever possible, cDNA was employed in the majority of cases due to the presence of either internal introns or because the product spanned a linker intron between two functional units.

After amplification, the PCR product was confirmed by electrophoresis through a 1.5% (w/v) agarose gel in TAE buffer (40 mM Tris, 20 mM acetic acid, 1 mM EDTA) at a pH of 8.3. The amplified product was purified using the Wizard® SV Gel and PCR Clean-Up Kit (PROMEGA) according to the manufacturer's instructions and sent for sequencing (Macrogen Europe). Sequence data was analysed on CLC Main Workbench v7.7 (QIAGEN), trimmed, and the forward and reverse sequencing data aligned to one another. The sequence was searched against the NCBI database using the BLASTn search algorithm to confirm the identity of the gene.

2.2.3 Comparison of haemocyanin sequence to antimicrobial peptides

After sequencing the C-terminal half of the haemocyanin gene, focus shifted to analysing the region for homology to other *Haliotis* haemocyanin sequences and to determining whether a putative antimicrobial peptide could be identified within the sequenced functional units. The collected sequences were split into their respective functional units and each functional unit was then searched against the antimicrobial peptide database (Wang et al. 2009) (http://aps.unmc.edu/AP/main.php). The APD3: Antimicrobial Peptide Calculator and Predictor function was used to determine whether or which of the functional units that had been sequenced included a potential antimicrobial peptide. The returned region was then analysed for factors that affect antimicrobial peptide functioning, such as the presence of small, amphipathic molecules with a high proportion of hydrophobic residues (Papagianni 2003) and a secondary structure that usually follows either an alpha-helical shape or a β-sheet (Dhople et al. 2006).

Once determined to be a potential antimicrobial peptide, the 3D structure of the amino acid sequence was predicted using the PHYRE2 engine (Kelley et al. 2015) and the output visualized and annotated using Chimera (Pettersen et al. 2004). The amphipathic nature of the molecule was examined using NetWheels (Mól et al. 2018), an online platform that assigns polarity to amino acid residues to visualize the α-helix in a way that shows the presence of polar and non-polar fronts.

2.3 Cloning into the vector pProEX and recombinant expression

An *H. midae* haemocyanin gene fragment, predicted to code for a putative antimicrobial peptide, was PCR amplified from genomic DNA and cloned into the expression vector pProEX (Figure 2.2). pProEX was chosen as it adds a polyhistidine-tag to the N-terminal end of the peptide for purification purposes, along with the trc promoter, which allows inducible control over the expression of the recombinant product.

2.3.1 Cloning of a putative antimicrobial peptide gene into the pProEX expression vector

PCR primers were designed to amplify the region of the *H. midae* haemocyanin gene that potentially coded for a putative antimicrobial peptide. These primers included restriction sites required for subcloning: *Nco*I on the forward primer and *Not*I on the reverse primer. The forward primer was designated *H. midae* haliotisin cloning Fwd (GCGCCCATGGAGCCTGAGGACACTTTTG) and the reverse primer *H. midae* haliotisin cloning Rev (CATAGCGGCCGCCACAGTTGCGGAAGTACC) (Table2.2). The PCR products were digested with *Nco*I-HF® (Bio-Labs) and *Not*I-HF® (Bio-Labs) for insertion into pProEX (Figure 2.2) to allow for transcription from the trc promoter. The produced mRNA could then be translated to form the recombinant haliotisin peptide with the 6-his tag included on the N-terminal end.

Table 2.2: PCR primers used for cloning and sequencing of Haliotisin into pProEX

Name of cloning PCR primer	**Sequence of primer**
H. midae haliotisin cloning Fwd (*NcoI*)	GCGCCCATGGAGCCTGAGGACACTTTTG
H. midae haliotisin cloning Rev (*NotI*)	CATAGCGGCCGCCACAGTTGCGGAAGTACC
pProEX sequencing Fwd (M13Rev)	GAGCGGATAACAATTTCACACAGG
pProEX sequencing Rev (pTrcHisRev)	GATTTAATCTGTATCAGG

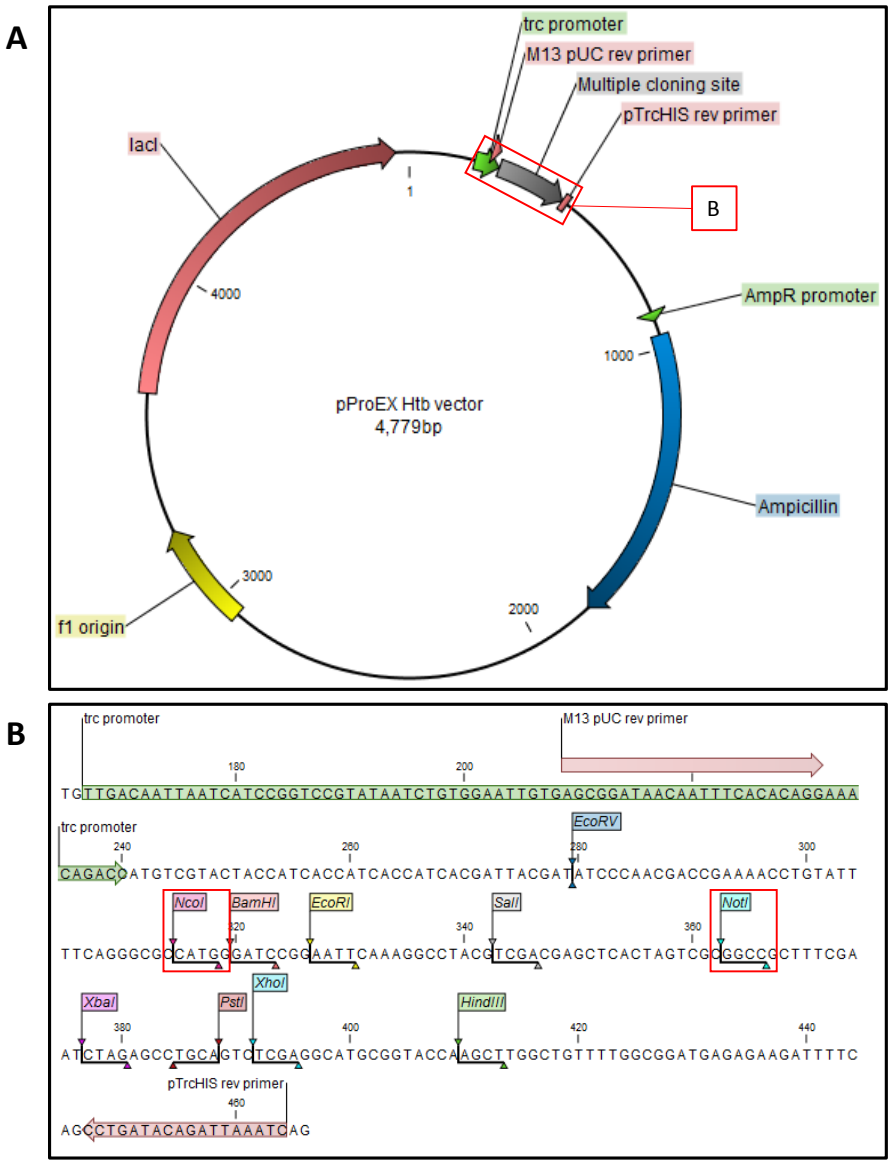

Figure 2.2: **A.** The nucleotide sequence of the vector pProEX HTb was obtained from Addgenes (https://www.addgene.org/browse/sequence_vdb/3835/) and annotated in CLC Main Workbench v7.7 (QIAGEN). Highlighted regions of interest include the f1 origin (yellow), the origin of replication of the vector; *lac*I gene (red), the lactose inducer gene; ampicillin (blue), the ampicillin resistance gene and its promoter (green); the multiple cloning site for fragment insertion (grey; expanded in **B**); the trc promoter (green), the promoter associated with the multiple cloning site; the two PCR primer binding sites (pink) for the sequencing primers M13 pUC rev primer and pTrcHIS rev primer.

B. Expanded region of the multiple cloning site showing the restriction enzyme recognition sites. The two enzymes used in this study, *Nco*I (340) and *Not*I (388), are highlighted in the red boxes.

PCR amplification was conducted using GoTaq® DNA polymerase (Promega) and genomic DNA as the template. The reaction cycles were 95°C for 5 minutes, 35 cycles of 95°C for 1 minute, 68°C for 1 minute (annealing temperature), 72°C for 1 minute for elongation and a final step at 72°C for 7 minutes to ensure thorough elongation.

The pProEX HTb vector was isolated from *E. coli* JM109 cells using a QIAprep Spin Miniprep Kit (Qiagen) as per the manufacturer's instructions and was quantified using a NanoDrop ND-100 spectrophotometer (NanoDrop Technologies, Inc.). The plasmid vector and PCR product were digested with *Nco*I and *Not*I overnight in a 37°C water bath. The vector was then electrophoresed through an ethidium bromide-stained agarose gel and visualised under low-wavelength UV in order to excise the appropriate DNA restriction fragment. The linear vector was cleaned using the Wizard® SV Gel and PCR Clean-Up Kit (Promega) as per the manufacturer's instructions. The ligation reaction was performed at room temperature overnight with a 1:5 molar ratio of vector to insert DNA using T4 DNA ligase (Bio-Labs). The recombinant vector was then transformed into *E. coli* JM109 cells, made competent according to the protocol presented in Dagert & Ehrlich (1979). The cells were transformed using the heat-shock method presented in Seidman et al. (1997).

The transformed cells were plated onto Luria agar (LA) supplemented with the selective antibiotic ampicillin (0.1 mg/ml final concentration). Appropriate controls were also performed to check the natural resistance of the strain, the transformation efficiency of an empty vector and the restriction digest of the vector. The positive colonies were screened for insert DNA using colony PCR with the primers used for subcloning and the primers that flank the DNA fragment inserted in the vector (sequencing primers). Colonies that showed the presence of insert DNA were incubated in Luria broth (LB) overnight and plasmids were extracted using the QIAprep Spin Miniprep Kit (QIAGEN) as per the manufacturer's protocol. The isolated plasmids were sent for sequencing at Macrogen Europe to ensure that the insert had not incurred any mutations as a consequence of PCR amplification, restriction digest, ligation and transformation. The sequences were analysed using CLC Main Workbench and compared to an *in silico* clone of the same region. The sequences were also searched against the NCBI database using BLASTn to ensure that the region contained similarities to the *H. midae* haemocyanin gene.

2.3.2 Recombinant protein production

Recombinant pProEX plasmids with the haliotisin insertion confirmed via DNA sequencing were transformed into chemically competent *E. coli* BL21 as described in section 2.3.1. Transformed cells were cultured on LA supplemented with ampicillin (final concentration 0.1 mg/ml) to select for the presence of

the vector. Colonies resistant to the antibiotic were analysed for the presence of the recombinant vector using colony PCR. A single colony was resuspended in 10 µl of water and used as the template of a PCR with the cloning primers or a combination of the forward sequencing primer and the reverse cloning primer. The colonies that exhibited the correct amplicon size were inoculated into LB for growth overnight at 30°C with shaking. This culture was stored in 200 µl aliquots supplemented with 25% glycerol (final conc.) at -80°C for later use in recombinant expression.

The three main factors that affect recombinant protein production are inducer concentration, the time from induction to harvesting and the temperature at which induction occurs. Other impactful factors include the optical density of the culture at the time of induction and the components of the media used to grow the cells. The BL21 cells containing the recombinant vector were grown overnight in LB at 30°C with shaking in order to generate a starter culture. The starter culture was used to inoculate 25 ml of LB in an 250 ml Erlenmeyer flask to a final optical density of 0.1 at 600 nm ($OD600_{nm}$ = 0.1). The 25 ml culture was grown to mid-log phase at 37°C with shaking (approximately 2 hours; $OD600_{nm}$ = 0.6). In order to induce the trc hybrid promoter present on the pProEX vector, a final concentration of 2 mM of isopropyl β-D-1-thiogalactopyranoside (IPTG) was added to the culture. The culture was induced for 4 hours at 37°C with shaking, and the cells harvested by centrifugation at 6 000 x g for 20 minutes and stored at -20°C until required for protein extraction.

2.3.3 Protein extraction

The cell pellet (section 2.3.2) was resuspended in a native buffer solution (100 mM Tris·Cl, 10 mM sodium chloride). The cell suspension was sonicated at an amplitude of between 6 and 10 µm for 30 second intervals and 15 second pauses for a total of 5 minutes. The cell suspension was kept cold in a methanol ice bath during sonication. Following initial lysis, the suspension was centrifuged at 20 000 x g for 15 minutes and the supernatant saved as the soluble protein fraction. The pellet was then resuspended in native buffer supplemented with 8 M urea and a pH adjusted to 8.0 (denaturing buffer). The suspension was sonicated and centrifuged as before, and the supernatant saved as the insoluble protein fraction. Both supernatants were analysed on a SDS-PAGE to determine whether the expected 11 kDa putative antimicrobial peptide was included in the insoluble or soluble protein fraction. The protein sizes were determined by comparison to a PageRuler™ Prestained Protein Ladder (Thermo Fisher Scientific). The identity of the protein bands was confirmed as being the his-tagged peptide by performing a western blot, using two different primary antibody probes, as described in section 2.3.5.

2.3.4 SDS-PAGE

SDS-PAGE gels were made up according to the protocol in the appendix (5.1.1). For all protein separation the samples were run on a 15% resolving and a 4% stacking SDS-PAGE. Before loading onto the gel, samples were mixed with a 5 X sample application buffer (1 M Tris-HCl pH 6.8, 50% glycerol, 25% SDS, 10 mg/ml bromophenol blue, 21% w/v dithiothreitol (DTT)) and boiled for 10 minutes. SDS-PAGE gel electrophoresis was performed at room temperature at 100V for 2 hour or until the dye front reached the end of the gel. Once complete, the gel was either stained to visualise the total proteins or the separated proteins bands were transferred to a nitrocellulose membrane for western blot analysis to detect the presence of the recombinant haemocyanin protein.

Staining was performed overnight at room temperature with shaking, using Coomassie stain (0.5 g Coomassie blue G-250, 225 ml methanol, 50 ml acetic acid and 225 ml dH_2O) and then destained using a destain solution (300 ml methanol, 100 ml acetic acid, 600 ml dH_2O) before being visualised on a Molecular Imager® ChemiDoc ™ XRS+ (Bio-Rad) and analysed using Image Lab V5.2.1 (Bio-Lab).

2.3.5 Western blot analysis

To confirm that the band detected via SDS-PAGE was the expected peptide, western blot analysis was performed on two separate membranes, one probed with an anti-HIS antibody (Sigma SAB4301134) and the other with an anti-KLH antibody (Agrisera AS99 001). Proteins separated by SDS-PAGE were transferred to the nitrocellulose membrane at 10V for 1 hour using a Trans-Blot® SD Semi Dry Transfer Cell (Bio-Rad), and the presence of total protein was confirmed using a Ponceau S (Merck) staining protocol. The stain was prepared by dissolving 0.1% (w/v) Ponceau S in 1% (v/v) acetic acid. Once the proteins had been transferred, and prior to blocking, the membrane was immersed in the stain for 5 minutes with shaking. After visualisation, the stain was removed via two rounds of washes with water for 5 minutes each.

Following staining, the membrane was blocked overnight using a 2% bovine serum albumin (BSA) phosphate-buffered saline (PBS) solution (137 mM NaCl, 10 mM phosphate, 2.7 mM KCl, pH 7.4). The membrane was then washed three times using a 2% Tween PBS (PBST) solution for 15 minutes per wash and a final wash of 1 x PBS. The primary anti-HIS antibody was diluted 1:2 000 and the primary anti-KLH antibody was diluted 1:10 000 in 2% BSA PBST. Each membrane was submerged in primary antibody suspension and incubated at 37°C with shaking for one hour. The primary was washed away with three sets of 15-minute washes with PBST and one 15-minute wash with PBS. The secondary antibody, Anti-

Rabbit IgG (whole molecule)–Peroxidase produced in goat (Sigma A6154), was diluted 1:5 000 in 2% BSA PBST and added to the membrane. The membrane was submerged in the secondary antibody solution and incubated for one hour at 37°C with shaking, following which the same set of washes as above were conducted. Finally, 2 ml of horseradish peroxidase substrate, TMB membrane peroxidase substrate (KPL), was added to each membrane and allowed to develop in the dark for 30 minutes. The membrane was then photographed using a Molecular Imager® ChemiDoc™ XRS+ (Bio-Rad) and analysed using Image Lab V5.2.1 (Bio-Rad).

2.4 Purification of the his-tagged putative AMP

After the presence of the correct peptide was confirmed using SDS-PAGE and western blot analysis it was necessary to purify the haemocyanin from the bacterial host proteins. This was done using the polyhistidine-tag presented by the pProEX vector and nickel affinity chromatography. Two methods were employed, batch purification and fast protein liquid chromatography (FPLC).

2.4.1 Batch purification of the his-tagged putative AMP

For the batch purification The QIAexpressionist™ handbook (5th edition)(Qiagen 2003) was used as a guide. Protocol 17: Batch purification of polyhistidine-tagged proteins from *E. coli* under denaturing conditions (Qiagen 2003) was followed with some minor alterations. In summary, 1 ml of HisPur™ Ni-NTA Resin (Thermo Fischer Scientific) was combined with 10 ml of the lysate and made up to a final volume of 15 ml using native buffer supplemented with 8 M urea. The suspension was incubated for one hour, according to the batch protocol, at room temperature on a rotisserie contained in a hybridization oven/shaker (Amersham Life Science) which was set at 10 revolutions per minute. The lysate was then carefully loaded into an empty Poly-Prep® Chromatography Colum (Bio-Rad). The bottom cap was removed and the flow-through collected. The column was then washed with three sets of 10 column volumes (CV) of denaturing buffer at pH 8, pH 7.4 and pH 6.7 respectively, collecting each of the fractions in 1.5 ml aliquots. Finally, the sample was eluted using the denaturing buffer supplemented with a final concentration of 250 mM imidazole.

All the fractions were analysed on a NanoDrop at an absorbance of 280 nm to determine relative protein concentrations. This information was used to generate an elution profile and determine which of the fractions contained proteins. All fractions containing proteins were analysed by SDS-PAGE in order to determine whether they contained the expected 11 kDa peptide in a purified form.

2.4.2 Dialysis to remove urea from the buffer containing the putative AMP

Dialysis was attempted in order to remove the urea from the buffer in which the purified peptide was suspended. A D-Tube™ Dialyzer Maxi (Merck), MWCO 6-8 kDa, was used for this purpose with the manufacturer's protocol acting as a guide. A two-step dialysis was performed: initially using the native buffer supplemented with 3 M urea as the dialysate; and then using the native buffer alone as the dialysate. One litre of dialysate was used to dialyse 700 µl of the sample. Each step was conducted over a 24-hour period with a single change of dialysate after 12 hours. The pH of the dialysate was altered with each change of buffer to reduce the overall pH from 8.0 to a more physiologically relevant 7.2 for downstream analysis. This was achieved by altering each solution to have a pH 0.2 lower than the solution it replaced. The resultant peptide was tested for activity in a radial diffusion assay (section 2.4.4), and the folding was examined using size exclusion chromatography (SEC). For SEC, the samples were filtered through a 0.2 µm filter and loaded onto a S75 16/600 column, the principle being that if the peptides within the sample all had the same configuration due to identical folding, the sample should elute in a single peak during the SEC.

2.4.3 FPLC on-column folding and purification of the His-tagged peptide

Using the method described by Oganesyan et al. (2005) as a guide, on-column refolding and purification of the *H. midae* putative antimicrobial peptide was attempted by changing the buffers during Fast Protein Liquid Chromatography (FPLC). After equilibration of the nickel-affinity column with the denaturing buffer (native buffer containing 8 M urea), the protein sample was loaded onto the column. The flow-through was collected and the column washed with 10 CV of 8 M urea, 20 mM Tris·Cl, 0.1 M NaCl at a pH of 8.0, following which 10 CV of the same solution at a pH of 6.7 was used to remove any non-specific binders. Five CV of the original denaturing buffer was then used to return the column to the original pH of 8.0.

The next stage focussed on refolding the protein. All renaturation steps were carried out in Buffer A (20 mM Tris·Cl, 0.1 M NaCl, pH 8.0), with various additions dependent on the purpose of the buffer. The column was washed with 10 CV of 20 mM Tris·Cl, pH 8.0 containing 0.1% Triton X-100 and 500 mM NaCl. Instead of performing this as a sudden buffer change, the addition of the Triton containing buffer was carried out using a gradient over 5 CV. The detergent was added to wash out the urea while maintaining the peptide in its denatured state. Subsequently, 10 CV of Buffer A containing 5 mM of β-cyclodextrin was added to remove the detergent and assist with folding the peptide bound to the column. An additional wash with just Buffer A was performed to remove excess β-cyclodextrin.

Finally, the bound proteins were eluted using an imidazole gradient from 0 to 300 mM in Buffer A. Each fraction collected over the course of the FPLC protocol was examined by spectrophotometry at 280 nm to detect the presence of proteins. All fractions of interest were analysed by SDS-PAGE to check for the presence of the haemocyanin peptide. To determine the concentration of the peptide, unknown samples were run alongside samples of BSA of known concentration to perform densitometric analysis. Set quantities of BSA were loaded onto an SDS-PAGE, ranging from 0.2 to 2.4 µg per well. After Coomassie staining, the optical density of the protein bands within the gel was measured and given a quantitative value for each sample. This was used to create a standard curve of the BSA sample that related protein quantity to optical density. The optical density of the peptide in the unknown samples was then measured and could be related back to quantity using the standard curve. By controlling the volume loaded onto the gel, protein concentration can also be determined.

2.4.4 Radial diffusion antimicrobial assay

The refolded putative antimicrobial peptide was examined for its ability to inhibit the growth of four bacteria. Two of the four were Gram-positive, *Bacillus subtilis and Staphylococcus aureus*, and two were Gram-negative, *Escherichia coli* and *Vibrio anguillarum*. The *Vibrio* species was the only marine bacterium tested and is the species that abalone encounter in their natural habitat, as well as being the primary cause for bacterial disease in farming conditions. *V. anguillarum* was grown in tryptic soy broth (TSB) (tryptone 17 g/l, peptone 3 g/l, glucose 2.5 g/l, NaCl 5 g/l and K_2HPO_4 2.5 g/l), while the other three bacteria were grown in Luria broth (LB) (tryptone 10 g/l, NaCl 10 g/l and yeast extract 5 g/l). *S. aureus* and *E. coli* were grown at 37°C with shaking, and *V. anguillarum* and *B. subtilis* were cultured at 30°C with shaking for 18 hours. The starter cultures were used to reinoculate fresh media to a final optical density at 600 nm of 0.1 ($OD600_{nm}$ = 0.1) which were subsequently incubated at the appropriate conditions to obtain mid-log phase cultures of each of the bacterial strains.

For the radial diffusion assay, two agar types were used – Luria agar and tryptic soy agar, made by the addition of 1 g of SeaKem® LE Agarose (Lonza) per 100 ml of LB or TSB respectively. To create a lawn of bacteria, 100 µl of mid-log phase (OD600nm = 0.6) culture was added to 7 ml of molten agar, vortexed and plated onto a petri dish. The agar was left to dry in a laminar flow for one hour. Using a modified pipette tip, wells of approximately 7 mm in diameter were made in the agar and 20 µl of either peptide solution or control solution was added to each well. The plates were then incubated overnight at 37°C for *E. coli* and *S. aureus,* or 30°C for *V. anguillarum* and *B. subtilis,* to allow the bacteria to grow. Solutions that inhibited the growth of the bacteria were expected to show a zone of inhibition, demonstrated by a

lack of growth in the bacteria surrounding the well. To better visualise this, the agar was stained using Coomassie stain (section 2.3.4) and then photographed. Control solutions included a negative control (the native buffer used during purification) and two positive controls (the denaturing buffer used during extraction, containing urea, and a solution of ampicillin at a similar concentration to the peptide). The native buffer was included to ensure that any zone of inhibition surrounding the peptide was not due to compounds contained within the buffer. The denaturing buffer was included to ensure that all urea had been removed from the peptide-containing solution. If the zone of inhibition from the denaturing buffer was of a similar sizes to the peptide solution it would imply there is residual urea in the peptide sample. The ampicillin solution was used to confirm that the assay was performed correctly; this solution should show a clear zone of inhibition.

2.4.5 Growth inhibition assay

To quantify the activity of the putative haemocyanin antimicrobial peptide, a growth inhibition assay was conducted. The bacterial species that showed positive results for the radial diffusion assay, indicating the peptide could inhibit their growth, was further analysed. Bacteria were grown to mid-log phase ($OD600_{nm} = 0.6$) and then diluted by performing a two-fold ten step serial dilution series. An aliquot (100 µl) of each dilution was added to the wells of a 96-well TPP® tissue culture plate (Merck). For each bacterial species, the samples were divided in half; one half was treated with 1 µg of the putative antimicrobial peptide (test wells), and the control half was treated with an equal volume of the native buffer (control wells). Each bacterium was tested in duplicate. The 96-well plate was incubated, with shaking, for two hours at the temperature appropriate for the strain being tested (section 2.4.4). The turbidity ($OD600_{nm}$) of the bacterial cultures in each well was then measured with a MultiSkan® Go (Thermo Fischer Scientific) spectrophotometer using SkanIt™ software v4.1 (Thermo Fischer Scientific). The turbidity of cultures were compared to the turbidity of control cultures. The inhibitory effects of 1 µg of putative AMP was indicated when the turbidity of test cultures was lower than the turbidity of the controls. Consequently, a student's T-test was conducted to compare the test and control wells for each stage of the two-fold dilutions.

3. Results

3.1 Sequencing and analysis

The full coding sequence of functional units e, f, g and h of the *H. midae* haemocyanin was determined (Supplementary Figure 5.1). The primer binding sites for the five sets of sequencing primers and the cloning primers are shown in Figure 3.1. The binding sites for the FU-e forward and the FU-h reverse primers were trimmed from the 5' and 3' ends, respectively, during sequence analysis. Figure 3.1 shows the location of each of the functional units as compared to the *H. tuberculata* haemocyanin sequence,

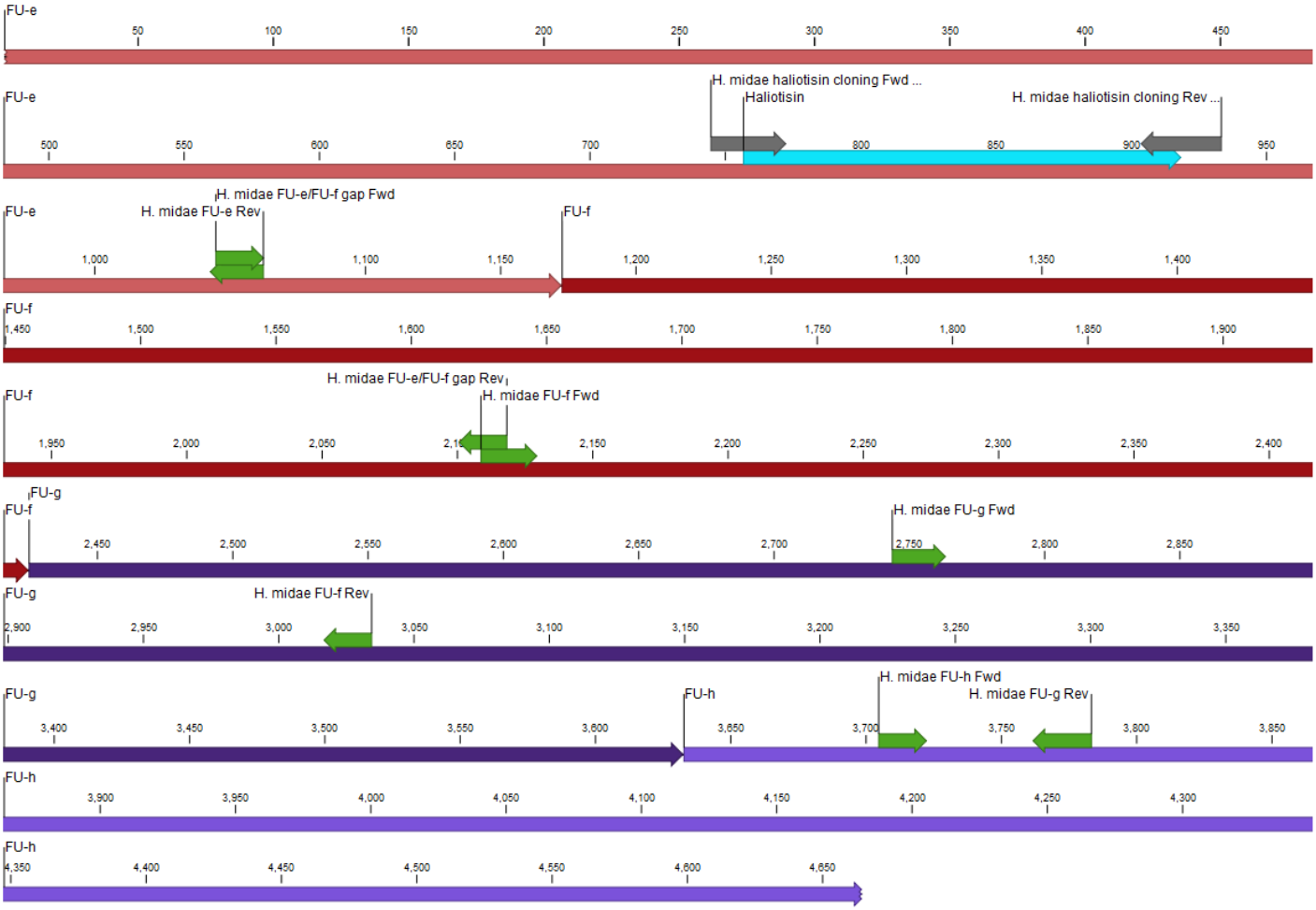

Figure 3.1: Diagram depicting annotated sequence data for *H. midae* haemocyanin 1 functional units a-h. Green arrows, binding regions for sequencing primers; grey arrows, binding regions for primers used for subcloning. Blue arrow indicates the haliotisin peptide region. The four sequenced functional units are: FU-e (light red), FU-f (dark red), FU-g (dark blue) and FU-h (purple). The complete sequence can be found in Supplementary Figure 5.1.

while Figure 3.2 illustrates the locations of the introns and exons in relation to *H. tuberculata* genomic and coding sequences. The region identified as being similar to the haliotisin peptide identified by Zhuang et al. (2015) is located in FU-e (Figure 3.1).

The presence of functional units e, f, g and h in the *H. midae* haemocyanin sequence was confirmed by aligning the *H. midae* sequence to the *H. rubra* coding sequence, the *H. tuberculata* coding sequence and the *H. tuberculata* genomic sequence (Figure 3.2). The *H. midae* haemocyanin sequence aligned between nucleotides 5101 and 9765 of *H. rubra*, indicating that it contained the majority of Fu-e, the entire FU-f and -g and most of FU-h, but excluding the final C-terminal portion.

A BLASTn search of the NCBI database revealed that the *H. midae* sequence was most similar to the

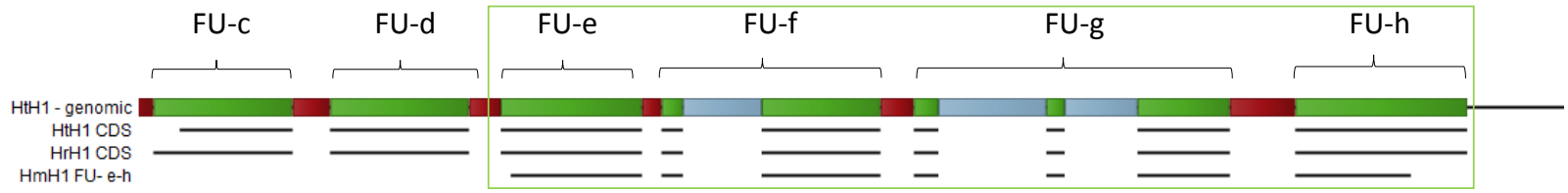

Figure 3.2: Alignment of the *Haliotis tuberculata* haemocyanin 1 sequence (HtH1 – genomic) with the coding sequences of *H. tuberculata* (HtH1 CDS), *H. rubra* (HrH1 CDS) and the *H. midae* HmH1 FU-e–h sequence obtained in this study. Exons located in the genomic sequence are highlighted in green and introns are highlighted in red (linker introns) or blue (internal introns).

haemocyanin of the Australian black lip abalone *H. rubra,* with a 97% identity and 100% query cover. The second hit was to the northeast Atlantic and Mediterranean *H. tuberculata* haemocyanin 1 with 90% identity and 100% query cover. The *H. tuberculata* haemocyanin 1 sequence is the most complete and annotated sequence available for molluscan haemocyanin, with both genomic and coding sequences available. The *H. tuberculata* haemocyanin 2 sequence had a lower query cover and identity (41% and 74% respectively) to the *H. midae* haemocyanin sequence, indicating that *H. midae* haemocyanin 1 is the sequence obtained in this study. The phylogeny of the abalone haemocyanin sequences is represented in the cladogram in Figure 3.3.

An *H. midae* contig (AJ749649.1) was most similar to the sequence obtained in this study (Figure 3.3). It must be noted, however, that this sequence is only 570 base pairs long and therefore does not align correctly with the other sequences included in the cladogram. The length of the other sequences included in the cladogram were trimmed to match the length of the four functional units (FU-e–h) obtained in this study. As noted previously, the *H. rubra* haemocyanin sequence shared the next most similarity with the

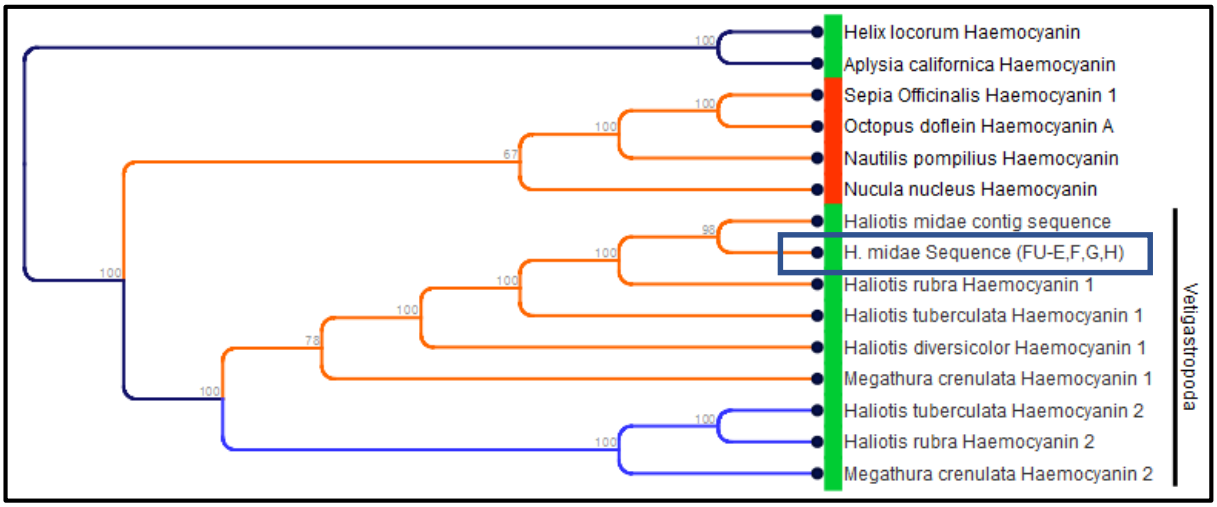

Figure 3.3: Cladogram showing sequence similarity between *H. midae* Sequence (FU-E,F,G,H) and other haemocyanin sequences from the NCBI database. *Helix locorum* (**GenBank: JF752344.1**), *Aplysia californica* (**GenBank: AJ556169.1**), *Sepia officinalis* (**GenBank: KF306341.1**), *Octopus dofleini* haemocyanin A (**GenBank: AY751301.1),** *Nautilis pompilus* haemocyanin (**GenBank: AJ619741.1**), *Nucula nucleus* haemocyanin (**GenBank: AJ786639.1),** *Haliotis tuberculata* haemocyanin 2 (**GenBank: AJ297475.1**), *Haliotis rubra* haemocyanin 2 (**GenBank: KU496943.1**), *Megathura crenulata* haemocyanin 2 (**GenBank: AJ698342.1**), *Megathura crenulata* haemocyanin 1 (**GenBank: AJ698341.2**), *Haliotis diversicolor* haemocyanin 1 (**GenBank: GQ352369.1**), *Haliotis tuberculata* haemocyanin 1 (**GenBank: AJ252741.1**), *Haliotis rubra* haemocyanin 1 (**GenBank: KU496942.1**), *Haliotis midae* contig sequence (**GenBank: AJ749649.1**).
Orange branches on the cladogram represent the haemocyanin 1 isoform, while the blue branch represents the haemocyanin 2 isoform. The green labels all the gastropod sequences. The red labels all the cephalopod sequences. Vetigastropoda includes the superfamilies Haliotidae and Fissurellidae. The cladogram was created using **CLC Genomics Workbench 7.0 (https://www.qiagenbioinformatics.com/).**

H. midae sequence obtained in this study and hence, is associated with the most recent branching event in the cladogram. Older evolutionary branching events can be distinguished for *H. tuberculata* and *H. diversicolor*. All these branching events contained a bootstrap value of 100, indicating that the nodes are well supported.

Haemocyanin 1 of the keyhole limpet *Megathura crenulata* has the highest sequence identity to the *H. midae* haemocyanin sequence in comparison to the other non-members of the Haliotidae superfamily (Figure 3.3). It should be noted that the commercially available antibody to haemocyanin used in this

study (section 3.2.1) was raised against this protein. The next Vetigastropoda clade consists of haemocyanin isoform 2 sequences, suggesting that the two haemocyanin isoforms are evolutionarily distinct.

The next cluster includes bivalve and cephalopod haemocyanin sequences from *Nucula nucleus* (clam), *Nautilus pompilus* (chambered nautilus), *Octopus dofleini* (giant Pacific octopus) and *Sepia officianalis* (common cuttlefish) (Figure 3.3). This cluster reflects haemocyanin sequence differences between cephalopods and gastropods, as well as the phylogeny of the two classes of invertebrates. The oldest branching event involves two gastropod haemocyanins from the terrestrial snail *Helix locorum* and the sea slug *Aplysia californica*.

3.1.1 Antimicrobial peptide analysis

The nucleotide sequence of the four functional units of the *H. midae* haemocyanin was translated using CLC Main Workbench v7.7 (QIAGEN) and divided into overlapping 70-amino-acid peptide sequences for input into the **APD3: Antimicrobial Peptide Calculator and Predictor**. This was necessary as the prediction engine is only able to process peptide sequences of 100 amino acids at a time. Each peptide sequence was searched against the database for similarity to antimicrobial peptide (AMP) structures and amino acid sequences of known antimicrobials. Whilst the majority of the fragments returned a potential helix structure, the highest similarity to known antimicrobials was only 31.1%. However, a 58-residue peptide located between amino acids 250 and 308 displayed 83.3% similarity to an AMP with accession number AP02446. Since this peptide is the haliotisin peptide from the abalone species *H. tuberculata* identified by Zhuang et al. (2015), it is likely that FU-e of the *H. midae* haemocyanin contains the same haliotisin peptide that occurs in other abalone species. The deduced amino acid sequence of the *H. midae* peptide was N - **DTFDYKKFGYRYDSLELEGRSIAHLDELIKERQEQDRTFAGLLKGFGTSAT** - C. This peptide has a total hydrophobic ratio of 29% and a total net charge of -3, while its protein-binding potential was determined to be 2.56 kcal/mol. Thus, the small size and a high proportion of hydrophobic residues in this region of the *H. midae* haemocyanin suggests that it is highly likely that it functions as an antimicrobial peptide.

Although peptide regions from functional units f and g also displayed similarities to the haliotisin peptide, the similarity was limited to 40.8% and 36.1% respectively. There was no similarity between FU-h and the haliotisin peptide or its derivatives. Conservation of amino acids comprising the haliotisin peptide region of haemocyanins from a number of molluscs is depicted in Figure 3.4. The full nucleotide sequence alignment between haemocyanins from *H. midae* and various molluscan species is included in the appendix (Supplementary Figure 5.2).

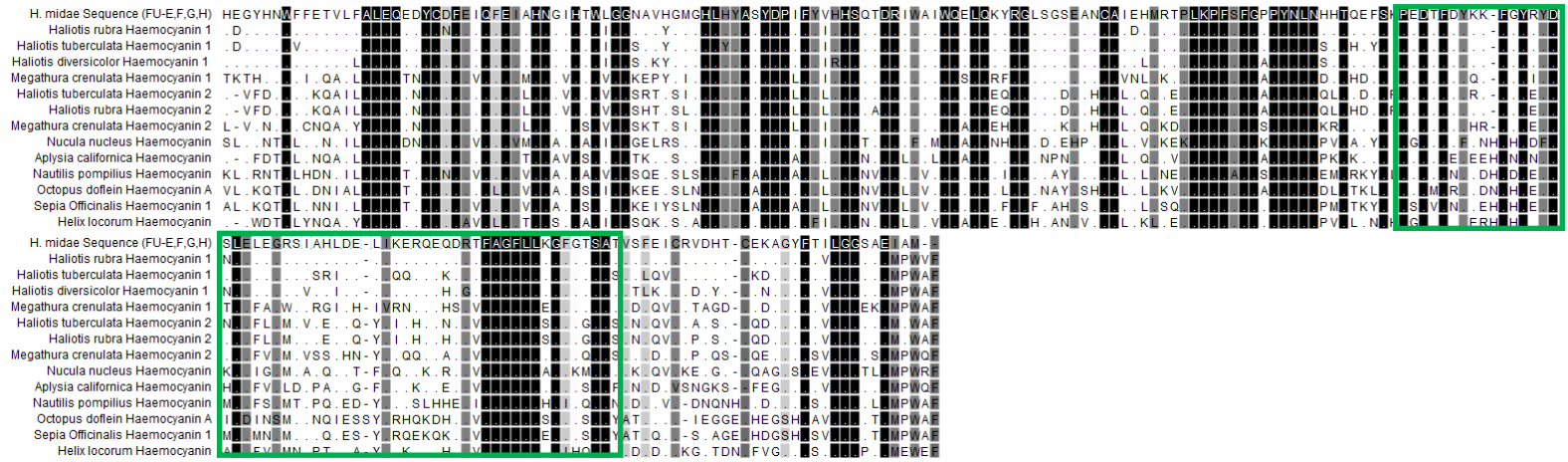

Figure 3.4: Multiple sequence alignment between the FU-e of haemocyanins from a number of molluscs, showing the degree of amino acid conservation (black-shaded regions are more highly conserved). Amino acids identical to that of the *H. midae* sequence are substituted with a dot. The region that includes the haliotisin peptide is marked by a green rectangle.

3.1.2 AMP structure analysis

The next step was to examine whether the haliotisin-like peptide identified in the *H. midae* haemocyanin contained β-sheets or α-helices and whether the helices, if present, were amphipathic in nature. Figure 3.5 shows the predicted 3D model of the peptide described in section 3.1.1. The peptide displays three secondary structures: an α-helix, a broken α-helix and a β-sheet domain, which is equivalent to the entire P3-P4-P5 peptide identified by Zhuang et al. (2015). Each specific domain also shows a high degree of hydrophobic amino acids (Figure 3.5B). The β-sheet specifically contains a majority of hydrophobic residues. Analysis of the full α-helix (**N – IAHLDELIKERQE – C**) for amphipathicity showed that the majority of non-polar residues were associated with one side of the helix (Figure 3.5C), thus demonstrating that the α-helix has an amphipathic structure and implying it is potentially capable of antimicrobial activity.

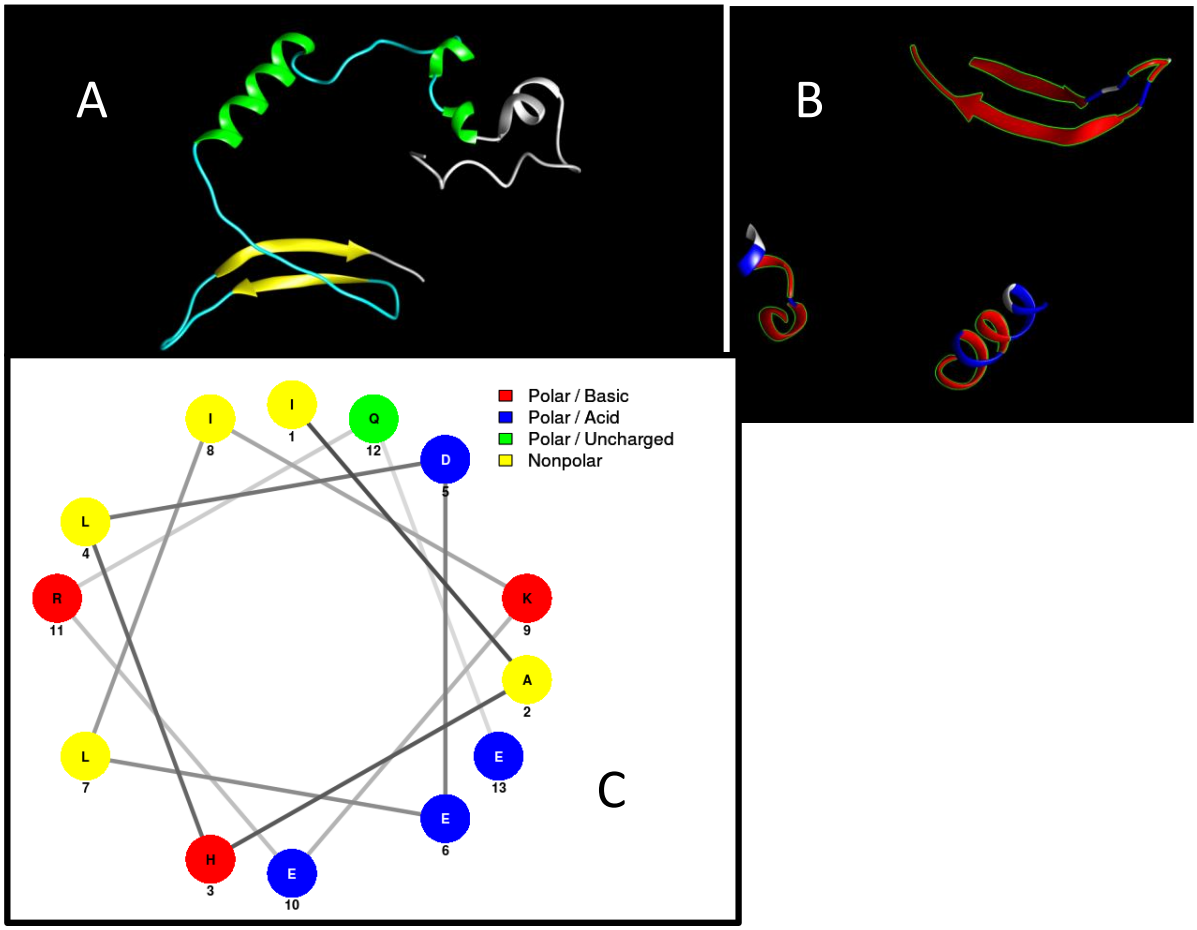

Figure 3.5: 3D ribbon structures of the Haliotisin peptide from *H. midae*. **A** Full ribbon depicting the three domains present: green, α-helix; yellow, β-sheet; white is a portion of the pProEX vector. **B** Shows the hydrophobic components of the domains, where red indicates hydrophobic residues and blue indicates hydrophilic residues. **C** Representation of the α-helix depicting polar and non-polar residues to imply amphipathicity.

3.2 Recombinant expression of AMP

PCR amplification was used to amplify the portion of the *H. midae* haemocyanin gene that coded for the putative haliotisin peptide for subsequent sub-cloning into the pProEX vector in order to recombinantly express the peptide. Agarose gel analysis of the PCR products obtained by colony PCR of the *E. coli* BL21 transformants confirmed sizes of the amplicons expected to be generated by the two sets of primers. The gene-specific primer pair (*H. midae* haliotisin cloning Fwd (*Nco1*) and *H. midae* haliotisin cloning Rev (*Not*I); Section 2.3.1: Table 2.2) yielded an amplification product of 178 base pairs, while amplification with the forward sequence primer (pProEX sequencing Fwd (M13Rev); Section 2.3.1: Table 3.1) and the

gene-specific reverse primer (*H. midae* haliotisin cloning Rev (*Not*I)) yielded an amplicon of 285 base pairs. DNA sequences of the amplicons confirming that the recombinant plasmids contained the correct haliotisin region are included in the appendix (Supplementary Figure 5.3).

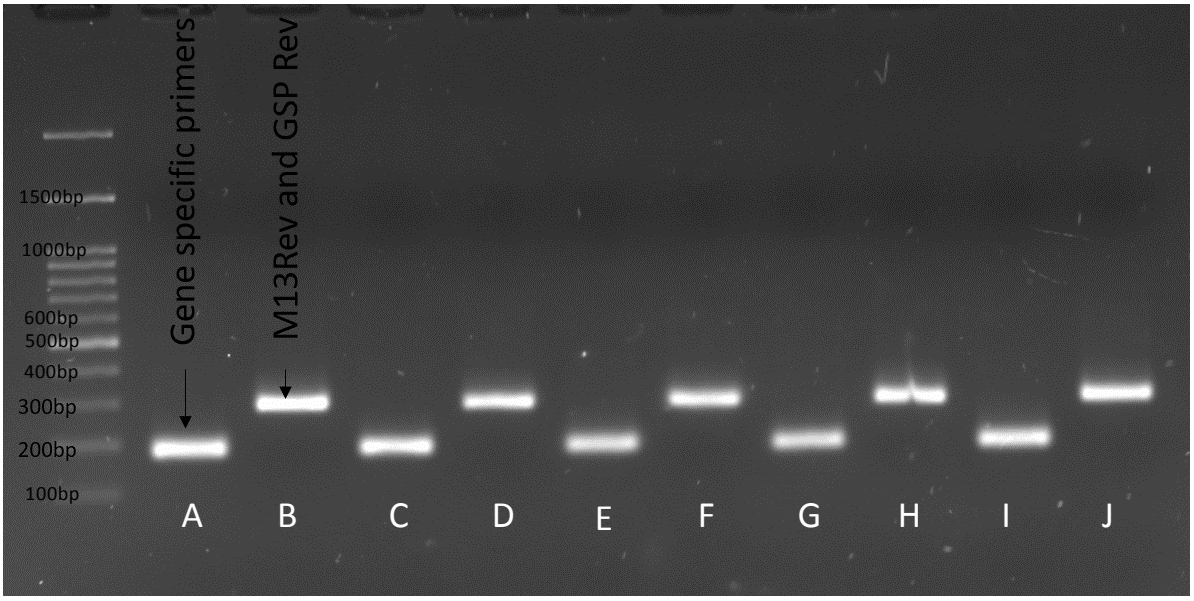

Figure 3.6: Colony PCR of *E. coli* BL21 colonies containing pProEX with the *H. midae* haliotisin peptide inserted in frame to the His-tag of the vector. Primer sets were gene specific (Lanes A, C, E, G, I) or the forward sequencing primer and the reverse gene specific primer (Section 2.3.1: Table 2.2) (B, D, F, H, J). Ladder used was OneMARK100 from GeneDirex.

3.2.1 Protein expression

Optimal expression of the *H. midae* haliotisin-like peptide in *E. coli* BL21 resulted by growing log-phase cells ($OD600_{nm}$ = 0.6) in the presence of IPTG at a final concentration of 2 mM for 4 hours at 37°C with shaking. The expressed peptide was detected in the insoluble *E. coli* protein fraction (Figure 3.7). Consequently, cells were lysed using the denaturing conditions described in section 2.3 to obtain increased peptide yields. The identity of the putative haliotisin was confirmed by western blot, using an antibody to the his-tag presented by the pProEX vector and a commercial haemocyanin antibody raised against keyhole limpet haemocyanin (KLH). Although non-specific bands are evident, a band situated just below the 15 kDa marker is evident in the induced samples and absent from the uninduced controls, indicating that the haliotisin-like peptide from *H. midae* was expressed in *E. coli* BL21 transformants (Figure 3.8).

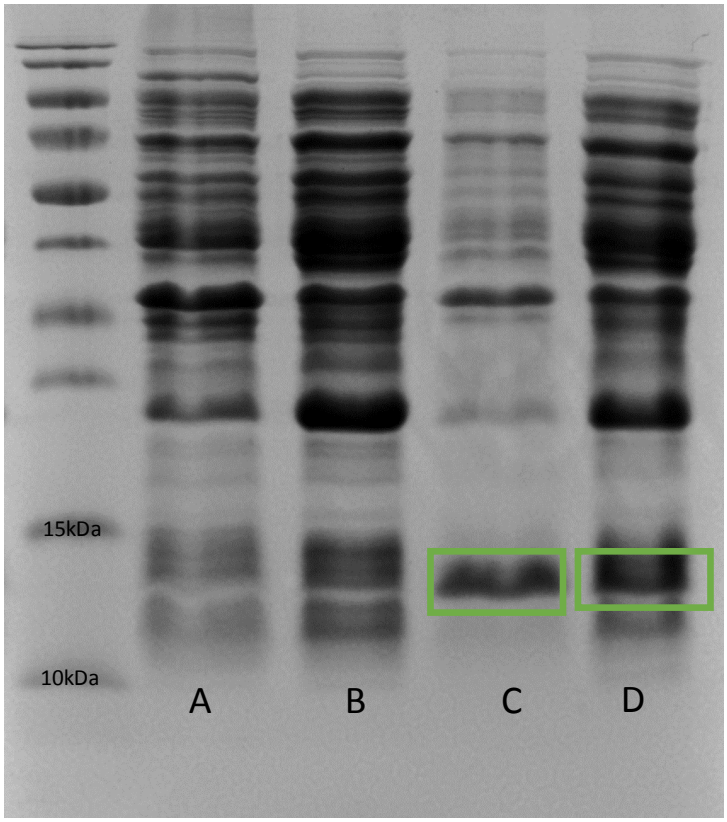

Figure 3.7: SDS-PAGE showing proteins extracted from *E. coli* BL21. **A** BL21 control cells lysed using native buffer. **B** Transformed cells lysed with native buffer. **C** Post-sonication pellet resuspended in denaturing buffer. **D** Transformed cells lysed using denaturing buffer. Putative haliotisin peptide highlighted in green box. Ladder used was PageRuler ™ Prestained protein ladder (Thermo Fisher Scientific).

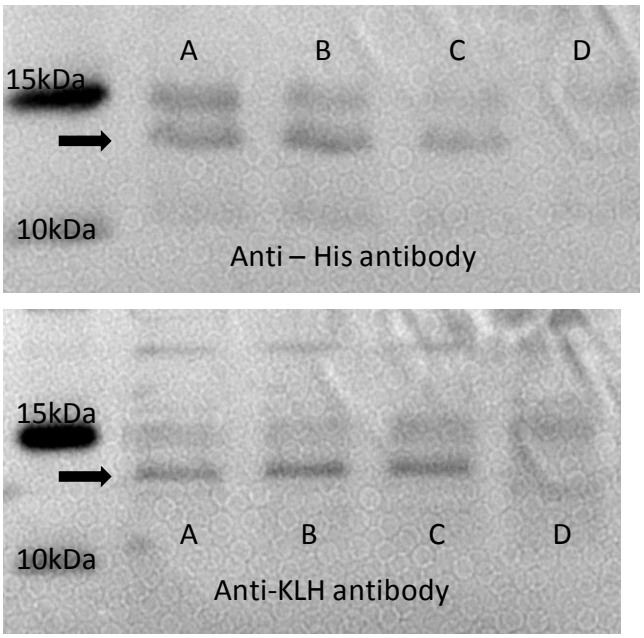

Figure 3.8: Western blots of protein extracted from haliotisin-expressing *E. coli* BL21 transformants. Protein extracted from cells induced for 4 (**A**), 6 (**B**) and 8 (**C**) hours compared to uninduced cells (**D**). Arrow indicates the band present in induced samples. Ladder was PageRuler™ Prestained protein ladder. (Thermo).

3.2.2 Purification of the *H. midae* haliotisin-like peptide

The putative haliotisin-like peptide expressed in *E. coli* BL21 was purified from the host proteins using the his-tag fused to the N-terminal end of the cloned *H. midae* haemocyanin fragment. Initial batch purification using HisPur™ Ni-NTA resin yielded positive results, with the peptide eluting at an imidazole concentration of 250 mM (Figure 3.9). However, additional proteins eluted together with the targeted peptide. Since a lower concentration of imidazole (20 mM) still seemed to elute the *H. midae* peptide, an alternate protocol for removing the non-specifically bound proteins was attempted which involved lowering the pH of the wash buffer from 8.0 (used for cell lysis) to 6.7. As can be seen in Figure 3.10, the revised protocol improved the purity of the haliotisin-like peptide, despite the presence of an additional protein (approximately 25 kDa) eluting from the HisPur™ Ni-NTA resin. Although still to be confirmed, this band may be a dimerised form of the *H. midae* peptide.

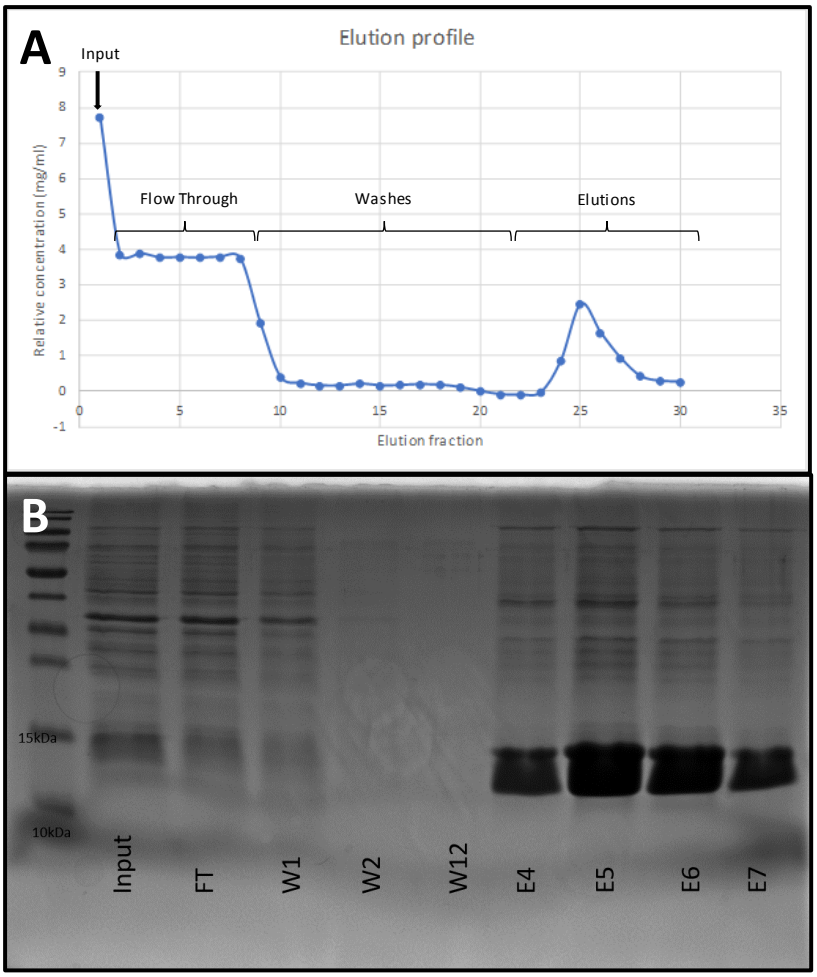

Figure 3.9: Batch purification using HisPur™ Ni-NTA resin. **A.** Elution profile showing an absorption peak at A280nm following the addition of imidazole at the start of the elution step. **B.** SDS-PAGE of the eluted samples (FT=Flow Through, W=Wash, E=Elution). The numbers correspond to the fraction number. Ladder: PageRuler ™ Prestained protein ladder (Thermo Fisher Scientific).

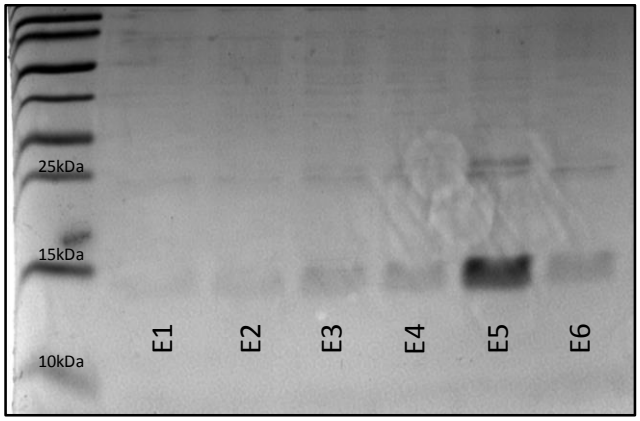

Figure 3.10: SDS PAGE of eluted fractions after washing with denaturing buffer at pH6.7. E: Elution fractions. Ladder: PageRuler™ Prestained protein ladder (Thermo Fisher Scientific)

3.2.3 Dialysis

In order to allow the purified *H. midae* haliotisin-like peptide to refold into the active state, it is necessary that the urea is removed from the sample buffer. Thus, removal of urea from the denaturing buffer was attempted by dialysis for a total of 48 hours (section 2.4.2). Size-exclusion chromatography (section 2.4.2) was used to investigate whether the peptide had indeed refolded to the active conformation, while a radial diffusion assay was employed to investigate the antimicrobial activity of the peptide (section 3.3; Figure 3.13i). Theoretically, if the peptide had folded correctly following dialysis to remove the urea, it should elute from the size-exclusion column as a single peak in the A280nm profile. However, no distinct peaks were visible in the elution profile, suggesting that the peptide had folded in a variety of conformations and consequently, had eluted throughout the size-exclusion column (Supplementary Figure 5.4), thus requiring an alternate protocol to obtain a correctly folded, biologically functional peptide.

3.2.4 Fast protein liquid chromatography

In collaboration with the Chemical Engineering Department at UCT, an on-column refolding and peptide purification protocol, adapted from Oganesyan et al. (2005), was performed using fast protein liquid chromatography, the elution profile for which can be seen in Figure 3.11.

It is evident that there is a peak in absorbance at the start of the protocol (Figure 3.11A). This is representative of proteins that were unable to bind to the column and flowed through in the initial buffer. The change in pH of the denaturing buffer causes a slight increase in the absorbance readings, barely detectable in the figure, which is representative of the non-specifically-bound proteins being eluted.

The erratic absorbance readings steadily increase as buffer containing the Triton detergent is added to the column (Figure 3.11B). Since Triton is known to absorb at 275 nm, a wavelength close to the 280 nm being examined, it is likely that the detergent is the cause of the increased absorbance. It is important to note that the absorbance values of the elution profile shown in Figure 3.11B are lower than those observed in the profile depicted in Figure 3.11A. The latter elution profile peaked at 5 000 mAU (milli-absorbance units), while the former (Figure 3.11B) peaked at around 1 800 mAU. The addition of β-cyclodextrin resulted in the final peak in the elution profile, presumably coinciding with the removal of the remaining Triton from the column (Figure 3.11B).

Four distinct peaks were evident in the elution profile generated during the elution stage of the fast protein liquid chromatography protocol (Figure 3.11C). The absorbance over the elution profile was much

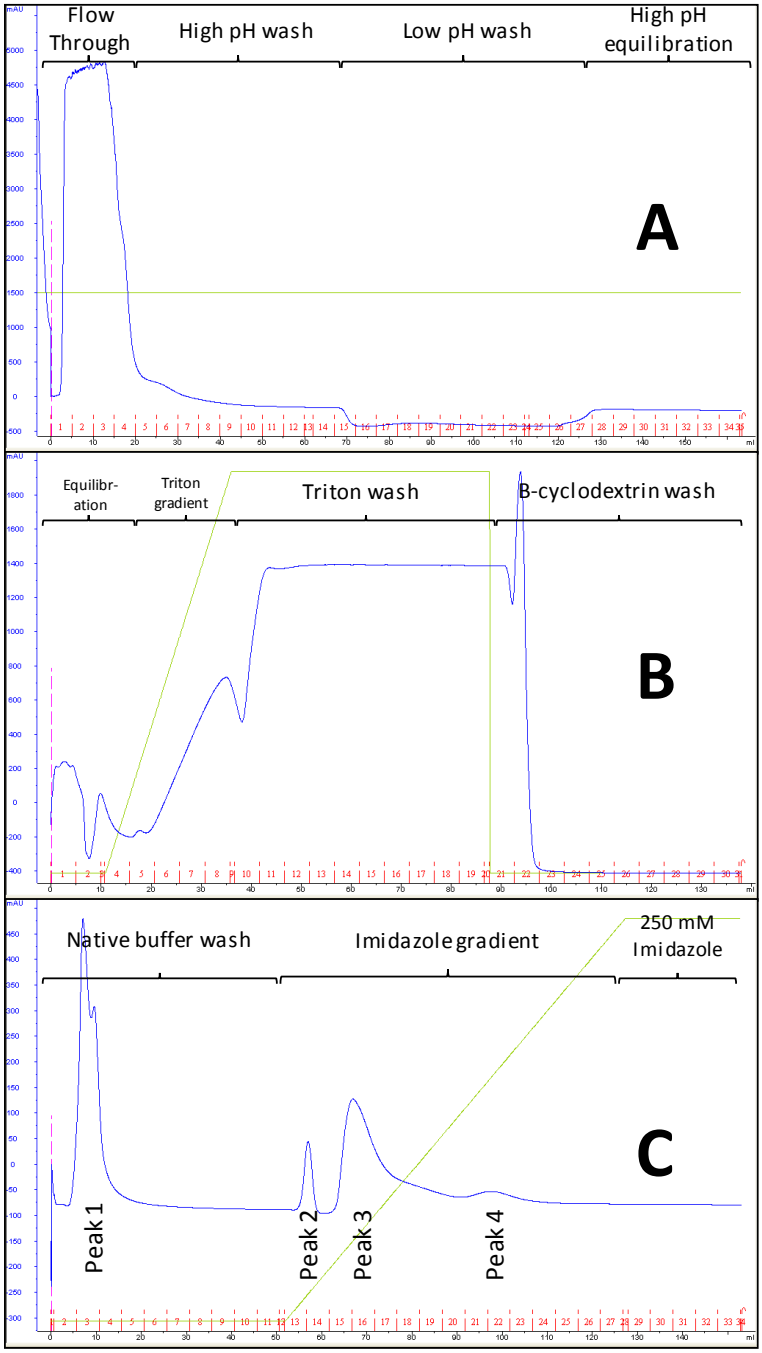

Figure 3.11: Elution profiles showing the three stages of the refolding and purification process performed with FPLC. Y-axis: absorbance at 280 nm normalised to the sample buffer. X-axis: the fraction number (red) and volume in ml (black). **A.** Elution profile for the initial flow-through and washes using a reduced pH urea buffer. **B.** The elution profile for the refolding step following addition of the detergent Triton and the cyclic oligosaccharide β-cyclodextrin. **C.** The elution step using an imidazole gradient. The blue line represents absorbance and the green line indicates the ratio of the two buffers. Each peak in absorbance has been labelled (1-4).

lower, peaking at only 450 mAU, which suggests that the concentration of the protein eluted from the column was very low.

All fractions obtained from the three stages of the fast protein liquid chromatography protocol that had absorbance readings higher than baseline were analysed by SDS-PAGE to determine the size of the proteins and the location of the recombinant haliotisin-like peptide. SDS-PAGE of the fractions containing the four peaks observed in the profile of the elution stage of the protocol (Figure 3.11C) showed that the fourth peak, located in fractions 21 and 22 of the elution profile (Figure 3.11C), included the purified *H. midae* peptide (Figure 3.12). The fourth peak (fractions 21 and 22) also appear to contain a double band for the recombinant protein. Fast protein liquid chromatography removed the large, non-specific proteins and returned the recombinant haliotisin-like peptide at a greater degree of purity. However, since elution was performed in 5 ml fractions, the concentration of the peptide was much lower than that obtained by batch HisPur™ Ni-NTA resin purification where the fractions were collected in 100 µl aliquots.

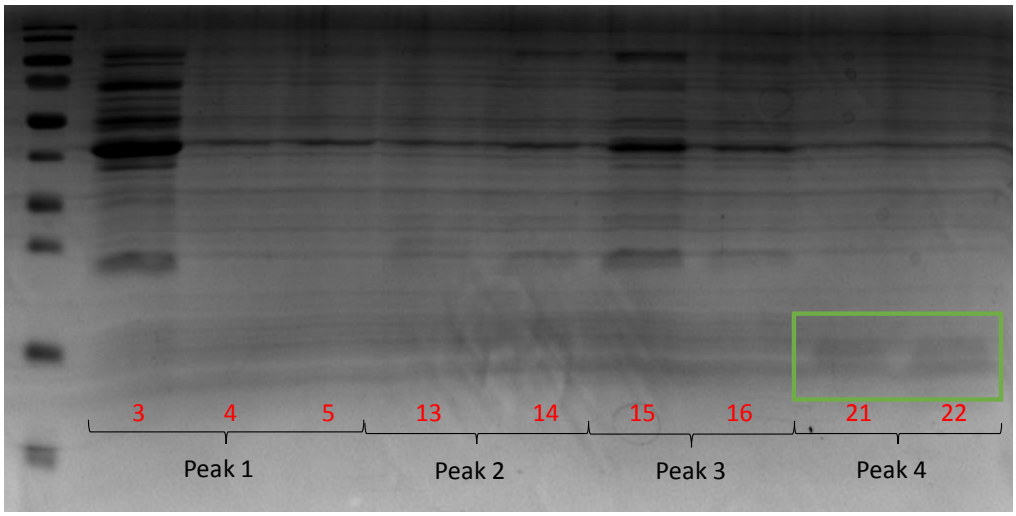

Figure 3.12: SDS-PAGE of elutions from FPLC refolding and purification. The four peaks indicated here correspond to the four peaks indicated in the profile of Figure 3.11C. The fraction numbers are in red to correspond with the red fraction numbers of Figure 3.11C. The green box indicates the faint band corresponding to the haliotisin-like peptide. Other bands indicate eluted non-specifically bound proteins.

The fractions containing the *H. midae* haliotisin-like peptide, as determined by SDS-PAGE (Figure 3.12), were pooled and concentrated to obtain a workable concentration that would allow screening of the antimicrobial potential of the peptide. Thus, the sample was placed in an Amicon ® Ultra with 3 kDa MWCO (molecular weight cut off) (Merck) and centrifuged at 5 000 x g until the total volume reached the minimum of 200 µl in accordance with the manufacturer's protocol. The concentrated sample containing the haliotisin-like peptide and known concentrations of bovine serum albumin (BSA) samples were

subjected to SDS-PAGE. After staining the polyacrylamide gel, the concentration of the haliotisin-like peptide could be determined by densitometric analysis (section 2.4.3) (Supplementary Figure 5.5). Even after the putative haliotisin peptide had been concentrated to the lowest possible volume using the Amicon® Ultra Centrifugal Filter (Merck), the final concentration of the purified protein remained low (between 50 and 100 µg/ml).

3.3 Antimicrobial activity

The most accurate strategy for determining whether a protein is correctly folded is to test the peptide for activity. Therefore, despite the low concentration of the purified haliotisin-like peptide, a radial diffusion assay was performed in order to examine whether the peptide could inhibit the growth of four different bacterial species. Zones of inhibition were evident in two of the four strains tested. The *E. coli* strain incubated with the batch-purified and dialysed haliotisin-like peptide sample (Figure 3.13i) and the *S. aureus* strain incubated with the concentrated FPLC-purified and refolded sample (Figure 3.13ii) both showed zones of inhibitions. The zone of inhibition for *E. coli* had a radius of 4 mm and the zone of inhibition for *S. aureus* had a radius of 7.5 mm. No zones of inhibition were visible for the native buffer in either of these radial diffusion assays. The two positive controls for the assay – the denaturing buffer and the ampicillin sample – both show zones of inhibition larger than that present in the peptide sample. The zone of inhibition for *E. coli* had a radius of 11 mm when treated with the denaturing buffer that contained urea, and the zone of inhibition for *S. aureus* had a radius of 15.5 mm when treated with ampicillin at a concentration equal to that of the peptide sample. The other two strains of bacteria tested, *B. subtilis* and *V. anguillarum,* showed no zones of inhibition (Supplementary Figure 5.6). The zones of inhibition in both the *E. coli* and *S. aureus* strains suggest that the putative haliotisin-like peptide from *H. midae* is able to inhibit the growth of these Gram-negative and Gram-positive bacterial species, although additional experiments are required to confirm this activity.

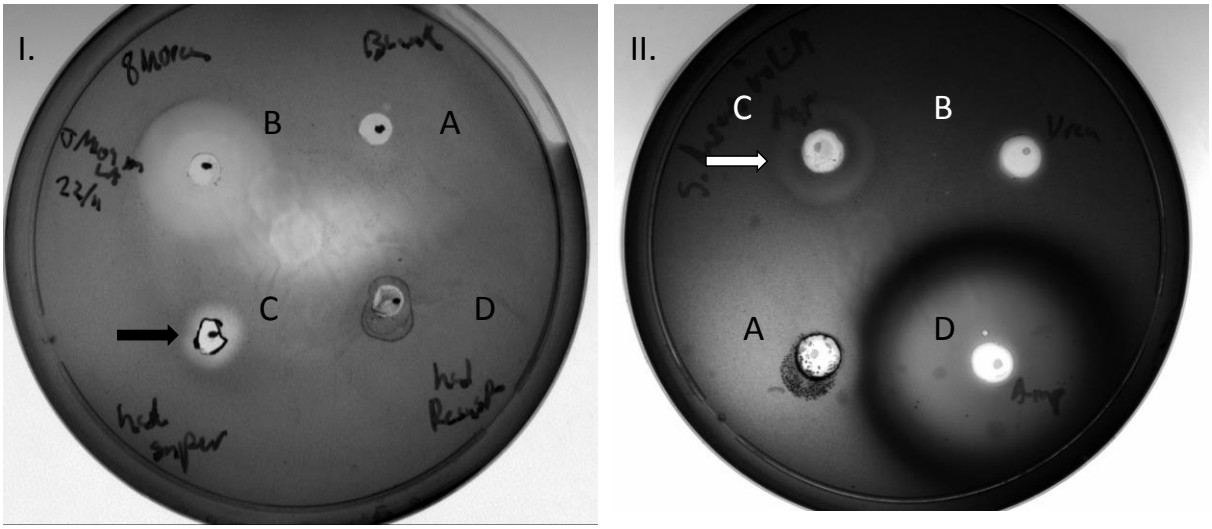

Figure 3.13: Stained agarose plates showing results of radial diffusion assay

i) *E. coli* exposed to water (**A**), 8M urea buffer (**B**), haliotisin peptide (**C**) and native buffer (**D**)

ii) *S. aureus* exposed to native buffer (**A**), 8M urea buffer (**B**), haliotisin peptide (**C**) and equal concentration of ampicillin (**D**).

3.3.1 Quantitative growth inhibition assay

Since the data obtained using the radial diffusion assay was only suggestive due to the qualitative nature of the assay the antimicrobial potential of the *H. midae* haliotisin-like peptide was further investigated using a quantitative growth inhibition assay. Only the two bacterial species that showed zones of inhibition (section 3.3) were tested. Two-fold serial dilutions of logarithmic growth-phase *E. coli* and *S. aureus* cultures were prepared and tested against 1 µg of the *H. midae* haliotisin-like peptide. Optical density of the *E. coli* cultures diluted from 1:128 to 1:512 showed significant decrease when incubated with the putative *H. midae* haliotisin-like peptide (Figure 3.14A). When incubated with the peptide, the *E. coli* cultures at lower dilutions (1:128, 1:256 and 1:512) achieved an optical density of only 34.8%, 18.9% and 13.7% respectively, relative to the control cultures at the corresponding dilutions. This shows that with less bacteria present, the low-concentration putative antimicrobial peptide was highly effective at inhibiting the growth of the Gram-negative *E. coli*.

Throughout the two-fold dilutions series, the optical density of the *S. aureus* cultures, when compared to corresponding uninhibited controls, showed a trend of being reduced when incubated with the putative *H. midae* haliotisin-like peptide (Figure 3.14B). Significant differences were only visible in four of the tested dilutions (undiluted, 1:2, 1:8 and 1:32) showing no trend, but this may be due to having only conducted

two technical repeats due to a limited amount of purified peptide available for the assay. The *S. aureus* strain, when incubated with peptide, was still able to achieve an optical density greater than 65% of that reached by the corresponding uninhibited controls, showing that the peptide had a weak inhibition of the *S. aureus* regardless of bacterial concentration. The data thus suggests that the *H. midae* haliotisin-like peptide is able to inhibit growth of both *E. coli* and *S. aureus*, but its ability to inhibit the growth of this Gram-positive bacterium is significantly less potent than its inhibitory effect on the Gram-negative bacterium.

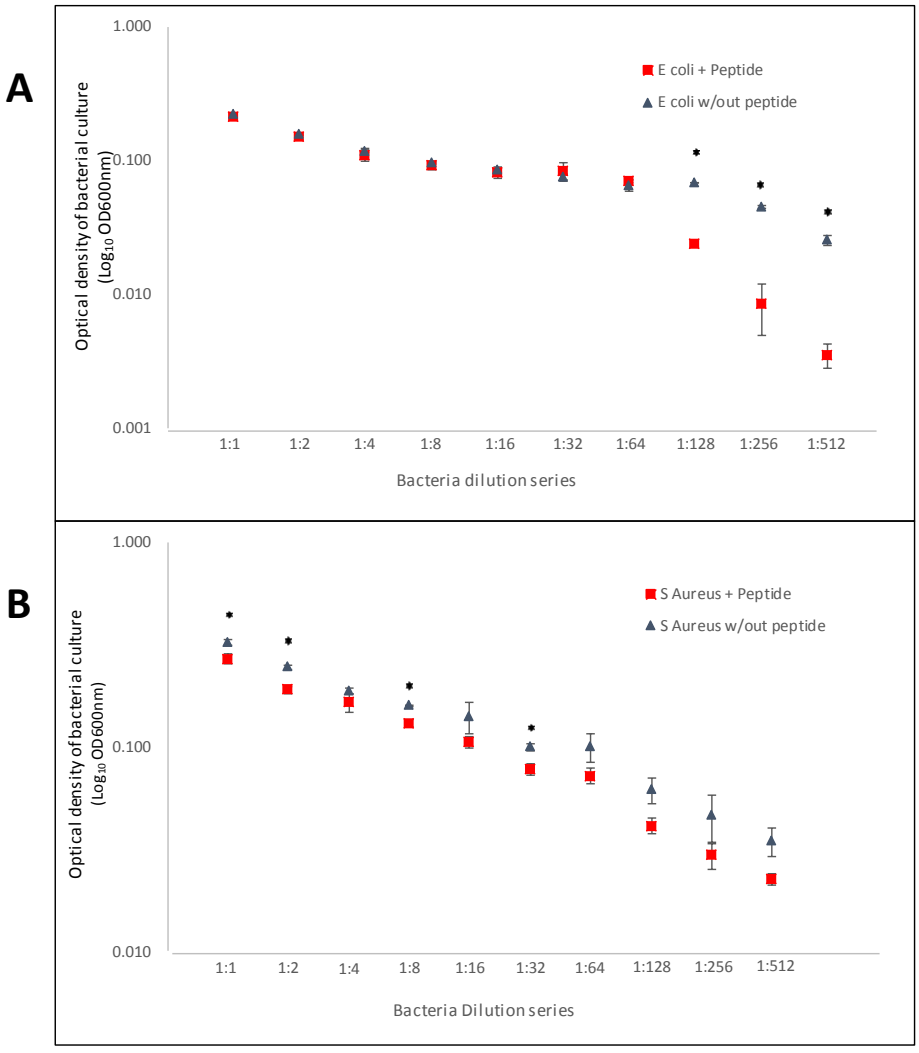

Figure 3.14: Optical density readings for bacterial cultures of *E. coli* (**A**) and *S. aureus* (**B**) incubated in the presence or absence of the haliotisin-like peptide from *H. midae*. * indicates significant decrease in growth when incubated with peptide compared to bacterial culture of the same starting concentration ($P<0.05$).

4. Discussion

4.1 Sequence analysis

Based on the upregulation of haemocyanin in response to *Vibrio* infection (Beltran 2015), further investigation of the role that haemocyanin, a large multimeric oxygen transporter, could have within the innate immune response of the South African abalone *H. midae* was undertaken. To start, a greater knowledge surrounding the sequence of the gene was required. The sequence presented in this study is the longest sequence of *H. midae* haemocyanin recorded to date. The gene showed high sequence similarity to the Australian black lip species *H. rubra* and demonstrated that the most prevalent haemocyanin present in *H. midae* is haemocyanin isoform 1. The two haemocyanin isoforms in Haliotidae seem to have evolved as a result of a duplication event that occurred *c*.350 million years ago (Streit et al. 2005), but the significance of there being two isoforms is still not completely understood. Primers designed with the second isoform of *H. rubra* as the template yielded no products when used for PCR amplification in this study, so it is not certain whether *H. midae* even contains the haemocyanin isoform 2. In some organisms, the expression of one isoform tends to dominate the other, and only arthropods are known to contain an equal ratio of the two haemocyanin isoforms. The two isoforms generally appear in a 3:1 ratio of isoform 1 : isoform 2 in abalone haemolymph (Altenhein et al. 2002; Keller et al. 1999).

4.1.1 Phylogeny of haemocyanin

The cladogram presented in Figure 3.2 agrees with data reported in other studies. Streit et al. (2005) found two clades present within the Haliotidae haemocyanin gene: a “short”-intron-possessing group of European and Australasian origin and a newer “long”-intron-possessing group, primarily from the North Pacific. Data from Streit et al. (2005) also provided evidence of a divergence from the superfamily Fissurellidae (represented by *Megathura crenulata* in Figure 3.2) *c*.260 million years ago, which accords with fossil records. For the current study, only the European and Australasian branch was utilised for the cladogram, but the divergence patterning and separation of the second isoform can be seen in both the data presented here and the data collected by Streit et al. (2005). The divergence of the gastropod species from the cephalopod species is also evidenced by the separation of the octopus, cuttlefish and nautilus sequences from the abalone and limpet sequences.

The *Haliotis* haemocyanin sequences all clustered together and associated with the *Megathura crenulata* sequence in a separate clade from the rest of the analysed haemocyanin sequences. The two

haemocyanin isoforms must have emerged after this divergence event, as evidenced by the grouping of isoform 2 sequences within the Vetigastropoda clade. The only peculiar finding in this figure is the isolation of the *Helix locorum* sequence away from the rest of the gastropod haemocyanin sequences. This terrestrial gastropod showed the earliest divergence away from the rest of the *Haliotis* species, suggesting that a large modification to the haemocyanin sequence was required for terrestrial life.

4.1.2 Functional unit e

Obtaining the full sequence of the haemocyanin gene was outside of the scope of this project, so for this study, the four subunits on the C-terminal end of *H. midae* haemocyanin were sequenced. This included the majority of FU-e and FU-h and the entirety of FU-f and FU-g, which had a maximum of 49% identity to one another at the protein level, in accord with the findings of previous studies (Lieb & Markl 2004). As Fu-e has been shown to play a role in the immune response (Zhuang et al. 2015; Dolashka & Voelter 2013; Zhu et al. 2014), it became the primary focus of a search for antimicrobial activity.

The linker region between the α-helix-rich domain and the β-sheet domain has been shown to have an impact on haemocyanin's function as a pro-phenoloxidase in molluscs, with structural alterations also associated with the conversion of haemocyanin into an immune-enzyme in crustaceans and chelicerates (Coates & Nairn 2014; Van Holde et al. 2001; Hristova et al. 2008; Kostadinova et al. 2013; Lee et al. 2003a). Zhuang et al. (2015) propose that haemocyanin is processed via an as yet uncharacterised proteolytic cleavage that causes the tertiary structure to loosen and enables the haemocyanin-derived phenoloxidase activity, which could also result in the release or generation of bioactive peptides such as haliotisin. Zhuang et al. (2015) further propose that a combination of host- and microbe-directed mechanisms could cause the release of haliotisin peptides by serine protease-like enzymes and, during the process, disturb the structural elements surrounding the dicopper centre of haemocyanin, which would allow phenols a mode of entry to the copper-bound O_2.

Dolashka et al. (2010) demonstrated the ability of glycosolated Fu-e isolated from *R. venosa*, the veined Rapa whelk, to stop viral replication of herpes simplex virus type 1. Additionally, Zhu et al. (2014), through work on *H. diversicolor*, demonstrated that when haemocyanin loses its inter-functional unit interactions, FU-e has an enhanced ability to oxidise diphenols. It is proposed that, during infection, enzymes target haemocyanin FU-e to signal the need for immune function through anti-viral activity (Dolashka & Voelter 2013), phenoloxidation (Zhu et al. 2014), the production of antimicrobial peptides such as haliotisin (Zhuang et al. 2015) or a combination of these responses.

4.1.3 Antimicrobial sequence analysis

The APD3 predictions returned a large number of potential helices for the inputted haemocyanin sequences, particularly on the N-terminal end of each functional unit, which accords with the data previously presented that found that this region contains a helix-rich domain (Lieb et al. 2000; Keller et al. 1999; Lieb et al. 2001). However, apart from the haliotisin-like region, none of these potential helices shared more than 30% identity with any other known antimicrobial peptide, suggesting that these helices are not likely to act as antimicrobial peptides. Some putative peptide fragments were predicted to have a cysteine-rich region, but again these showed low similarity to known AMPs.

The hydrophobicity of the peptide found in FU-e of *H. midae* was determined to be 29%, very close to the 28% hydrophobicity content of the haliotisin peptide reported by Zhuang et al. (2015). The protein-binding potential was also very similar: 2.56 kcal/mol for this study's peptide and 2.82 kcal/mol reported in the Zhuang et al (2015) study. The protein-binding potential of the peptide is unrelated to this study, as the potential membrane-binding function of the peptide involves lipids rather than proteins (Boman 2003). These findings suggest that the peptide isolated from FU-e of *H. midae* in this study should have the same bioactivity as the haliotisin peptides synthetically created by Zhuang et al. (2015).

Regions with a degree of similarity to the haliotisin peptide were also found in FU-f and FU-g, but these were partial alignments and not the full peptide sequence observed in FU-e. This indicates that either the haliotisin peptide-coding region was present within all the functional units after the duplication event and subsequently, portions of it in FU-f and FU-g were lost due to deletions; or an ancestral version of the peptide was present in each functional unit after the duplication event, and only FU- e adapted this coding region to form the haliotisin-like peptide.

The 3D-structure prediction of the haliotisin-like peptide shows the same features presented by Zhuang et al (2015) and is compared in Figure 4.1, where the P3, P4 and P5 peptide regions are shown to be contained within the cloned segment of haliotisin used in this study. The red-highlighted region represents the P3 peptide, which Zhuang et al. (2015) found to have high anti-proliferating activity against the Gram-positive bacterium *B. subtilis*, while a combination of P4 (green) and P5 (blue) exhibited the highest activity against the tested *E. carotovora* strain, representing Gram-negative bacteria. This indicates that the peptide used in this study contains all three motifs presented by Zhuang et al. (2015) and should have similar effects on both Gram-negative and -positive bacteria. The P3-P4-P5 is thought to contribute one continuous peptide with antimicrobial properties.

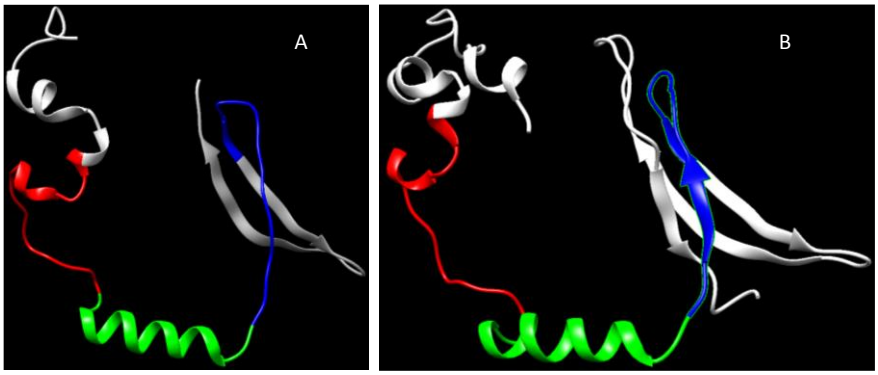

Figure 4.1: 3D ribbon models of (**A**) The haliotisin-like peptide investigated in this study and (**B**) The haliotisin peptide identified by Zhuang et al. (2015). Red indicates the P3 peptide described in the Zhuang study, green indicates the P4 peptide and blue indicates the P5 peptide.

The organisation of amphipathicity within the helix (Figure 3.5C) shows that it is most likely to associate with the membrane of the bacterial cell wall and cause disruption. The portion of the helix that contains an abundance of non-polar residues will most likely associate with the lipid core of the bacterial membrane and cause the formation of pores through one of the three proposed methods by Brogden (2005) and described in section 1.2.1, although which specific method is not known. Zhuang et al. (2015) used transmission electron microscopy to show cell wall abnormalities, demonstrating that the haliotisin peptide inhibits growth through lesions in the bacterial cell wall. Because the alpha helix present in the haliotisin-like peptide of this study demonstrates a high degree of similarity to the one presented by Zhuang et al. (2015), it is likely that the two peptides have a similar function.

4.2 Recombinant production of the peptide

During the recombinant production of the haliotisin-like peptide, the growth and induction conditions yielded the peptide within the insoluble fraction of the lysed *E. coli* cells. The growth conditions were modified in an attempt to obtain a soluble version of the peptide, but this resulted in reduced growth of the hosting *E. coli* cells. Induction at a lower temperature for a longer period of time should allow for the cells to produce and correctly fold the peptide, as it does not contain many complex features and should thus fold correctly in a prokaryotic organism such as *E. coli*. However, there was a significant reduction in the optical density of the culture when these conditions were tested (incubation at 20°C for between 12 and 18 hours after inducing with 2 mM of IPTG), implying a reduced number of cells. The uninduced controls were able to grow sufficiently over this time period, suggesting that the reduction in cell density is directly related to the production of the peptide over this period. The reduction in *E. coli* growth and

replication under these conditions may be a result of resource-intensive recombinant protein production, leaving insufficient energy for culture maintenance. An alternative hypothesis is that the peptide was produced and correctly folded, becoming functionally active as an AMP and inhibiting the growth of the bacteria. Consequently, it was decided that the best course of action would be to induce at a higher temperature for a shorter period of time to encourage the cells to form inclusion bodies of the peptide and then isolate the haliotisin-like peptide from the insoluble fraction post-lysis for purification and refolding at a later stage.

The process could be improved by initially lysing the *E. coli* with the native buffer and then resuspending the insoluble fraction in the denaturing buffer, as was done for the results presented in Figure 3.7. This would allow for an initial purification step to eliminate all the *E. coli* cytoplasmic host proteins from further purification steps. The insoluble proteins alone could be used for batch purification or FPLC purification, which would result in a reduced chance of non-specific binding due to fewer proteins in the sample. Reducing the total number of proteins in the sample would also reduce the likelihood of the peptide binding to another protein during refolding protocols.

During the batch purification the incubation of the cell lysate with the affinity resin could be increased to 24 hours, which may increase the yield of purified protein produced. The binding process is generally a slow one and by only binding for one hour it is possible that a lot of the target protein is being washed off during later steps. By increasing the binding time, it is possible that more protein will bind to the column and therefore could be eluted later.

4.2.1 Size-exclusion chromatography of dialysed sample

Size-exclusion chromatography (SEC) of the haliotisin-like peptide that underwent dialysis did not result in significant peaks in the elution profile (Supplementary Figure 5.4), indicating that either the concentration of the sample was too low to induce a noticeable peak within the $A280_{nm}$ readings and hence no peak was visible on the elution profile, or the peptide present was not in a uniform conformation and was eluted over the entire time interval of the SEC. However, the sample still showed some antimicrobial functioning (Figure 3.13i), an indication that at least some of the haliotisin-like peptides that were present in the sample had folded correctly and were functionally active.

4.2.2 FPLC purification and refolding

To keep the peptide in a charged state so that electrostatic repulsion would stop the peptide from aggregating on the column (Bondos & Bicknell 2003), the pH of the denaturing buffer was lowered to only

6.7. This value was chosen as it remained one pH unit higher than the predicted isoelectric point (pI) of the peptide at 5.8.

In the FPLC protein refolding and purification, a peak in the $A280_{nm}$ profile was present during the Triton wash of the samples (Figure 3.11 B), probably because Triton X-100 absorbs at a 275 nm which is close to the wavelength measured here for protein concentration. It is unlikely to represent any protein being eluted at this stage, regardless the fractions from this range were examined on an SDS-PAGE and found to contain no proteins. The fractions that did contain the haliotisin-like peptide were 21 and 22 which corresponded to the final peak in the elution profile shown in Figure 3.11C. This indicates that the peptide bound with a higher affinity to the resin than any other protein within the sample and shows that the peptide must contain the 6-His residues at the N-terminal end, and that only with an imidazole concentration over 100 mM was it able to elute out. Figure 3.12 shows that the protein eluted separated at two slightly different sizes in the SDS-PAGE. This could be due to limited proteolytic activity and could also explain why Figure 3.13 shows two zones of clearing for the active peptide. However, due to the low quality of the gel and the limited sample these possibilities could not be explored in this study. It is important to note that while this demonstrates the haliotisin-like peptide was appropriately purified using FPLC, it does not give any indication as to whether or not the peptide folded in the correct manner.

4.2.3 Concentration of the haliotisin-like peptide

Even after using the Amicon® Ultra, the concentration of the haliotisin-like peptide was still only between 50 and 100 µg/ml. This may be because the starting culture for recombinant protein expression was only 25 ml, whereas culture volumes of over a litre are usually utilised for the recombinant expression of proteins. Using a greater culture volume would increase the total number of *E. coli* cells present and able to produce the required peptide, resulting in more total peptide being produced. However, the present study remains a proof of concept that the haliotisin-like peptide from *H. midae* could be produced in the *E. coli* BL21 cells and be purified using nickel affinity chromatography.

The concentration of the haliotisin-like peptide was calculated to be 8.35 nM when used for the activity screening, which is significantly less than the 10 µM concentrations used by Zhuang et al. (2015) for their radial diffusion assays. Although the concentration of the *H. midae* haliotisin-like peptide is closer to the 300 – 1 000 nM concentration range that Zhuang et al. (2015) found to be the minimum inhibitory concentration (MIC) of the P3 peptide against *B. subtilis*, the concentration of the *H. midae* peptide is still almost a hundred-fold lower. Thus, a higher concentration of the peptide could lead to a more consistent result with regard to the activity assays.

4.3 Activity screening

The correct folding of the haliotisin-like peptide post-FPLC refolding and purification was not examined in detail in this study. This could have been performed as previously described through size exclusion chromatography (SEC), or more accurately using circular dichroism (Clarke 2011) or X-ray crystallography (Kataoka & Goto 1996). However, these methods all require a high concentration of starting peptide and could therefore not be performed on the sample obtained in this study.

Two of the qualitative radial diffusion assays demonstrated that the peptide was active as an antimicrobial peptide. Activity against *E. coli* (Figure 3.13i) and *S. aureus* (Figure 3.13ii) demonstrates that this peptide was able to inhibit the growth of both a Gram-negative and -positive bacterium. It also demonstrates that the regions of the *H. midae* haemocyanin analogous to the P3 and P4-P5 regions identified by Zhuang et al. (2015) exhibit a similar anti-proliferating activity. The primary issue was that the purified peptide was at a low concentration, which limited the choice of the available assays that could be performed. A higher concentration of peptide would have been optimal to determine the MIC of the peptide against specific bacterium and accurately determine the mode of action of inhibition. As the quantity of peptide was limited, the concentration of the bacterial cultures was adjusted to conclude an appropriate starting concentration at which the peptide could potentially inhibit *E. coli* and *S. aureus*.

4.3.1 Growth-inhibition assay

A significant decrease in growth was observed when a low starting concentration of the Gram-negative bacterium, *E. coli,* was incubated with approximately 1 µg of the haliotisin-like peptide (Figure 3.14). The Gram-positive bacterium, *S. aureus*, generally showed less growth in the presence of the peptide, but not to the same degree as *E. coli*, indicating that the peptide was better able to inhibit the growth of the Gram-negative bacterium.

The majority of bacterial organisms present in the marine environment are Gram-negative, except in the sediment (Gontang et al. 2007). As abalone inhabit primarily rocky shoreline regions, it is logical that the majority of the bacterial species that they would encounter are primarily Gram-negative and that their immune response would thus be better suited to preventing infection by members of the bacterial group that possess the thinner peptidoglycan layer.

In this assay, the thicker peptidoglycan layer present in the cell wall of *S. aureus* may inhibit the action of haliotisin because the AMP has to first pass through the peptidoglycan layer in order to gain access to the phospholipid bilayer (Neelay et al. 2017). The variability in thickness between Gram-positive and -negative

bacteria may account for the differing efficacy of the AMP to inhibit the growth of the two strains. While visualising bacterial cells under transmission electron microscopy, Zhuang et al. (2015) observed that the Gram-negative strain they tested displayed cell wall abnormalities, appearing damaged and irregular when incubated with the P4 region of their haliotisin peptide. This indicates that the P4 region, which matches the full helix found in this study, was interacting with the cell wall and disturbing it in some way; the peptide may be effectively interacting with the *E. coli* cell walls and damaging them in order to cause cell leakage and bacterial death. The isolated peptide showed inconclusive results for *V. anguillarum* in this study. The strain of *V. anguillarum* was not uniform in its growth on the plate (Supplementary Figure 5.6). This resulted in an inability to detect a zone of clearing with reference to the peptide. Due to the low quantity of peptide isolated the test could not be repeated. It is possible that because *V. anguillarum* was grown on tryptic soy agar, and the other bacteria were all grown on LA, that the additional sugar meant that the *Vibrio* were able to grow faster than the peptide was able to kill them. This can bee seen by a lack of a zone of clearing in the ampicillin control of *V. anguillarum*.

Zhuang et al. (2015) determined that the N-terminal amino acids were required for the proper functioning of the P3 peptide against the Gram-positive strain included in their study and suggested that this may be caused by these groups interacting with a specific epitope present on the *B. subtilis* cell wall. If this N-terminal portion is that important, it is possible that the his-tag present on the N-terminal end of the haliotisin-like peptide isolated in his study is inhibiting the antimicrobial action of the related P3 region when incubated with the two Gram-positive bacteria (*B. subtilis* and *S. aureus*), which could explain why the peptide showed lesser inhibitory effects against the *S. aureus* strain. To determine whether the his-tag blocks the activity of the P3 portion of the haliotisin-like peptide produced in the current study, the his-tag can be removed through treatment with a TEV protease which targets a site included in the pProEX vector.

4.4 Conclusion

In conclusion, functional units e–h of the *H. midae* haemocyanin were sequenced and showed phylogeny within the European and Australasian clade of Haliotidae evolution. The sequence showed the highest degree of similarity to the Australian black lip abalone, *H. rubra*. The isoform present in *H. midae* was the initial, older isoform 1 and no evidence of isoform 2 was found. The sequenced functional units contained FU-e, which has been shown to play a role in the immune response of invertebrates and this functional unit contained a region that matched the haliotisin peptide identified by Zhuang et al. (2015) with a high degree of similarity.

This haliotisin-like region was amplified from haemocyte DNA and cloned into an expression vector for recombinant expression in *E. coli* cells. The peptide obtained through recombinant expression was confirmed throughout several stages of this research project: the insert cloned into the vector was confirmed to have the correct DNA sequence; the size of the peptide produced was correct, as evidenced through SDS-PAGE analysis; the peptide contained the his-tag from the pProEX vector as evidenced through western blot analysis (Figure 3.8A) and because it bound to both the batch purification and the FPLC nickel-affinity column; and the peptide produced was bound by the anti-KLH antibody, indicating a region similar to that found within haemocyanin – which the *E. coli* host proteins lacked. Collectively, this information provides sufficient evidence to suggest that the produced peptide was the haliotisin-like peptide identified through sequence alignment.

After purification, this peptide showed activity against both a Gram-negative and -positive bacterial strain. The peptide was able to significantly inhibit the growth of *E. coli*, demonstrating a greater anti-proliferation activity against the Gram-negative bacterium. However, more testing must be conducted in order to gain further insight into this haliotisin-like peptide derived from the *H. midae* haemocyanin in terms of its regulation and function as a component of the abalone immune response.

This research has provided a basis of knowledge around haemocyanin, and more specifically haliotisin, within the *H. midae* immune response. This acts as confirmation that the haemocyanin protein that was found to be upregulated in response to bacterial infection previously, is having an effect in the immune response of abalone. Therefore, this research acts as a starting point for further study on haemocyanin, and haliotisin, so that one day it could be used as a marker for the identification and diagnosis of disease within abalone. If haemocyanin is being upregulated when *H. midae* is under bacterial challenge and having an effect on the immune response as shown, then by testing for elevated levels of haemocyanin within abalone it would act as a proxy for bacterial infection. However, more research needs to be conducted in order to gain a complete picture and this study acts as the starting point for said research.

5. Appendix

5.1 Supplementary data

5.1.1 SDS-PAGE gel recipe

In preparation for casting the electrophoresis gel a 4 X Tris·Cl SDS pH 8.8 (1.5 M Tris, 0.4% SDS) and a 4 X Tris·Cl SDS pH 6.8 (1.5 M Tris, 0.4% SDS) were made up and stored at 4°C. A 15% resolving gel was made up using 1 ml of acrylamide/bis-acrylamide 37:1 ratio (Merck) in a 1 X Tris·Cl SDS pH 8.8 solution made to a final volume of 5 ml. To initiate polymerisation, 50 µl of fresh ammonium persulfate (APS) and 5 µl of N, N, N', N'- tetramethyl ethylenediamine (TEMED) was added. This solution was cast into secured 10.1 x 7.3 cm glass plates, and 1 ml of isopropanol was added to ensure a smooth layer on the upper surface.

A 4% stacking gel was made up in a similar fashion, using 0.25 ml of acrylamide/bis-acrylamide 37:1 ratio (Merck) in a 1 X Tris·Cl SDS pH 6.8 solution to a final volume of 2.5 ml. The isopropanol was thoroughly removed from the gel rigging after an hour, when the resolving gel had set. To initiate polymerisation, 25 µl of fresh APS and 5 µl of TEMED was added to the stacking gel. The stacking gel was added above the resolving gel in the gel rigging. A comb was placed into the stacking gel to create appropriate spaces for sample loading. The stacking gel was allowed to set for one hour before being placed into the electrophoresis tank, the comb being removed, and the tank filled with 1 X running buffer (25 mM Tris, 192 mM glycine, 0.1% SDS).

5.1.2 Supplementary figures

A

>Partial *H. midae* haemocyanin DNA sequence (FU-e,f,g and h)

GTCAGAGCTTTGGAGGGAATGCAGAATGATCACTCCGCTGATGGATACCAAGCCATCGCTTCTTTCCATGCCCTGCCGCCACTC
TGCCCTAATCCAGCTGCAGCTCACCGTTTTGCTTGTTGTGTCCACGGTATGGCTACATTCCCCCAGTGGCACAGGCTGTACACT
GTACAGTTCCAGGATGCACTGAGAAGACATGGTTCACTTGTTGGTGTTCCGTACTGGGACTGGACGAAGCCAGTCGCCGAATT
ACCCAAGCTTCTTTCTTCGGAGACATTTCATGATCCAATCCACAATATTAATATTTCAAATCCATTCTTCCAAGCTGATATAGAAT
TCGAAGGAGCGGGCGTTCATACCGAGAGGCACATAAATGAAGATCGCCTGTTTCACAGTGGAGATCATGAGGGATACCATAA
CTGGTTCTTTGAGACTGTTCTCTTTGCTTTGGAACAGGAAGATTACTGCGATTTTGAAATACAGTTTGAGATAGCCCATAATGG
CATTCACACATGGCTTGGTGGAAACGCAGTACATGGCATGGGACACCTTCACTATGCTTCTTATGATCCAATCTTCTACGTCCAC
CATTCACAGACAGACAGAATATGGGCTATTTGGCAAGAGCTGCAGAAGTACAGGGGCCTATCTGGTTCAGAAGCAAACTGTG
CCATTGAACATATGAGAACACCTTTGAAGCCCTTCAGCTTTGGGCCACCTTACAATTTGAATCATCATACGCAAGAATTTTCAAA
GCCTGAGGACACTTTTGACTATAAGAAGTTTGGATACAGATATGATAGTCTGGAATTGGAGGGACGGTCAATTGCTCATCTTG
ATGAACTTATCAAGGAAAGACAGGAGCAAGACAGAACTTTTGCAGGGTTCCTTCTTAAAGGTTTTGGTACTTCCGCAACTGTGT
CATTCGAAATTTGCAGAGTTGATCACACCTGTGAAAAAGCCGGGTATTTCACTATTCTGGGAGGATCCGCAGAAATGCCATGG
GTGTTCGACAGGCTCTACAAGTACGACATTACTAAAACTCTCCACGATATGCACCTGAGGCCCGAGGATACCTTCTCTGTAAAA
GTAACTGTCACTTCTTACAATGGAACAGTACTCTCGGGAGACCTCATCCAGACACCGTCCATCATATTTGTACCTGGGCGCCAT
AAGCTAAATTCACGGAAACATGCACCTAACAAGATCCGCCATGAGTTAAGTAGCCTTAGTTCCCGTAACATAGCAAGCTTGAA
GGCTGCGTTGACAAGTCTTCAACATGATAGTGGAACTGATGGTTATCAAGCCACTGCTGCATTCCATGGCGTCCCTGCGCAGT
GCCACGATGCATCTGGACGTGAGATCGCTTGTTGCATCCATGGTATGGCGACATTCCCCGACTGGCACAGGTTGTACACCCTCC
AGTTGGAACAGGCCTTGAGCAGACATGGTTCCAGTGTTGCGGTGCCTTACTGGGATTGGACCAAGCCAATTACTGAACTACCA
CACCTTTTGACAGATGGAGAATATTACGATGTTTGGCAAAATGCCGTCATAACCAATCCATTTGCAAGAGGTTATGTGAAATTT
AAAGATGCATTCACAGTGAGAAATGTCCAGGAAGGTCTGTTCAAAATGTCAACTTTTGGAAAGCACTCACTTCTGTTTGACCAG
GCTTTGTTGGCTCTTGAACAAACTGACTACTGTGACTTCGAAGTTCAGTTTGAAGTGATGCACAACACGATCCACTATCTCGTTG
GAGGACGTCAAACGTACGCCTTCTCCTCTCTTGAGTATTCATCATACGATCCAATCTTCTTTATCCATCACTCATTTGTTGACAAA
ATATGGCCTGTATGGCAAGAACTGCAAAGCAGGAGACATCTACAGTATAAGGCAGCTGATTGTGCTGTGCGGCTAATGAGTA
AGGCAATGAGACCTTTCAACAAGGATTTCAACCACAACTCATTCACGAAGAAGCATGCAGTTCCAAATACAGTATTTGACTATG
AAGATCTTGGCTATAACTATGACAACCTTGAACTCAGTGGTTTGAACCTGAATGAAATCGAGGCGTTGATATCAAAACGAAAG
TCACATGCTAGAGTCTTTGCTGGTTTCCTGTTGTTTGGACTAGGAACCTCGGCTGATATACATCTGGACATTTGCAAGACATCC
GAAAACTGCCATCATGCTGGTGTGATCTTCATCCTGGGAGGTTCTGCAGAGATGCATTGGGCATACAACCGACTCTACAAGTA
TGATATTACAGAAGCACTGCATGAATTTGACATCAACCCTGAAGATGTTTTCCATGCTGATGAACCATTTTTCCTGAAGCTGTCT
GTGGTTGCTGTGGATGGGACTGTCATTCCATCGCCTCGCCTTCACCAGCCAACAATAATTTATGAACCAGGAGAAGGTCATCAT
GATGACCACGAGTCGGGAAGCATAGCAGGATCTGGTGTCCGCAAGGACGTGAACACCCTTACAAAAGCTGAGACTGACAACC
TGAGGGAAGCACTTCAAGGTGTAATGGACGACCATGGTCCCAATGGCTTTCAAGCCATTGCTGCTTTCCATGGAAAACCAGCT
TTGTGTCCCATGCCTGATGGTCACAACTACTCATGTTGCACTCATGGCATGGCTACCTTCCCACACTGGCATCGCCTCTACACGA
AGCACATGGAAGATGCATTGAAGGCTCACGGATCTCTCGTTGGCCTCCCCTACTGGGACTGGACTACTGCCTTTACCCATCTGC
CAACACTTGTCACCGACACCGAAAACAACCCTTTCAACCATGGCCACATTGAGTATCTCAATGTCGACACAACCCGTTCTCCCAG
AGACATGCTGTTCAACGACCCCGAGCACGGATCAGAGTCGTTCTTCTACAGACAAGTCCTTTTTGCTCTGGAGCAAACTGATTT
CTGCAAGTTCGAGGTTCAGTATGAGATAACCCACAATGCTATCCATTCCTGGACAGGTGGCCACAGTCCTTATGGTATGTCCAC
TCTCGACTTCACTGCCTACGATCCACTGTTCTGGCTACATCACTCCAACACGGATAGAATCTGGGCTATCTGGCAAGCTTTGCAA
GAATACAGAGGACTCCCATACAACCATGCCAATTGTGAGATCCAGGCAATGAAAACGCCCCTGAGGCCTTTCAGTGACGATAT
CAACCATAATCCAGTCACAAAGGCTAACTCAAAGCCGGTAGATGTGTTCGAGTATAATCGGTTAAGCTTCCAGTACGACACCCT
CATTTTCCATGGGTATAGTATTCCGGAACTTGATCACATGCTTGAAGAAAGGAAGAAGGAAGACAGAATATTTGCCGCCTTCCT
TCTCAGTGGAATCAAGCAAAGTGCTGATGTAGTTTTCGATGTATGCCAACCAGGTCACGAATGTGTGTTTGCAGGCACTTTTGC
GATCTTGGGAGGAGAGCTTGAAATGCCCTGGTCCTTTGACAGACTGTTCCGCTATGACATCACCAAAGTCATGAAACAGCTGC
ACCTGAGACACGATTCGGACTTTACGTTTAGGGTGAAGATTGTCGGCACTGACGAACACGAGCTTCCTTCTGACAGTTTCAAA

GCACCAACTATTGAATTTGAACCAGGGGTACACGACGGAGAGAAACACGACGGTGGTCATCATGACGACAGACACTCAGATG
TCCTGATCAGAAAAGAAGTTGACTTCCTCTCCCTGCAGGAGGCCAATGCCATTAAGGATGCACTGTACAAGCTCCAGAATGAC
AACGGTAAAGGAGGCTTTGAGGCCATAGCTGGCTATCACGGGTATCCTAATATGTGCCCAGAAAAAGAGACCGACAAGTATC
CGTGCTGCGTCCATGAAATGCCTGTGTTCCCTCACTGGCATCGCCTGCATACCATTCAGATGGAGAGAGCTCTTAAAAACCATG
GTTCGCCGATGGGCATTCCTTATTGGGATTGGACAAAGAAGATGTCGAGTCTTCCAGCATTCTTTGCAGATTCCGGTAATGGCA
ACCCCTTCTACAAATATCATATAAGGGGTGTGCAACATGAAACAACCAGGGAAATTAATCCTAGTATCTTTAATCAGACCAAGT
TTGGTGAATATGATTACCTATACTACCTGACTCTGCAAGTCCTGGAAGAAAACTCATACTGCGACTTTGAGGTACAGTATGAGA
TCCTTCACAACGCCATCCATGCCTGGCTTGGAGGATCTGGAAAGTATTCAATGTCTACCCTTGAGTATTCAGCTTTTGACCCTGT
CTTCATGATTCATCACTCTAGTTTGGATAGAATCTGGATCCTTTGGCAGAAGTTGCAAAAGAGAAGAATGAAGCCTTACTACGC
AATAGACTGTGCTGGAGATAGACTAATGAAGTCCCCCTTGCATCCCTTTAACTACGAAACCGTCAATGAAGATGAGTTCACTCG
AATCAACTCTTACCCAAACATAGTGTTTGACCACTACAGGTTCAACTATGAATACGATAACTTGAGAGTCAGAGGTCATGACAT
ACATGAGCTTGAAGACGTACTTAAGGAATTAAGACACAAAGATCGCATATTTGCTGGTTTTGTTTTGTCGGGCTTACGGATATC
AGCTACAGTGAAAGTATTCATTCATTCGAAAAATGCAACAAGTCACGAAGAATATGC

B

> Amino acid sequence of the *H. midae* carboxyl portion of the haemocyanin derived from the nucleotide sequence

VRALEGMQNDHSADGYQAIASFHALPPLCPNPAAAHRFACCVHGMATFPQWHRLYTVQFQDALRRHGSLVGVPYWDWTKPVA
ELPKLLSSETFHDPIHNINISNPFFQADIEFEGAGVHTERHINEDRLFHSGDHEGYHNWFFETVLFALEQEDYCDFEIQFEIAHNGIHT
WLGGNAVHGMGHLHYASYDPIFYVHHSQTDRIWAIWQELQKYRGLSGSEANCAIEHMRTPLKPFSFGPPYNLNHHTQEFSKPEDT
FDYKKFGYRYDSLELEGRSIAHLDELIKERQEQDRTFAGFLLKGFGTSATVSFEICRVDHTCEKAGYFTILGGSAEMPWVFDRLYKYDIT
KTLHDMHLRPEDTFSVKVTVTSYNGTVLSGDLIQTPSIIFVPGRHKLNSRKHAPNKIRHELSSLSSRNIASLKAALTSLQHDSGTDGYQA
TAAFHGVPAQCHDASGREIACCIHGMATFPDWHRLYTLQLEQALSRHGSSVAVPYWDWTKPITELPHLLTDGEYYDVWQNAVITN
PFARGYVKFKDAFTVRNVQEGLFKMSTFGKHSLLFDQALLALEQTDYCDFEVQFEVMHNTIHYLVGGRQTYAFSSLEYSSYDPIFFIH
HSFVDKIWPVWQELQSRRHLQYKAADCAVRLMSKAMRPFNKDFNHNSFTKKHAVPNTVFDYEDLGYNYDNLELSGLNLNEIEALIS
KRKSHARVFAGFLLFGLGTSADIHLDICKTSENCHHAGVIFILGGSAEMHWAYNRLYKYDITEALHEFDINPEDVFHADEPFFLKLSVV
AVDGTVIPSPRLHQPTIIYEPGEGHHDDHESGSIAGSGVRKDVNTLTKAETDNLREALQGVMDDHGPNGFQAIAAFHGKPALCPM
PDGHNYSCCTHGMATFPHWHRLYTKHMEDALKAHGSLVGLPYWDWTTAFTHLPTLVTDTENNPFNHGHIEYLNVDTTRSPRDM
LFNDPEHGSESFFYRQVLFALEQTDFCKFEVQYEITHNAIHSWTGGHSPYGMSTLDFTAYDPLFWLHHSNTDRIWAIWQALQEYRG
LPYNHANCEIQAMKTPLRPFSDDINHNPVTKANSKPVDVFEYNRLSFQYDTLIFHGYSIPELDHMLEERKKEDRIFAAFLLSGIKQSAD
VVFDVCQPGHECVFAGTFAILGGELEMPWSFDRLFRYDITKVMKQLHLRHDSDFTFRVKIVGTDEHELPSDSFKAPTIEFEPGVHDG
EKHDGGHHDDRHSDVLIRKEVDFLSLQEANAIKDALYKLQNDNGKGGFEAIAGYHGYPNMCPEKETDKYPCCVHEMPVFPHWHR
LHTIQMERALKNHGSPMGIPYWDWTKKMSSLPAFFADSGNGNPFYKYHIRGVQHETTREINPSIFNQTKFGEYDYLYYLTLQVLEEN
SYCDFEVQYEILHNAIHAWLGGSGKYSMSTLEYSAFDPVFMIHHSSLDRIWILWQKLQKRRMKPYYAIDCAGDRLMKSPLHPFNYET
VNEDEFTRINSYPNIVFDHYRFNYEYDNLRVRGHDIHELEDVLKELRHKDRIFAGFVLSGLRISATVKVFIHSKNATSHEEY

Supplementary Figure 5.1: **A** The partial DNA sequence of haemocyanin from *H. midae* obtained through this study. Sequencing primer regions highlighted in green. Cloning primer sites highlighted in grey. **B** Translated region of frame +1 with the haliotisin peptide region highlighted in blue.

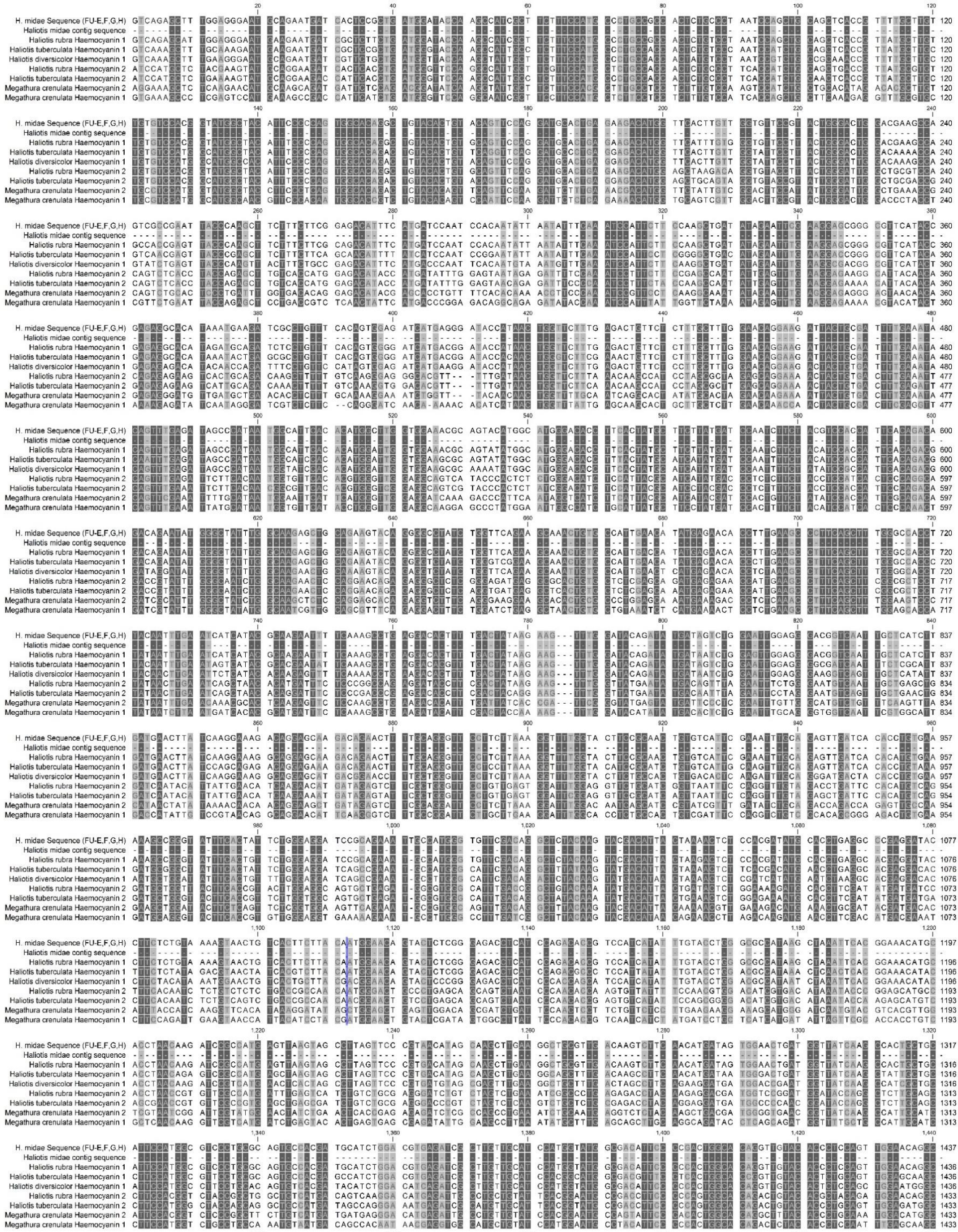
H. midae Sequence (FU-E,F,G,H)
Haliotis midae contig sequence
Haliotis rubra Haemocyanin 1
Haliotis tuberculata Haemocyanin 1
Haliotis diversicolor Haemocyanin 1
Haliotis rubra Haemocyanin 2
Haliotis tuberculata Haemocyanin 2
Megathura crenulata Haemocyanin 2
Megathura crenulata Haemocyanin 1

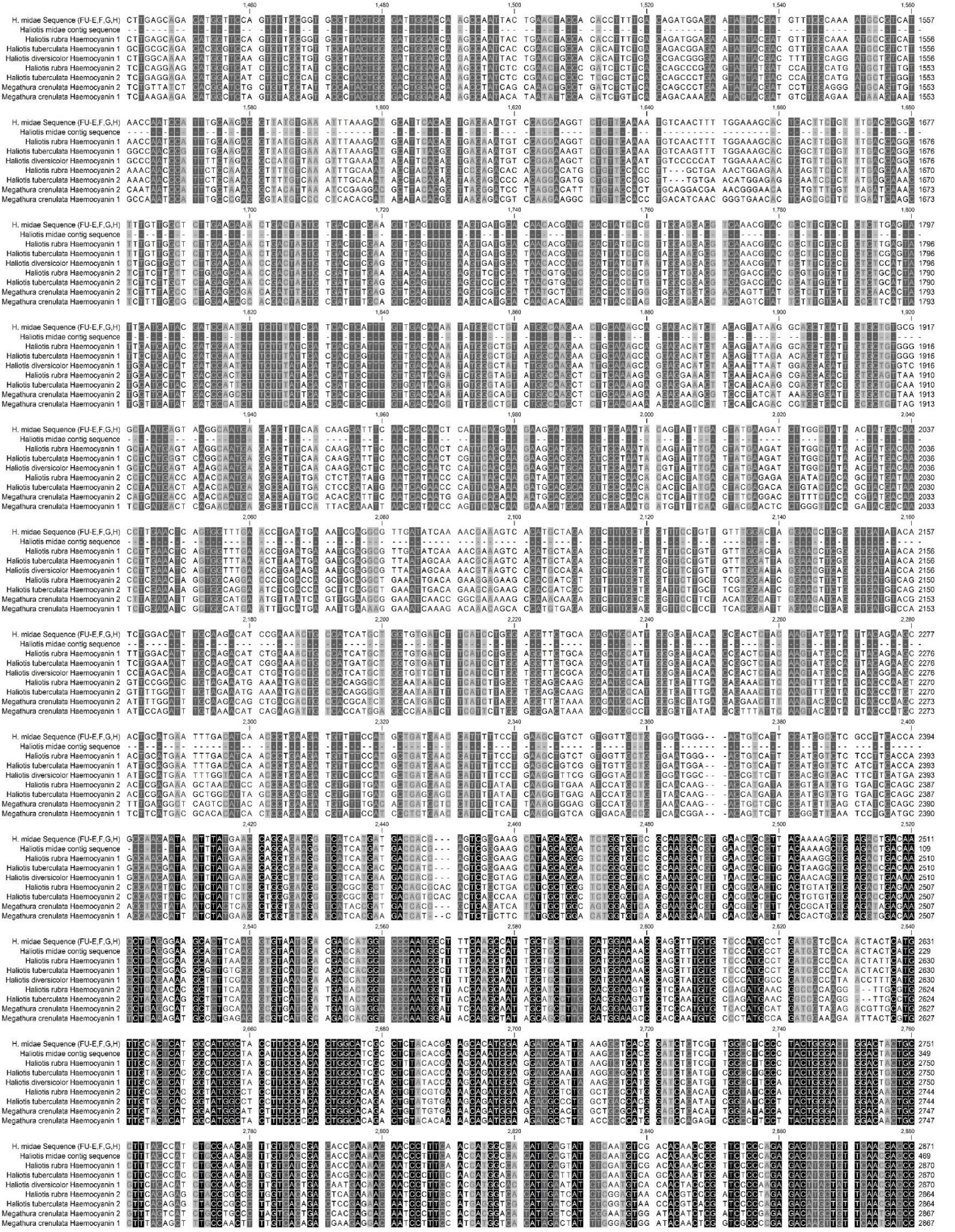
H. midae Sequence (FU-E,F,G,H)
Haliotis midae contig sequence
Haliotis rubra Haemocyanin 1
Haliotis tuberculata Haemocyanin 1
Haliotis diversicolor Haemocyanin 1
Haliotis rubra Haemocyanin 2
Haliotis tuberculata Haemocyanin 2
Megathura crenulata Haemocyanin 2
Megathura crenulata Haemocyanin 1

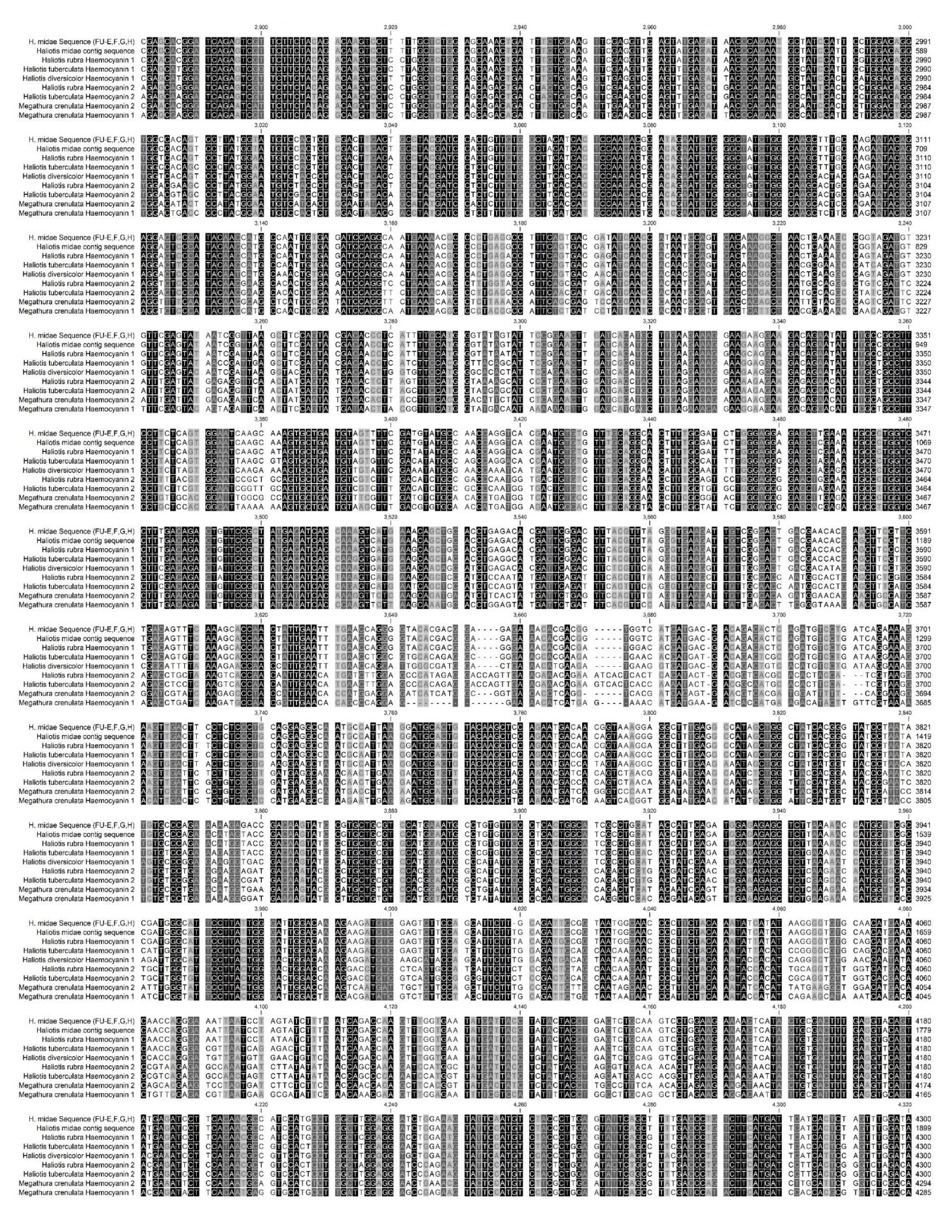
H. midae Sequence (FU-E,F,G,H)
Haliotis midae contig sequence
Haliotis rubra Haemocyanin 1
Haliotis tuberculata Haemocyanin 1
Haliotis diversicolor Haemocyanin 1
Haliotis rubra Haemocyanin 2
Haliotis tuberculata Haemocyanin 2
Megathura crenulata Haemocyanin 2
Megathura crenulata Haemocyanin 1

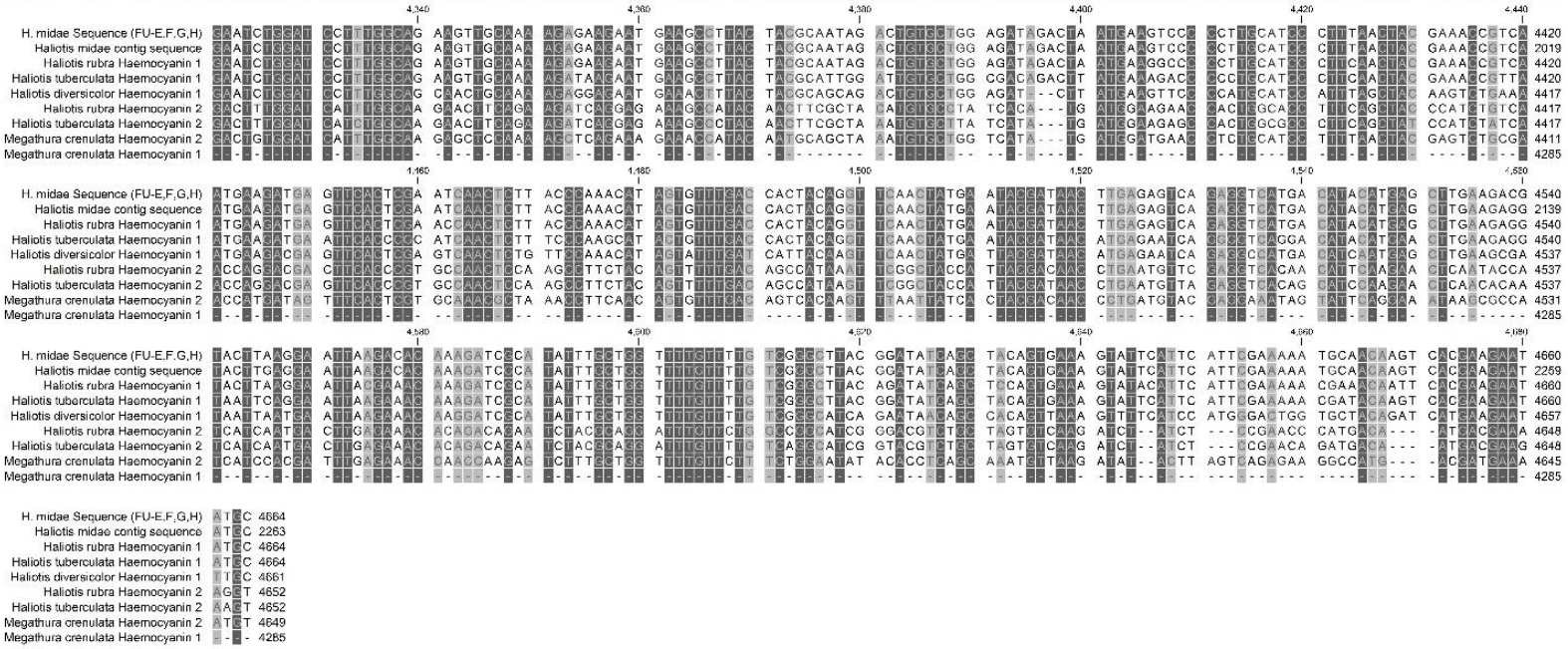

Supplementary Figure 5.2: Full sequence obtained for carboxyl portion of the *H. midae* haemocyanin (*H. midae* sequence (FU-E, F, G, H)) aligned to other haemocyanin sequences from the NCBI database. The darker shaded regions indicate conserved nucleotide residues.

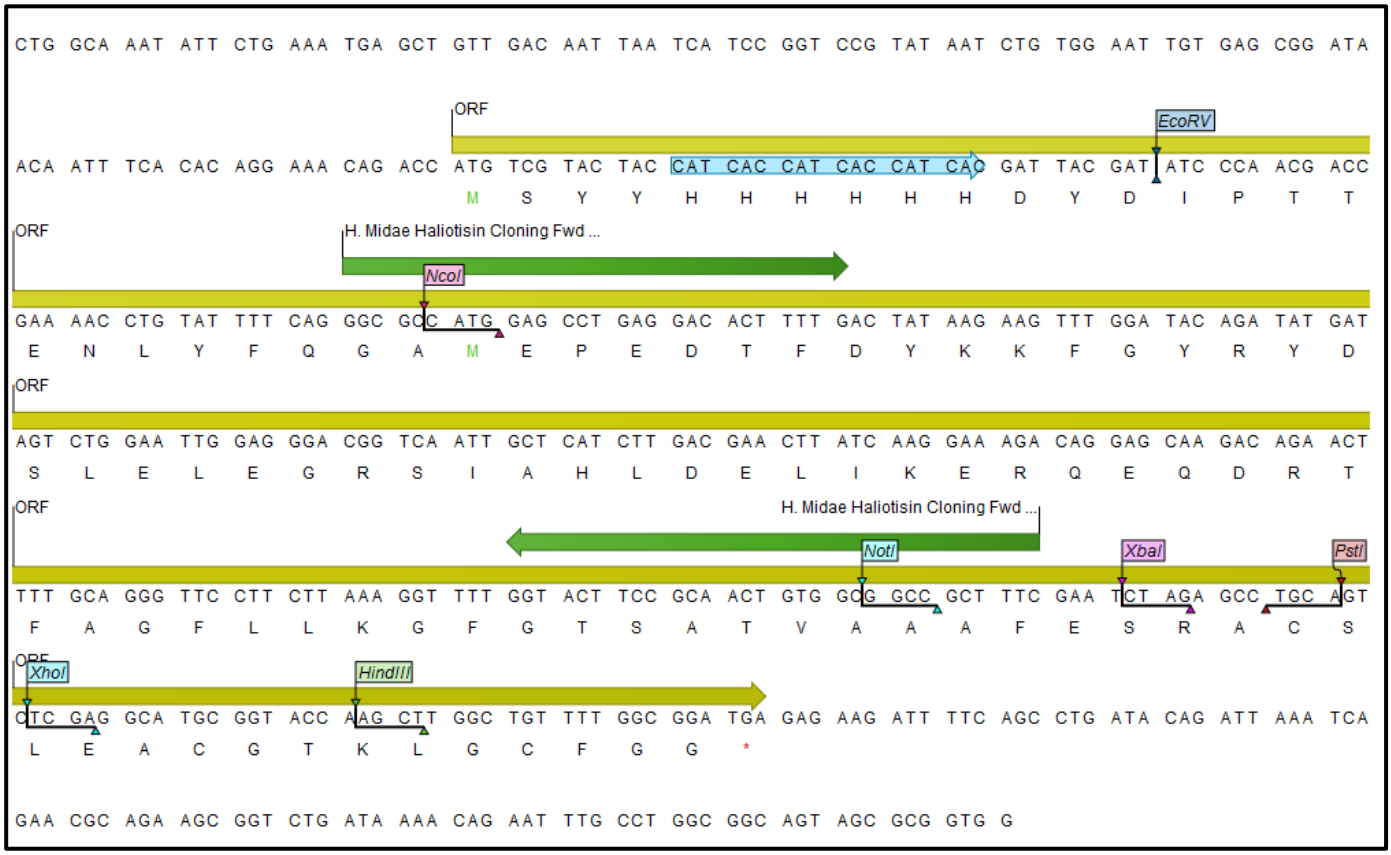

Supplementary Figure 5.3: Sequencing results of the cloned region of haliotisin within the pProEX vector. Yellow arrow indicates the open reading frame (ORF) for the multiple cloning site including the expected haliotisin peptide. The blue arrow indicates the 6-his tag presented by the pProEX vector.

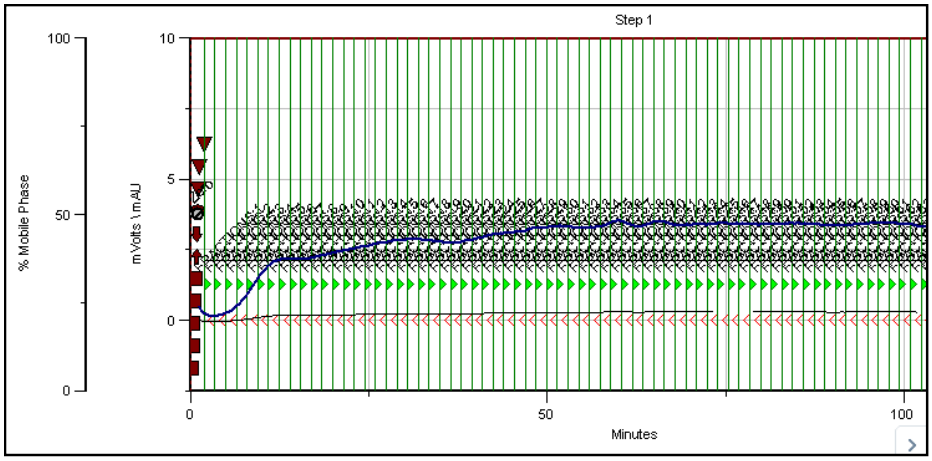

Supplementary Figure 5.4: Profile of the size exclusion chromatography of dialysed samples containing haliotisin peptide.

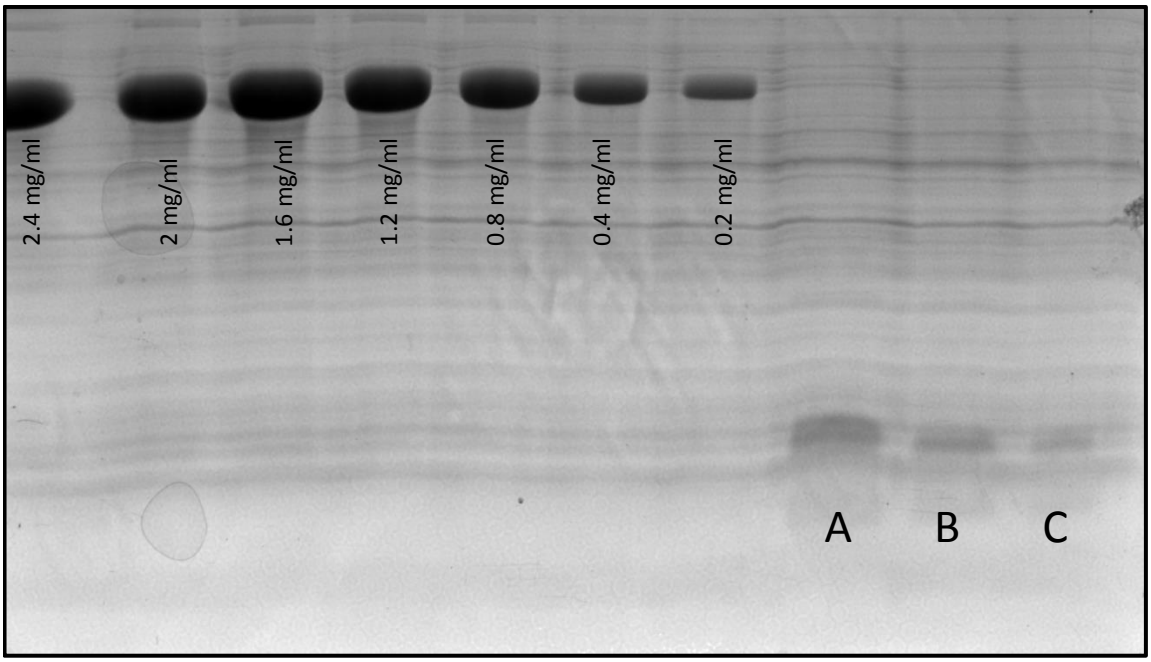

Supplementary Figure 5.5: SDS-PAGE showing the deduced concentrations of the *H. midae* peptide samples compared to known amounts of BSA. The concentration of BSA ranged between 0.2 mg/ml to 2.4 mg/ml as indicated in the figure. The *H. midae* peptide was added undiluted (A), 1:2 dilution (B) and 1:5 dilution (C)

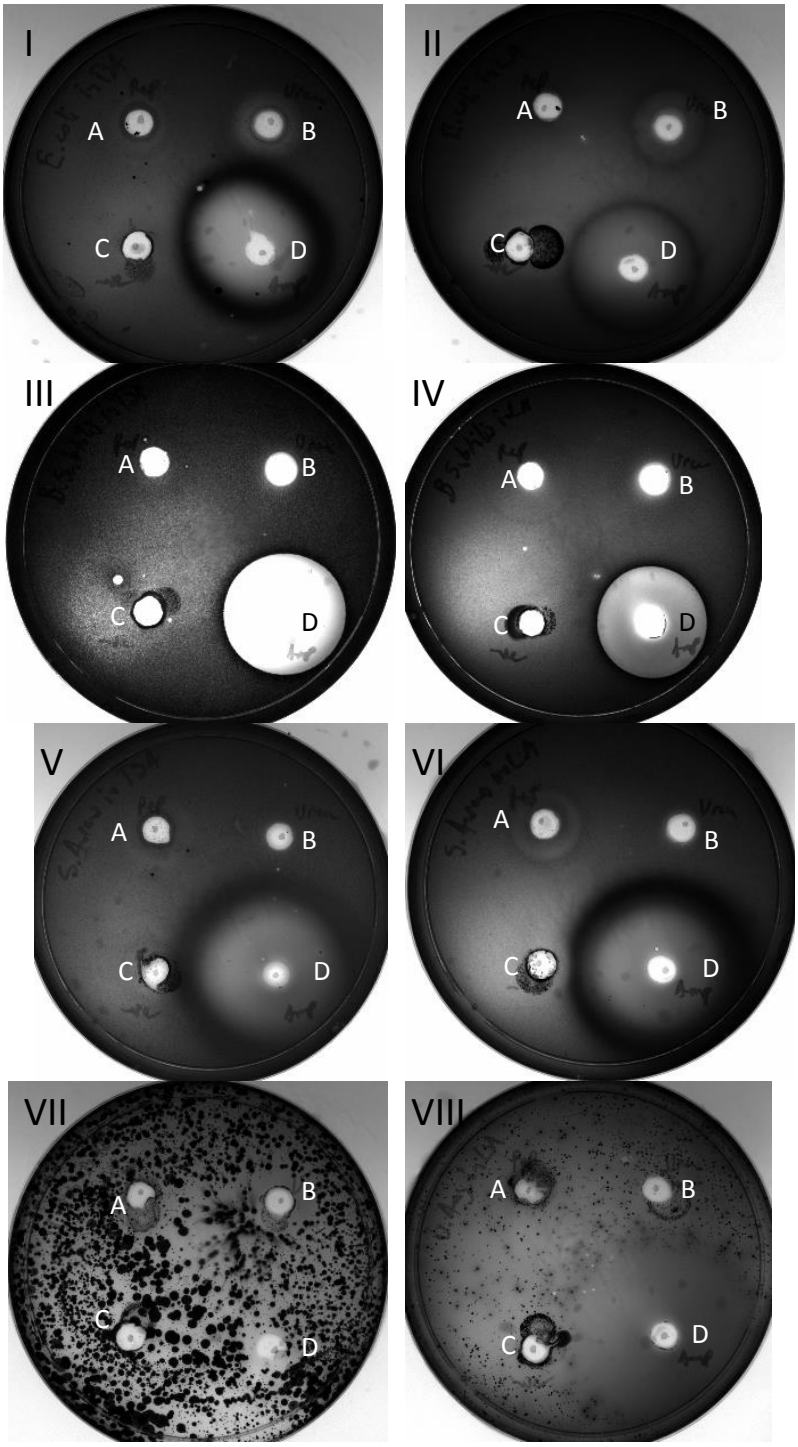

Supplementary Figure 5.6: Coomassie stained bacterial spread plates of the 4 different strains tested by the radial diffusion assay for susceptibility to the putative *H. midae* haliotisin-like peptide. *E. coli* on TSA (I) and LA (II), *B. subtilis* on TSA (III) and LA (IV), *S. aureus* on TSA (V) and LA (VI) and *V. anguillarum* on TSA (VII) and LA (VIII). Each strain was tested against the peptide solution purified by FPLC (A), 8M urea buffer (B), native buffer (C) and an equal concentration of ampicillin (D).

5.2 Cited Literature

Adachi, K. et al., 2005. An oxygen transporter hemocyanin can act on the late pathway of melanin synthesis. *Pigment Cell Research*, 19(3), pp.214–219.

Altenhein, B., Markl, J. & Lieb, B., 2002. Gene structure and hemocyanin isoform HtH2 from the mollusc Haliotis tuberculata indicate early and late intron hot spots. *Gene*, 301(1–2), pp.53–60. Available at: http://www.ncbi.nlm.nih.gov/pubmed/12490323.

Altschul, S.F. et al., 1990. Basic local alignment search tool. *Journal of Molecular Biology*, 215(3), pp.403–410.

Arechavala-Lopez, P. et al., 2013. Reared fish, farmed escapees and wild fish stocks - A triangle of pathogen transmission of concern to Mediterranean aquaculture management. *Aquaculture Environment Interactions*, 3(2), pp.153–161.

Balcázar, J.L. et al., 2006. The role of probiotics in aquaculture. *Veterinary Microbiology*, 114(3–4), pp.173–186.

Bayne, C.J., 1990. Phagocytosis and Non-Self Recognition in Invertebrates. *Bioscience*, 40(10), pp.723–731.

Beltran, C.G.G., 2015. *A Proteomic Investigation of the immune response of the South African Abalone, Haliotis Midae*. University of Cape Town.

Bierbaum, G. & Sahl, H.-G., 1985. Induction of autolysis of staphylococci by the basic peptide antibiotics Pep 5 and nisin and their influence on the activity of autolytic enzymes. *Archives of Microbiology*, 141(3), pp.249–254. Available at: https://doi.org/10.1007/BF00408067.

Boman, H.G., 2003. Antibacterial peptides: Basic facts and emerging concepts. *Journal of Internal Medicine*, 254(3), pp.197–215.

Bondad-Reantaso, M.G. et al., 2005. Disease and health management in Asian aquaculture. *veterinary parasitology*, (4), pp.157–170.

Bondos, S.E. & Bicknell, A., 2003. Detection and prevention of protein aggregation before, during, and after purification. *Analytical Biochemistry*, 316(2), pp.223–231. Available at: http://www.sciencedirect.com/science/article/pii/S0003269703000599.

Bower, S.M., McGladdery, S.E. & Price, I.M., 1994. Synopsis of infectious diseases and parasites of commercially exploited shellfish. *Annual Review of Fish Diseases*, 4, pp.1–199. Available at: http://www.sciencedirect.com/science/article/pii/0959803094900280.

Brogden, K.A., 2005. Antimicrobial peptides: Pore formers or metabolic inhibitors in bacteria? *Nature Reviews Microbiology*, 3(3), pp.238–250.

Bulet, P., Stöcklin, R. & Menin, L., 2004. Anti-microbial peptides: from invertebrates to vertebrates. *Immunological Reviews*, 198, pp.169–184. Available at: http://www.ncbi.nlm.nih.gov/pubmed/15199962.

Canesi, L. et al., 2002. Bacteria–hemocyte interactions and phagocytosis in marine bivalves. *Microscopy Research and Technique*, 57(6), pp.469–476. Available at: https://doi.org/10.1002/jemt.10100.

Canesi, L. et al., 2006. Cell signalling in the immune response of mussel hemocytes. *Developmental &*

Comparative Immunology, 26(4), pp.325–334.

Cardinaud, M. et al., 2015. The early stages of the immune response of the European abalone Haliotis tuberculata to a Vibrio harveyi infection. *Developmental and Comparative Immunology*, 51(2), pp.287–297.

Casas, S.M. et al., 2011. Comparison of antibacterial activity in the hemolymph of marine bivalves from Galicia (NW Spain). *Journal of Invertebrate Pathology*, 106(2), pp.343–345.

Cerenius, L., Lee, B.L. & Söderhäll, K., 2008. The proPO-system: pros and cons for its role in invertebrate immunity. *Trends in Immunology*, 29(6), pp.263–271.

Chacon, O. et al., 2003. Circadian metabolic rate and short-term response of juvenile Green abalone (Haliotis Fulgens Philippi) to three anesthetics. *Journal of shellfish Research*, 22(May 2014), pp.415–421.

Clarke, D.T., 2011. Circular Dichroism and Its Use in Protein-Folding Studies BT - Protein Folding, Misfolding, and Disease: Methods and Protocols. In A. F. Hill et al., eds. Totowa, NJ: Humana Press, pp. 59–72. Available at: https://doi.org/10.1007/978-1-60327-223-0_5.

Coates, C.J. & Nairn, J., 2014. Diverse immune functions of hemocyanins. *Developmental and Comparative Immunology*, 45(1), pp.43–55.

Cook, P. & Gordon H, R., 2010. World Abalone supply, markets and pricing. *Journal of Shellfish Research*, 29(3), pp.569–571.

Cook, P.A., 2014. The Worldwide Abalone Industry. *Scientific Research*, 5(December), pp.1181–1186.

Corbeil, S. et al., 2016. Australian abalone (Haliotis laevigata, H. rubra and H. conicopora) are susceptible to infection by multiple abalone herpesvirus genotypes. *Diseses of aquatic organisms*, 119(5), pp.101–106.

Dagert, M. & Ehrlich, D., 1979. Prolonged incubation In calcium chloride improves the competence Of Escherichia coli cells. *Gene*, 6, pp.23–28. Available at: https://journals-scholarsportal-info.libaccess.lib.mcmaster.ca/pdf/03781119/v06i0001/23_piiccitcoecc.xml.

Dang, V.T., Benkendorff, K. & Speck, P., 2011. In vitro antiviral activity against herpes simplex virus in the abalone Haliotis laevigata. *Journal of General Virology*, 92(3), pp.627–637.

Decker, H. et al., 2007. Minireview: Recent progress in hemocyanin research. *Integrative and Comparative Biology*, 47(4), pp.631–644.

Department of Agriculture Forestry and Fisheries, 2016. *Aquaculture Yearbook 2016 South Africa*, Available at: https://www.nda.agric.za/doaDev/sideMenu/fisheries/03_areasofwork/Aquaculture/AquaDocumentation/DAFF Yearbook 2016.5Mb.pdf.

Destoumieux-Garzón, D. et al., 2001. Crustacean immunity: Antifungal peptides are generated from the C terminus of shrimp hemocyanin in response to microbial challenge. *Journal of Biological Chemistry*, 276(50), pp.47070–47077.

Dhople, V., Krukemeyer, A. & Ramamoorthy, A., 2006. The human beta-defensin-3 , an antibacterial peptide with multiple biological functions. , 1758, pp.1499–1512.

Dimarcq, J.-L. et al., 1998. Cysteine-Rich Antimicrobial Peptides in Invertebrates. *Peptide Science*, 47(January), pp.465–477.

Dixon, J., Gulliver, A. & Gibbon, D., 2001. Farming Systems and Poverty. In M. Hall, ed. *Farming Systems and Poverty*. FAO and the World Bank.

Dixon, M.G., Hecht, T. & Brandt, C.R., 1991. Identification and treatment of a Clostridium and Vibrio infection in South African abalone, Haliotis midae L. *Journal of Fish Diseases*, 14(6), pp.693–695. Available at: https://doi.org/10.1111/j.1365-2761.1991.tb00629.x.

Dolashka, P. & Voelter, W., 2013. Antiviral activity of hemocyanins. *International Journal of Science*, 10, pp.120–127. Available at: http://www.isj.unimo.it/articoli/ISJ301.pdf.

Ellis, R.P. et al., 2011. Immunological function in marine invertebrates: Responses to environmental perturbation. *Fish and Shellfish Immunology*, 30(6), pp.1209–1222.

FAO, 2016. Brief on fisheries , aquaculture and climate change in the AR5. *Food and Agriculture Organisation*.

Franchini, P., Van Der Merwe, M. & Roodt-Wilding, R., 2011. Transcriptome characterization of the South African abalone Haliotis midae using. *BMC Research Notes*, 4(59).

Fredrick, W.S. & Ravichandran, S., 2012. Hemolymph proteins in marine crustaceans. *Asian Pacific Journal of Tropical Biomedicine*, 2(6), pp.496–502.

Ghosh, J. et al., 2011. Invertebrate immune diversity. *Developmental and Comparative Immunology*, 35(9), pp.959–974.

Girón-pérez, M.I., 2010. Relationships between innate immunity in bivalve molluscs and environmental pollution. *Exposure*, 7(2), pp.149–156. Available at: http://www.isj.unimo.it/articoli/ISJ212.pdf.

Gontang, E.A., Fenical, W. & Jensen, P.R., 2007. Phylogenetic diversity of gram-positive bacteria cultured from marine sediments. *Applied and Environmental Microbiology*, 73(10), pp.3272–3282.

Haldar, S. & Chatterjee, S., 2012. Vibrio Related Diseases in Aquaculture and Development of Rapid and Accurate Identification Methods. *Journal of Marine Science: Research & Development*, 1. Available at: https://www.omicsonline.org/vibrio-related-diseases-in-aquaculture-and-development-of-rapid-and-accurate-identification-methods-2155-9910.S1-002.php?aid=6125.

Handlinger, J. et al., 2005. Bacterial infection in Tasmanian farmed abalone: causes, pathology, farm factors and control options. *Diseases in Asian aquaculture 5: proceedings of the fifth Symposium on Diseases in Asian Aquaculture, 24-28 November 2002, Queensland, Australia.*, pp.11–299. Available at: http://search.proquest.com/docview/19380684?accountid=14643%5Cnhttp://mlbsfx.sibi.usp.br:3410/sfxlcl41?url_ver=Z39.88-2004&rft_val_fmt=info:ofi/fmt:kev:mtx:book&genre=conference&sid=ProQ:Aquatic+Science+&+Fisheries+Abstracts+(ASFA)+Aquaculture+Abstracts&a.

Harris, J.R. et al., 2000. Haliotis tuberculata hemocyanin (HtH): Analysis of oligomeric stability of HtH1 and HtH2, and comparison with keyhole limpet hemocyanin KLH1 and KLH2. *Micron*, 31(6), pp.613–622.

Van Holde, K.E., Miller, K.I. & Decker, H., 2001. Hemocyanins and Invertebrate Evolution. *Journal of*

Biological Chemistry, 276(19), pp.15563–15566.

Hooper, C. et al., 2011. Effect of movement stress on immune function in farmed Australian abalone (hybrid Haliotis laevigata and Haliotis rubra). *Aquaculture*, (May).

Hooper, C. et al., 2014. Effects of severe heat stress on immune function, biochemistry and histopathology in farmed Australian abalone (hybrid Haliotis laevigata×Haliotis rubra). *Aquaculture*, 432(October), pp.26–37. Available at: http://dx.doi.org/10.1016/j.aquaculture.2014.03.032.

Hooper, C. et al., 2007. Stress and immune responses in abalone: Limitations in current knowledge and investigative methods based on other models. *Fish and Shellfish Immunology*, 22(4), pp.363–379.

Horstman, D.A. et al., 1991. Red tides in False Bay , 1959-1989 , with particular reference to recent blooms of Gymnodinium sp . *Transactions of the Royal Society of South Africa*, 47(September), pp.611–628.

Hristova, R. et al., 2008. o-Diphenol oxidase activity of molluscan hemocyanins. *Comparative Biochemistry and Physiology*, 149(3), pp.439–446.

James, N., 2018. Aquaculture outlook 2018 : a mixed bag. *Perspectives in aquaculture*, (february), p.2018.

Kataoka, M. & Goto, Y., 1996. X-ray solution scattering studies of protein folding. *Folding and Design*, 1(5), pp.107–114.

Keller, H. et al., 1999. Abalone (Haliotis tuberculata) hemocyanin type 1 (HtH1. *European Journal of Biochemistry*, 264(1), pp.27–38.

Kelley, L.A. et al., 2015. The Phyre2 web portal for protein modeling, prediction and analysis. *Nature Protocols*, 10, p.845. Available at: https://doi.org/10.1038/nprot.2015.053.

Kesarcodi-Watson, A. et al., 2008. Probiotics in aquaculture: The need, principles and mechanisms of action and screening processes. *Aquaculture*, 274(1), pp.1–14.

Kilian, A., 2016. Abalone spearheading SA's aquaculture sector. *Engineering News*. Available at: http://www.engineeringnews.co.za/article/abalone-spearheading-sas-aquaculture-sector-2016-03-09 [Accessed January 1, 2019].

Kostadinova, E. et al., 2013. Positions of the glycans in molluscan hemocyanin, determined by fluorescence spectroscopy. *Journal of Fluorescence*, 23(4), pp.753–760.

Koutsogiannaki, S. & Kaloyianni, M., 2010. Signaling molecules involved in immune responses in mussels Abstract Immune system of molluscs is constituted by hemocytes and humoral factors that cooperate for the protection of the organism , triggering a wide range of immune responses . In molluscs , . *Zoology*, pp.11–21.

Kragol, G. et al., 2001. The antibacterial peptide pyrrhocoricin inhibits the ATPase actions of DnaK and prevents chaperone-assisted protein folding. *Biochemistry*, 40(10), pp.3016–3026.

Lafferty, K.D. et al., 2015. Infectious Diseases Affect Marine Fisheries and Aquaculture Economics. *Annual Review of Marine Science*, 7, pp.471–96.

Lafferty, K.D. & Kuris, A.M., 1993. Mass mortality of abalone Haliotis cracherodii on the California Channel Islands: tests of epidemiological hypotheses. *Marine Ecology Progress Series*, 96(3),

pp.239–248.

Lee, K.-K., Liu, P.-C. & Huang, C.-Y., 2003. Vibrio parahaemolyticus infectious for both humans and edible mollusk abalone. *Microbes and Infection*, 5(6), pp.481–485. Available at: http://www.sciencedirect.com/science/article/pii/S1286457903000650.

Lee, S.Y., Lee, B.L. & Söderhäll, K., 2003. Processing of an antibacterial peptide from hemocyanin of the freshwater crayfish Pacifastacus leniusculus. *Journal of Biological Chemistry*, 278(10), pp.7927–7933.

Lieb, B. et al., 2001. Structures of two molluscan hemocyanin genes: Significance for gene evolution. *Proceedings of the National Academy of Sciences*, 98(8), pp.4546–4551. Available at: http://www.pnas.org/cgi/doi/10.1073/pnas.071049998.

Lieb, B., Altenhein, B. & Markl, J., 2000. The sequence of a gastropod hemocyanin (HtH1 from Haliotis tuberculata). *Journal of Biological Chemistry*, 275(8), pp.5675–5681.

Lieb, B. & Markl, J., 2004. Evolution of molluscan hemocyanins as deduced from DNA sequencing. *Micron*, 35(1–2), pp.117–119.

Loker, E.S. et al., 2004. Invertebrate immune systems-not homogonous, not simple, not well understood. *Immunological Reviews*, 198, pp.10–24.

Macey, B.M., Christison, K.W. & Mouton, A., 2011. Halioticida noduliformans isolated from cultured abalone (Haliotis midae)in South Africa. *Aquaculture*, 315(3–4), pp.187–195. Available at: http://dx.doi.org/10.1016/j.aquaculture.2011.02.004.

Malham, S.K. et al., 2003. Evidence for a direct link between stress and immunity in the mollusc Haliotis tuberculata. *Journal of Experimental Zoology Part A: Comparative Experimental Biology*, 295A(2), pp.136–144. Available at: https://doi.org/10.1002/jez.a.10222.

Markl, J., 2013. Evolution of molluscan hemocyanin structures. *Biochimica et Biophysica Acta - Proteins and Proteomics*, 1834(9), pp.1840–1852. Available at: http://dx.doi.org/10.1016/j.bbapap.2013.02.020.

Marmaras, V.J. & Lampropoulou, M., 2009. Regulators and signalling in insect haemocyte immunity. *Cellular Signalling*, 21(2), pp.186–195. Available at: http://www.sciencedirect.com/science/article/pii/S089865680800257X.

Marshall, O.J., 2004. PerlPrimer: cross-platform, graphical primer design for standard, bisulphite and real-time PCR. *Bioinformatics (Oxford, England)*, 20(15), pp.2471–2472.

Matsuzaki, K., 2001. Why and how are peptide-lipid interactions utilized for self defence? *Biochemical Society Transactions*, 29(4), pp.598–601.

Mau, A. & Jha, R., 2018. Aquaculture of two commercially important molluscs (abalone and limpet): existing knowledge and future prospects. *Reviews in Aquaculture*, 10(3), pp.611–625.

May, R.M., 1988. How Many Species Are There on Earth. *Science*, 241(4872), pp.1441–1449. Available at: http://links.jstor.org/sici?sici=0036-8075%2819880916%293%3A241%3A4872%3C1441%3AHMSATO%3E2.0.CO%3B2-B.

Mayfield, S. et al., 2011. Survey estimates of fishable biomass following a mass mortality in an Australian molluscan fishery. *Journal of Fish Diseases*, 34(4), pp.287–302. Available at:

https://doi.org/10.1111/j.1365-2761.2011.01241.x.

Miller, K.I. et al., 1998. Sequence of the Octopus dofleini hemocyanin subunit: structural and evolutionary implications. *Journal of molecular biology*, 278(22), pp.827–842.

Mogensen, T.H., 2009. Pathogen recognition and inflammatory signaling in innate immune defenses. *Clinical Microbiology Reviews*, 22(2), pp.240–273.

Mól, A., Castro, M. & Fontes, W., 2018. A web application to create high quality peptide helical wheel and net projections. *bioRxiv*, pp.1–7. Available at: http://lbqp.unb.br/NetWheels/.

Morash, A.J. & Alter, K., 2016. Effects of environmental and farm stress on abalone physiology: perspectives for abalone aquaculture in the face of global climate change. *Reviews in Aquaculture*, 8(4), pp.342–368.

Mouton, A. & Gummow, B., 2011. The occurrence of gut associated parasites in the South African abalone, Haliotis midae, in Western Cape aquaculture facilities. *Aquaculture*, 313(1–4), pp.1–6.

Nappi, A.J. & Ottaviani, E., 2000. Cytotoxicity and cytotoxic molecules in invertebrates. *BioEssays*, 22(5), pp.469–480. Available at: https://doi.org/10.1002/(SICI)1521-1878(200005)22:5%3C469::AID-BIES9%3E3.0.CO.

Neelay, O.P. et al., 2017. Antimicrobial peptides interact with peptidoglycan. *Journal of Molecular Structure*, 1146, pp.329–336. Available at: http://dx.doi.org/10.1016/j.molstruc.2017.06.018.

Nicolas, J.L. et al., 2002. Vibrio carchariae , a pathogen of the abalone Haliotis tuberculata. *Diseases of aquatic orgnanisms*, 50(June), pp.35–43.

Ottaviani, E., Valensin, S. & Franceschi, C., 1998. The neuro-immunological interface in an evolutionary perspective: the dynamic relationship between effector and recognition systems. *Frontiers in Bioscience*, 3, pp.431–435. Available at: http://www.ncbi.nlm.nih.gov/pubmed/9545439.

Paillard, C., Le Roux, F. & Borrego, J.J., 2004. Bacterial disease in marine bivalves, a review of recent studies: Trends and evolution. *Aquat. Living Resour.*, 17(4), pp.477–498. Available at: https://doi.org/10.1051/alr:2004054.

Pang, Z. et al., 2014. Distinct regulation patterns of the two prophenoloxidase activating enzymes corresponding to bacteria challenge and their compensatory over expression feature in white shrimp (Litopenaeus vannamei). *Fish & Shellfish Immunology*, 39(2), pp.158–167. Available at: http://www.sciencedirect.com/science/article/pii/S1050464814001429.

Papagianni, M., 2003. Ribosomally synthesized peptides with antimicrobial properties: biosynthesis, structure, function, and applications. *Biotechnology Advances*, 21(6), pp.465–499. Available at: http://www.sciencedirect.com/science/article/pii/S0734975003000776.

Pettersen, E.F. et al., 2004. UCSF Chimera — A Visualization System for Exploratory Research and Analysis.

Pitcher, G.C. et al., 2019. Devastating farmed abalone mortalities attributed to yessotoxin-producing dinoflagellates. *Harmful Algae*, 81(May 2018), pp.30–41. Available at: https://doi.org/10.1016/j.hal.2018.11.006.

Pitcher, G.C. et al., 2001. Paralytic Shellfish Poisoning in the abalone Haliotis midae on the West Coast of South Africa. *J. Shellfish Res.*, 20(2), pp.895–904.

Qiagen, 2003. *The QIAexpressionist™ A handbook for high-level expression and purification of 6xHis-tagged proteins* 5th ed., Available at: http://kirschner.med.harvard.edu/files/protocols/QIAGEN_QIAexpressionist_EN.pdf.

Qiu, C. et al., 2014. Molecular Cloning of Hemocyanin cDNA from Fenneropenaeus chinensis and Antimicrobial Analysis of Two C-terminal Fragments. *Marine Biotechnology*, 16(1), pp.46–53. Available at: https://doi.org/10.1007/s10126-013-9519-y.

Raemaekers, S. et al., 2011. Review of the causes of the rise of the illegal South African abalone fishery and consequent closure of the rights-based fishery. *Ocean and Coastal Management*, 54(6), pp.433–445. Available at: http://dx.doi.org/10.1016/j.ocecoaman.2011.02.001.

Riciluca, K.C.T. et al., 2012. Rondonin an antifungal peptide from spider (Acanthoscurria rondoniae) haemolymph. *Results in Immunology*, 2, pp.66–71. Available at: http://dx.doi.org/10.1016/j.rinim.2012.03.001.

Romeo, D. et al., 1988. Structure and bactericidal activity of an antibiotic dodecapeptide purified from bovine neutrophils. *Journal of Biological Chemistry*, 263(20), pp.9573–9575.

Rowley, A.F. & Powell, A., 2007. Invertebrate Immune Systems-Specific, Quasi-Specific, or Nonspecific? *The Journal of Immunology*, 179(11), pp.7209–7214. Available at: http://www.jimmunol.org/cgi/doi/10.4049/jimmunol.179.11.7209.

Sales, J. & Britz, P.J., 2001. Research on abalone (Haliotis midae L .) cultivation in South Africa. *Aquaculture Research*, 32(11), pp.863–874.

Sales, J. & Britz, P.J., 2001. Research on abalone (Haliotis midae L.) cultivation in South Africa. *Aquaculture Research*, 32(11), pp.863–874.

Sawabe, T. et al., 2007. Mass Mortality of Japanese Abalone Haliotis discus hannai Caused by Vibrio harveyi Infection. *Microbes and Environment*, 22(3), pp.300–308.

Schwarz, S., Kehrenberg, C. & Walsh, T.R., 2001. Use of antimicrobial agents in veterinary medicine and food animal production. *International Journal of Antimicrobial Agents*, 17(6), pp.431–437. Available at: http://www.sciencedirect.com/science/article/pii/S0924857901002977.

Seidman, C.E. et al., 1997. Introduction of plasmid DNA into cells. In *Current protocols in molecular biology*. pp. 1–8.

Selsted, M.E. et al., 1985. Primary structures of three human neutrophil defensins. *Journal of Clinical Investigation*, 76(4), pp.1436–1439.

Simmaco, M., Mignogna, G. & Barra, D., 1998. Antimicrobial peptides from amphibian skin: What do they tell us? *Peptide Science*, 47(6), pp.435–450. Available at: https://doi.org/10.1002/(SICI)1097-0282(1998)47:6%3C435::AID-BIP3%3E3.0.CO.

Sindermann, C.J., 1984. Disease in marine aquaculture. *Helgolander meeresuntersuchungen*, 37, pp.505–530.

Slattery, M. et al., 2012. Marine Proteomics: A Critical Assessment of an Emerging Technology. *Journal of Natural Products*, 75(10), pp.1833–1877. Available at: https://doi.org/10.1021/np300366a.

Söderhäll, K. & Cerenius, L., 1998. Role of the prophenoloxidase-activating system in invertebrate immunity. *Current Opinion in Immunology*, 10(1), pp.23–28.

Song, Y.L. et al., 2003. Haemolymph parameters of Pacific white shrimp (Litopenaeus vannamei) infected with Taura syndrome virus. *Fish and Shellfish Immunology*, 14(4), pp.317–331.

Spotte, S.H., 1970. Fish and invertebrate culture: water management in closed systems. In *Fish and invertebrate culture*. p. 145.

Steinberg, J., 2005. The illicit abalone trade in South Africa. *Institute for Security Studies.*, 105(April), p.16.

Steiner, H. et al., 1981. Sequence and specificity of two antibacterial proteins involved in insect immunity. *Nature*, 292, p.246. Available at: https://doi.org/10.1038/292246a0.

Streit, K., Geiger, D.L. & Lieb, B., 2005. Molecular Phylogeny and the Geographic Origin of Haliotidae Traced by Haemocyanin Sequences. *Journal of Molluscan Studies Advanced Access*, (September), pp.1–6.

Terwilliger, N.B., 2007. Hemocyanins and the immune response: Defense against the dark arts. *Integrative and Comparative Biology*, 47(4), pp.662–665.

Tiscar, P.. & Mosca, F., 2004. Defense Mechanisms in Farmed Marine Molluscs. *Veterinary Research Communications*, pp.57–62.

Travers, M.A. et al., 2010. Gene expression patterns of abalone, Haliotis tuberculata, during successive infections by the pathogen Vibrio harveyi. *Journal of Invertebrate Pathology*, 105(3), pp.289–297.

Travers, M.A. et al., 2008. Morphologic, cytometric and functional characterisation of abalone (Haliotis tuberculata) haemocytes. *Fish and Shellfish Immunology*, 24(4), pp.400–411.

Troell, M. et al., 2006. Abalone farming in South Africa : An overview with perspectives on kelp resources , abalone feed , potential for on-farm seaweed production and socio-economic importance. , 257, pp.266–281.

Troell, M. et al., 2006. Abalone farming in South Africa: An overview with perspectives on kelp resources, abalone feed, potential for on-farm seaweed production and socio-economic importance. *Aquaculture*, 257(1–4), pp.266–281.

Vosloo, A., Laas, A. & Vosloo, D., 2013. Differential responses of juvenile and adult South African abalone (Haliotis midae Linnaeus) to low and high oxygen levels. *Comparative Biochemistry and Physiology - A Molecular and Integrative Physiology*, 164(1), pp.192–199. Available at: http://dx.doi.org/10.1016/j.cbpa.2012.09.002.

Wang, G., Li, X. & Wang, Z., 2009. APD2: The updated antimicrobial peptide database and its application in peptide design. *Nucleic Acids Research*, 37(SUPPL. 1).

Wang, J. et al., 2013. Molecular cloning and transcriptional regulation of an allograft inflammatory factor-1 (AIF-1) in Zhikong scallop Chlamys farreri. *Gene*, 530(2), pp.178–184. Available at: http://www.sciencedirect.com/science/article/pii/S0378111913010937.

Westerhoff, H. V. et al., 1989. Magainins and the disruption of membrane-linked free-energy transduction. *Proceedings of the National Academy of Sciences*, 86(17), pp.6597–6601. Available at: http://www.pnas.org/cgi/doi/10.1073/pnas.86.17.6597.

Wood, A.D. & Buxton, C.D., 1996. Aspects of the biology of the abalone haliotis midae (Linne, 1758) on the east coast of south Africa. 1. Feeding biology. *South African Journal of Marine Science*, 17,

pp.61–68.

Yang, L. et al., 2000. Crystallization of antimicrobial pores in membranes: Magainin and protegrin. *Biophysical Journal*, 79(4), pp.2002–2009. Available at: http://dx.doi.org/10.1016/S0006-3495(00)76448-4.

Zanjani, N.T. et al., 2016. Abalone Hemocyanin Blocks the Entry of Herpes Simplex Virus 1 into Cells : a Potential New Antiviral Strategy. *Antimicrobial Agents and Chemotherapy*, 60(2), pp.1003–1012.

Zasloff, M., 2002. Antimicrobial peptides of multicellular organisms. *Nature*, 415(389), pp.389–395.

Zhang, X., Huang, C. & Qin, Q., 2004. Antiviral properties of hemocyanin isolated from shrimp Penaeus monodon. *Antiviral Research*, 61(2), pp.93–99.

Zhu, H. et al., 2014. Cryo-EM structure of isomeric molluscan hemocyanin triggered by viral infection. *PLoS ONE*, 9(6), pp.1–8.

Zhuang, J. et al., 2015. Identification of candidate antimicrobial peptides derived from abalone hemocyanin. *Developmental and Comparative Immunology*, 49(1), pp.96–102.

Zosloff, M., 1988. Magainlns, a Class of Antimicrobial Peptldes from Xenopus Skin: Isolation, Characterization of Two Active Forms, and Partial cDNA Sequence of a Precursor. *Journal of Occupational and Environmental Medicine*, 30(6), p.470. Available at: http://content.wkhealth.com/linkback/openurl?sid=WKPTLP:landingpage&an=00043764-198806000-00004.

De Zoysa, M., Nikapitiya, C., et al., 2011. Microarray analysis of gene expression in disk abalone Haliotis discus discus after bacterial challenge. *Fish & Shellfish Immunology*, 30(2), pp.661–673. Available at: http://www.sciencedirect.com/science/article/pii/S1050464810004079.

De Zoysa, M., Whang, I., et al., 2011. Transcriptional analysis of disk abalone (Haliotis discus discus) antioxidant enzymes against marine bacteria and virus challenge. *Fish & Shellfish Immunology*, 31(1), pp.155–160. Available at: http://www.sciencedirect.com/science/article/pii/S105046481100129X.